POLSKA AKADEMIA NAUK
KOMITET FIZYKI

ACTA PHYSICA POLONICA

KWARTALNIK

Vol. XII — Fasc. 1

WARSZAWA 1953

Содержание

POLSKA AKADEMIA NAUK
KOMITET FIZYKI

ACTA PHYSICA POLONICA

KWARTALNIK

Volumen XII

WARSZAWA 1953

PAŃSTWOWE WYDAWNICTWO NAUKOWE

Czasopismo ukazuje się corocznie w jednym tomie złożonym z czterech kwartalnych zeszytów.

Журнал издаваемый ежегодно в одном томе состоящем из четырех выпусков.

The periodical appears yearly in one volume of four quarterly issues.

Le periodique parit dans un volume par an en quatre fascicules trimestriels.

Die Zeitschrift erscheint in einem Bande von vier Heften jährlich.

Adres Redakcji — Адрес Редакции — Adresse de la Rédaction:
Kraków 2, al. Słowackiego 15 m. 9

Cena zeszytu pojedynczego wynosi 12 zł,
prenumerata roczna 48 zł, półroczna 24 zł
Adres Państwowego Wydawnictwa Naukowego:
Warszawa, Krakowskie Przedmieście 79

Volumen XII

CONTENTS

FASCICULUS 1

FASCICULUS 2

FASCICULUS 3-4

Laboratory Equipment and Techniques

Letters to the Editor

AUTHOR INDEX

СОДЕРЖАНИЕ

Выпуск 1

Письма в редакцию

Выпуск 2

Выпуск 3—4

УКАЗАТЕЛЬ АВТОРОВ

ON A GRAPHIC METHOD OF ELIMINATING THE BACKGROUND IN PHOTOGRAPHIC SPECTROPHOTOMETRY

By Maria D. Kunisz

Institute of Experimental Physics, Jagellonian University, Kraków

(received February 2, 1952)

Dorgelo's spectrophotometric method cannot be employed directly if the spectral lines appear on a background of a continuous spectrum which cannot be eliminated by laboratory means. A graphic method of eliminating the background is suggested and employed to determine the ratio of intensities of spectral lines of the composed triplet $4d^3D - 4p^3P^0 ZnI$

Introduction

The intensity ratio of spectral lines appearing on an unblackened plate is determined by Dorgello's method in the following way. Let $\mathcal{J}_{l_1}$ and $\mathcal{J}_{l_2}$ be the line intensities of wave-lengths λ_1 and λ_2, and let $I^i_{l_1}$ and $I^i_{l_2}$ be the intensities after passing through the i-th section of a step filter or a rotating sector. Then we obtain

$$I_{l_1} \cdot p_i = \mathcal{J}^i_{l_1} \qquad (1)$$

where p_i (a proper fraction) is the transparency of the given section of the filter.

Curves of the dependence of plate-blackening on light intensity $S_{l_1}(I^i_{l_1})$, $S_{l_2}(I^i_{l_2})$ are plotted for both lines (see Fig. 1) on the basis of a microphotogram of spectral lines photographed through a step filter or a rotating sector. A typical diagram of this relation is shown in Fig. 1; where p is plotted in a logarithmic scale.

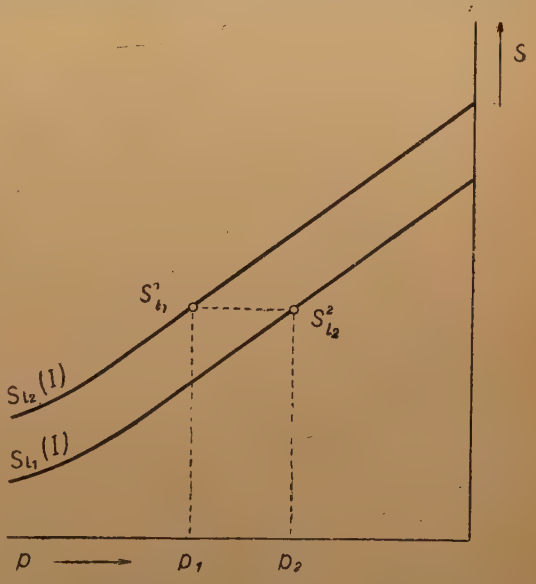

Fig. 1. Blackening of a plate as a function of light intensity for two photometered lines

Let us consider any plate blackening values for both lines which fulfil the condition $S^1_{l_1} = S^2_{l_2}$. Assuming that the wave lengths λ_1 and λ_2 are sufficiently near each other, so that the spectral difference of sensitiveness of the photographic plate may be neglected, we may conclude that the intensities of light falling on

the plate are equal, i. e. $I^1_{l_1} = I^2_{l_2}$. Therefore in view of equation (1) $\mathcal{J}_{l_1} \cdot p_1 = \mathcal{J}_{l_2} \cdot p_2$ and the desired ratio of intensity of the lines λ_1 and λ_2 may be represented by

$$\frac{\mathcal{J}_{l_1}}{\mathcal{J}_{l_2}} = \frac{p_2}{p_1} \qquad (2)$$

I. The method of objective monochromatic spectrophotometry of lines appearing on the background of a continuous spectrum

The above method cannot be directly applied for determining the ratio of intensities of lines appearing on the background of a continuous spectrum, as may be proved by the following reasoning:

let $S_{l_1+t_1}$ and $S_{l_2+t_2}$ represent the plate-blackening for lines of wave-lengths λ_1

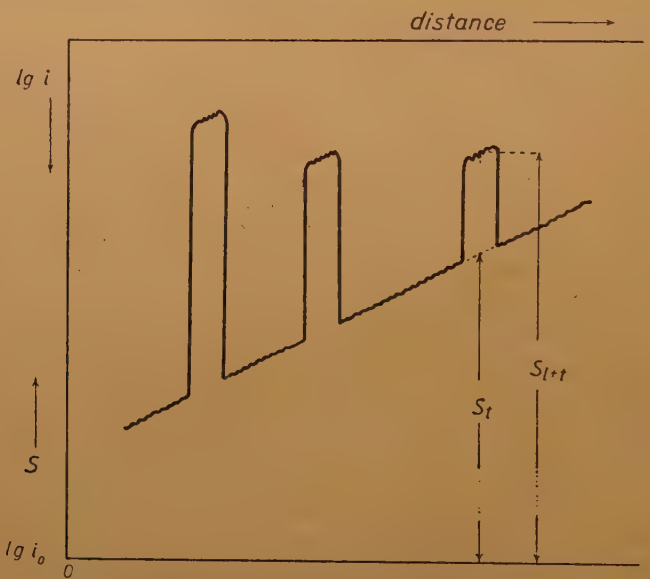

Fig. 2. The microphotogram: i denotes the current intensity in the galvanometer of the microphotometer, and i_0 the current intensity in the galvanometer for the unblackened plate

and λ_2 respectively, determined together with the background, and S_{t_1} and S_{t_2} the plate-blackening for the continuous spectrum for the same wave-lengths (see Fig. 2). The S_t values are the mean values calculated by interpolation of values of the plate-blackening for the background in the vicinity of the lines.

Dorgello's method directly applied enables us to calculate the ratio of intensities:

$$\frac{\mathcal{J}_{l_1+t_1}}{\mathcal{J}_{l_2+t_2}} = \frac{\mathcal{J}_{l_1} + \mathcal{J}_{t_1}}{\mathcal{J}_{l_2} + \mathcal{J}_{t_2}} \mp \frac{\mathcal{J}_{l_1}}{\mathcal{J}_{l_2}} \qquad \text{if} \quad \frac{\mathcal{J}_{l_1}}{\mathcal{J}_{l_2}} \mp \frac{\mathcal{J}_{t_1}}{\mathcal{J}_{t_2}}$$

This value obviously does not, in general, represent the ratio of the line intensities.

If the intensity of the continuous spectrum is constant in the examined range of wave-lengths ($\mathcal{J}_{t_1} = \mathcal{J}_{t_2}$) the background may be eliminated by two methods;

in the case of a continuous spectrum of variable intensity only the second method is available.

Method 1. The following ratios may be determined by Dorgelo's usual method from the curves of the dependence of the plate-blackening on light intensity for lines observed together with the background and for the background itself: $S_{l_1+t_1}(\mathrm{I})$, $S_{l_2+t_2}(\mathrm{I})$, $S_{t_1}(\mathrm{I})$, $S_{t_2}(\mathrm{I})$

$$\frac{\mathcal{J}_{l_1+t_1}}{\mathcal{J}_{t_1}}; \quad \frac{\mathcal{J}_{l_2+t_2}}{\mathcal{J}_{t_2}}$$

However, as $\mathcal{J}_{l_1+t_1} = \mathcal{J}_{l_1} + \mathcal{J}_{t_1}$ therefore $\frac{\mathcal{J}_{l_1+t_1}}{\mathcal{J}_{t_1}} = \frac{\mathcal{J}_{t_1} + \mathcal{J}_{t_1}}{\mathcal{J}_{t}}$ and accordingly $\frac{\mathcal{J}_{l_1}}{\mathcal{J}_{t_1}} = \frac{\mathcal{J}_{l_1+t_1}}{\mathcal{J}_{t_1}} - 1$ $\frac{\mathcal{J}_{l_2}}{\mathcal{J}_{t_2}} = \frac{\mathcal{J}_{l_2+t_2}}{\mathcal{J}_{t_2}} - 1$

Thus the ratio of the line intensity measured together with the background and the background intensity determines unequivocally the ratio of intensities o the line and the background.

Hence, assuming that the background in the considered range is constant, i. e. $\mathcal{J}_{t_1} = \mathcal{J}_{t_2}$, the ratio of intensities of the lines may be directly calculated:

$$\frac{\mathcal{J}_{l_1}}{\mathcal{J}_{l_2}} = \frac{\mathcal{J}_{l_1}}{\mathcal{J}_{t_1}} : \frac{\mathcal{J}_{l_2}}{\mathcal{J}_{t_2}} = \frac{\frac{\mathcal{J}_{l_1+t_1}}{\mathcal{J}_{t_1}} - 1}{\frac{\mathcal{J}_{l_2+t_2}}{\mathcal{J}_{t_2}} - 1}$$

Method 2. Using the same curves as above we can plot curves of the relation of the plate-blackening and the light intensity, corresponding with the lines $S_{l_1}(\mathrm{I})$ and $S_{l_2}(I)$ without the background. For this purpose we reason on the basis of Fig. 3 as follows.

On Fig. 3, two curves are plotted, one of which, $S_{l+t}(I)$, represents the dependence of plate-blackening on light intensity calculated for the line together with the background, and the second, $S_t(I)$, the dependence of plate-blackening on light intensity calculated for the background alone. For a certain value of transparency p_1, the line intensity calculated with the background intensity amounts to $I^1_{t_1} = \mathcal{J}_t \cdot p_1$ and the corresponding blackening of the plate to S^1_t.

As point 2 we choose a point in which the blackening due to the background alone possesses a value equal to the blackening due to the line together with the background in point 1.

The appearance of a line with the intensity $\mathcal{J}_l$ on the background of a continuous spectrum of intensity $\mathcal{J}_t$ deepens the plate-blackening by $S^1_{l+t} - S^1_t$, and therefore has the same effect as increasing the light intensity by $I^2_t - I^1_t$. Equal blackening of the plate for the same wave-length proves that the light in-

tensity is the same, provided all other conditions remain unchanged. This means that $I_t^3 = I_{l+t}^1$ or $\mathcal{J}_t \cdot p_2 = \mathcal{J}_{l+t} \cdot p_1 = (\mathcal{J}_l + \mathcal{J}_t) \cdot p_1$. Therefore $I_l^1 = \mathcal{J}_l \cdot p_1 = \mathcal{J}_t \cdot (p_2 - p_1) = I_t^2 - I_t^1 = I_t^3$, where $p_3 = p_2 - p_1$.

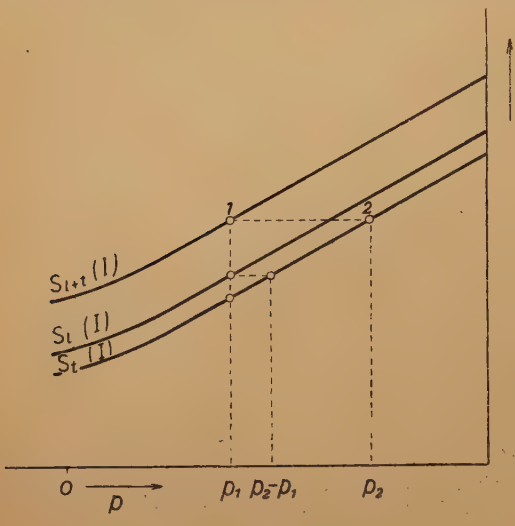

Fig. 3. Graphic elimination of the bac kground

The background intensity $I_t^2 - I_t^1$ corresponds to the blackening S_t^1, equal to the blackening which would be caused by a line weakened by p_1, if it appeared on a non-blackened photographic plate.

Calculating in this way the blackening of the plate for several values of the weakening p we may plot the curve of the dependence of the plate-blackening on the light intensity of the line. After plotting corresponding curves for all lines which have been observed we may calculate by the usual Dorgelo method the ratio of their intensities.

II. Determination of the ratio of spectral line intensities of an arc spectrum of the Zn composed triplet $4d^3D - 4p^3P^0$

A carbon arc with an anode filled with a mixture of powdered $ZnSO_4$ and carbon in weight proportion 2 : 3 was used as the source of light. The spectrum was photographed with the help of a large quartz spectrograph produced by C. Zeiss (Jena), with a dispersion of 18,4—19 Å/mm in the given range of wave-lengths. "Omega" antihalo orthochromatic plates produced by "Film Polski" were used. A six-step rotating sector was employed, weakening the light in the proportion 100 : 50 : 25 : 12,5 : 6,25 : 3,125 : 1,5625. The spectrum was photometered with a photoelectric microphotometer produced by C. Zeiss (Jena). The zinc spectrum obtained appeared on the background of a continuous spectrum of varying intensity.

Diagrams $S_{l+t}(I)$, $S_t(I)$ and $S_l(I)$ for wave-lengths *3345* Å, *3303* Å and *3282* Å respectively were plotted by the method described above (I, 2).

The following results were obtained for various conditions of glowing of the arc:

No	$\mathcal{J}_{3345}$	$\mathcal{J}_{3303}$	$\mathcal{J}_{3282}$
1	100	61 ± 1	22 ± 3
2	100	60 ± 1	21 ± 2
3	100	61 ± 1	23 ± 3
4	100	61 ± 1	24 ± 3
5	100	60 ± 1	19 ± 2

These results contain an experimental error due to neglecting differences of sensitiveness of the plate for the observed lines.

The results obtained, except for No 4, agree with the sum rule, which gives $\mathcal{J}_{3344} : \mathcal{J}_{3303} : \mathcal{J}_{3282} = 100 : 60 : 20$

The author wishes to express her thanks to Professor H. Niewodniczanski for suggesting the subject of this paper and for numerous discussions during its execution. She would also like to thank other members of the staff of the Institute of Experimental Physics of Jagellonian University for help received from them.

REFERENCE

Dorgelo H. B., *Z. Phys.*, **26**, 756 (1925).

КРАТКОЕ СОДЕРЖАНИЕ

М. Д. Куниш, *Графический метод исключения фона при спектральной фотографической фотометрии.*

Метод спектральной фотометрии Доргело не может быть применен в том случае, когда спектральные линии выступают на фоне непрерывного спектра, от которого лабораторным путем нельзя избавиться.

В настоящей работе приведен графический метод исключения фона, который был применен для определения отношения интенсивностей спектральных линий сложного триплета

$$4d^3D - 4p^3P^0 \; Zn\,I.$$

ON A STATISTICAL PHOTOGRAPHIC METHOD OF DETERMINING THE CROSS-SECTIONS FOR THE ABSORPTION OF SLOW NEUTRONS

By M. Wielowiejska

Physical Laboratory, Jagellonian University, Kraków

(received February 21, 1952)

A statistical photographic method of measuring the cross-sections for the absorption of thermal neutrons (0,025 eV) in aluminium and lead has been elaborated. The flux of photoneutrons from the reaction $^9Be(\gamma,n)2\alpha$ slowed down in paraffin wax was determined by evaluating the density of the $^3_1$H and $^4_2$He tracks in the emulsions of 100μ Ilford C2 nuclear research plates loaded with lithium. This method was applied to the determination of the cross-section of Al and Pb atoms for the total absorption of thermal neutrons. The results are in good agreement with those obtained by other methods.

Apparatus and method of measurements

A source of photoneutrons from the reaction $^9\mathrm{Be}(\gamma,n)\,2^4_2\mathrm{He}$ was used. The neutrons were sent through a layer of paraffin wax 6 cm thick with the purpose of slowing them down to so-called thermic velocities. About 13 mg of radium in radioactive equilibrium with its derivatives was used in the experiments. The radium was placed in a small cardboard cylinder contained in a larger cylinder of 6 cm diameter and 6 cm height. The larger cylinder was filled with beryllium so that the radioactive source was symmetrically surrounded by it on all sides. The source of neutrons was surrounded with a 6 cm layer of paraffin wax. It is known that with this thickness of paraffin wax, the highest possible number of neutrons (of initial energy 0,2 and 0,6 MeV) is slowed down to the thermal energy of room temperature.

To protect the experimenter against radium γ-radiation the whole apparatus was screened with a 5 cm layer of lead. The particulars are given in Fig. 1, where the experimental arrangement is shown in a horizontal cross-section.

Ilford nuclear research plates, type C2, emulsion thickness 100μ, saturated with lithium, were placed perpendicularly to the direction of the neutron flux. The plates were screened by a 5 cm lead filter. Because of the use of this filter the neutron flux was weakened to ¼, but this was necessary in order to bring down the γ-photon background in the emulsion to a sufficiently low level.

As the neutron source was weak, the time of exposition adopted for all measurements amounted to 96 hrs; the geometry of the experiment remained unchan-

ged during the whole time. Exposed plates were developed with the help of the temperature method of Dilworth et al. (1948).

A serious difficulty appeared during developing of the plates, as some plates were so darkened that their observation under a microscope was impossible. After a series of experiments it appeared that the only way to get rid of this darkening was to bathe the plates for 12-16 hours in the fixing solution at room temperature. This solution was changed from time to time. The α particle tracks do not undergo any changes during such long bathing; they are as distinct as after the usual developing. Besides, sometimes after developing the emulsion was covered on its surface with a thin layer of silver, which could not be removed mechanically, but the long bath in the fixing solution removed it completely.

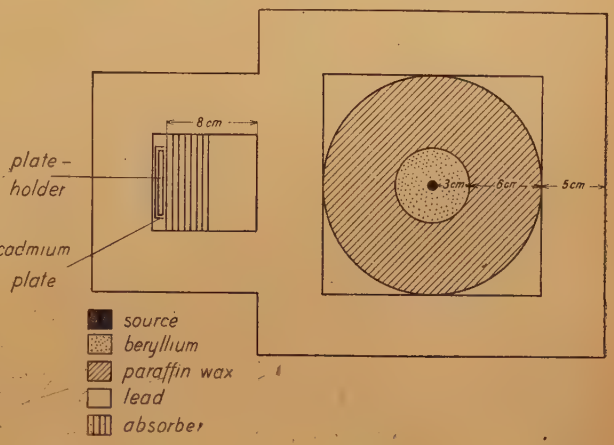

Fig. 1. Horizontal cross-section of the apparatus

After exposition and development each plate was examined under a Zeiss microscope with a depth micrometer. The microscope possessed a stage with cross movement. The magnification used during the observations was 588. This was chosen in consideration of the length of the measured tracks, since according to Titterton (1949) and Locqueneux (1950) in the reaction $^6\mathrm{Li}(n,\alpha)^3\mathrm{H}$ the joint track length of tritonium and the α-particle amounts to about 42μ. It is assumed that the length of the road is constant and that the distribution is isotropic.

Usually the tracks do not appear in the plane of observation in the microscope but are inclined towards it at an angle. In that case only projections are observed on a plane parallel to the emulsion surface. Traces whose components parallel to the emulsion surface were of the length $12—42\mu$ were counted. This range was chosen on the basis of the statistical material.

The shrinking of the emulsion during developing was taken into account. The shrinkage coefficient was calculated on the basis of Vigneron's paper (1949). For Ilford C2 plates with emulsion thickness of 100μ it amounts to $S = 2{,}16 \pm 0{,}07$. Every component perpendicular to the emulsion surface was therefore multiplied by this coefficient.

Statistics of tracks were prepared from the point of view of the length of their components. The results of the measurements were collected in a table. The horizontal column A contains the number of traces for which the statistics were prepared. B contains the lengths of components parallel to the emulsion

surface, C the mean lengths of components perpendicular to the emulsion surface after multiplying by the shrinkage coefficient, and D the values of the perpendicular components calculated on theoretical grounds. The estimated probable errors of the measurements were $\pm 1\mu$.

Table 1

A	45	49	47	50	48	49	49
B	9μ	12	15	18	24	30	36
C	$12 + 2\mu$	16	15	14	12,2	12,3	7
D	19μ	18,5	18	17	15	13	9

Comparing the experimental values in column C with theoretical ones in column D we see that beginning with the length of the parallel component 12μ almost all tracks, whose projections on a horizontal plane possess a length $12—42\mu$, may be attributed to tracks due to the reaction $^6\mathrm{Li}(n, \alpha)^3\mathrm{H}$. On the other hand, tracks possessing parallel components of length lower than 12μ, as for instance 9μ in Table 1, differ too much from the calculated theoretical values. In other words it is difficult to identify them with tracks due to the reaction $^6\mathrm{Li}(n, \alpha)^3\mathrm{H}$.

Measurements and their discussion

The calculation of the flux of neutrons falling on the surface of the emulsion was based on the following reasoning: Let N be the number of neutrons falling normally during 1 sec on 1 cm^2 of the emulsion of thickness e, containing M atoms of the given element in 1 ccm; and let n be the number of neutrons which cause the reaction. Then in agreement with the definition of the cross-section

$$\delta(v) = \frac{n}{N} \cdot \frac{1}{M \cdot e} \cdot$$

where v is the velocity. Therefore

$$N = \frac{1}{\delta(v)} \cdot \frac{n}{M \cdot e} \cdot$$

Let $n_0 = n/e$ be the number of reactions per unit volume. Then $N = \frac{1}{\delta(v)} \cdot \frac{n_0}{M}$. If we find n_0, i. e. the number of reactions per unit volume of the emulsion then, with given δ and M, we may calculate N.

To establish the value of n_0, statistics of fields with various absorber thickness were prepared. Each time traces were counted for 213 fields, in other words, the number of tracks were counted whose projections on the plane of the field of view were contained in cylinders of equal diameter and height.

The results of the measurements are shown on diagrams representing the relation between the number of fields and the number of traces. As it appeared, for every thickness of the absorber the values are distributed on a Gaussian error curve around a most probable value. For instance, with an aluminium layer of 5,2 cm most fields contain two tracks (see Fig. 2).

Statistics for several plates which have been developed without a previous

exposition have been prepared to find out whether in an unexposed emulsion there are present traces due to the reaction $^6Li(n, \alpha)^3H$ caused by stray neutrons. It appeared that such traces do exist, but in so few fields that this neutron background was not taken into account.

The number of neutrons passing through a given thickness of the absorber is determined by utilizing the most probable values obtained on the basis of the diagrams. Assuming that the thickness of the emulsion amounts to 100 μ, that the lithium concentration (according to Ilford) amounts to 0,016 g/ccm and that the cross-section for lithium (mean value for both isotopes ^6Li and ^7Li) amounts to $\delta = 64$ barns, the following tables were dressed:

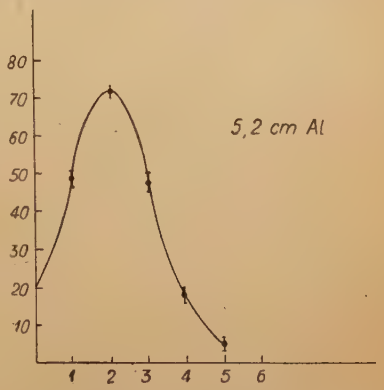

Fig. 2. Number of fields as function of the number of tracks in one field

Table 2

Aluminium absorber, thickness	1,2	2,4	5,2	8
$n_0 = \frac{n}{e}$	$23{,}88 \times 10^4$	$20{,}69 \times 10^4$	$15{,}92 \times 10^4$	$11{,}94 \times 10^4$
$N = \frac{1}{\delta(v)} \cdot \frac{n_0}{M}$	$2{,}683 \times 10^6$	$2{,}325 \times 10^6$	$1{,}789 \times 10^6$	$1{,}34 \times 10^6$

Table 3

Lead absorber, thickness	0,6	1,2	2	3
$n_0 = \frac{n}{e}$	$23{,}88 \times 10^4$	$19{,}90 \times 10^4$	$15{,}92 \times 10^4$	$11{,}94 \times 10^4$
$N = \frac{1}{\delta(v)} \cdot \frac{n_0}{M}$	$2{,}683 \times 10^6$	$2{,}236 \times 10^6$	$1{,}789 \times 10^6$	$1{,}34 \times 10^6$

On the basis of these tables absorption curves for aluminium and lead were plotted (Fig. 3 and 4). These diagrams show the logarithms of the neutron number intensity N as function of the mass of the absorber per one cm^2. Both curves are straight lines inclined at an angle φ to the abscissae axis. The cross-section may be calculated from the equation

$$\delta = \frac{m}{lge} \cdot tg\,\varphi,$$

where m is the atomic mass of the absorber.

The calculated values of the cross-section amounted to $\delta = 1{,}64$ barns for aluminium and $\delta = 8{,}63$ barns for lead. The error committed during the calculation of these values on the basis of the diagram amounts to about ± 2 percent. These values agree with results obtained by other authors. According to Goldsmith et al. (1947) the cross-section for slow neutrons of 0,025 eV energy has the value $\delta = 8{,}7$ barns for lead and $\delta = 1{,}5$—$1{,}6$ barns for aluminium.

In these measurements systematic as well as accidental errors may appear. The uncertainty in the value of the lithium concentration given by the producing firm (2 percent) belongs to the first group.

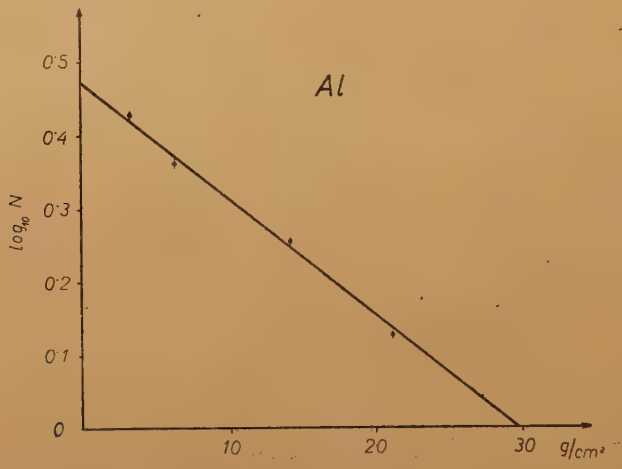

Fig. 3. Diagram of the logarithm of neutron number as function of the mass of the absorber per 1 cm² for Al

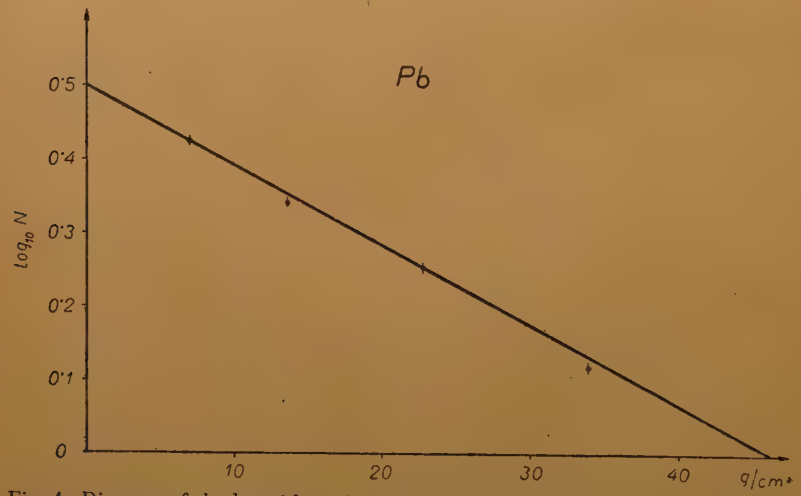

Fig. 4. Diagram of the logarithm of neutron number as function of the mass of the absorber per 1 cm² for Pb

There were also noticed discontinuous tracks consisting of separate shorter groups, which could be caused by inhomogeneity of the AgBr distribution in the emulsion.

Perhaps the largest error is due to the fact that not all of the tracks are completely contained in the emulsion.

The aluminium and lead employed in the measurements were spectrometrially tested. Small amounts of copper and nickel impurities were present but

no trace of cadmium or boron, possessing especially high cross-sections for thermic neutron capture, were found.

Summary of results

A method of measuring the crossection for the absorption of thermal neutrons of 0,025 eV energy based on statistical measurements with the help of photographic emulsion was worked out. The values of the cross-sections were found to be $\sigma = 1{,}64$ barns for Al and $\sigma = 8{,}63$ barns for Pb.

The possibility was also established of measuring with this method the surface density of the number of evenly distributed neutrons of the order of $10^6/cm^2$. The order of magnitude of this density amounted to 10^8 in Titterton's (1949) and to 10^{10} in Locqueneux's (1950) measurements. Hence, the method elaborated in this paper is suitable for measuring weak fluxes of thermal neutrons.

In this research only photoneutrons were used; this involves a strong flux of γ-rays. These sources are known to have a very low efficiency, about 10 times smaller than the neutron sources employing the reaction (α, n). To obtain a strong enough neutron dose the time of exposition must be suitably extended. This leads to a stronger irradiation of the emulsion with γ-rays. To diminish the background a lead filter was used. As it appeared, with so weak a source (13 mg Ra) and such a long period of exposition the background was diminished by the lead filter of 5 cm thickness to such an extent that it did not hinder the observations.

It is a pleasure to thank Professor H. Niewodniczański for suggesting the subject of this paper and for his supervision during its execution, and to thank all those who by their friendly attitude facilitated its succesful accomplishment.

REFERENCES

Dilworth C. C., Occhialini G. P., and Payne R. M., *Nature*, **162** (1948).
Goldsmith H., Ibser H. W., and Feld B. T., *Rev. Mod. Phys.*, **19**, 259 (1947).
Locqueneux R., *J. Phys. Radium*, **11**, 144 (1950).
Titterton E. W., *Nature*, **163**, 990 (1949).
Vigneron L., *J. Phys. Radium*, **10**, 305, (1949).

КРАТКОЕ СОДЕРЖАНИЕ

М. Велёвейская, *Статистический фотографический метод измерения эффективного сечения поглощения медленных нейтронов.*

Разработан статистический фотографический метод измерения эффективного сечения поглощения термических нейтронов (0,0025 eV) атомами аллюминия и свинца. Поток нейтронов, получаемых в реакции $^9Be(\gamma,n)2\alpha$ и замедляемых парафином, определялся путем оценки плотности следов ^3H и ^4He в ядерных пластинках Ильфорда 100—C2, пропитанных литием. Этот метод был применен для определения полного эффективного сечения поглощения термических нейтронов атомами Al и Pb. Результаты совпадают с результатами, полученными другими методами.

CONSERVATION LAWS IN NON-LOCAL FIELD THEORIES

By J. Rzewuski

Physical Institute, Nicholas Copernicus University, Toruń

(received June 1, 1953)

The purpose of this paper is to investigate to what extent conservation laws are satisfied in non-local field theories.

Introduction

The conception of non-local interaction is equivalent to the conception of structure of the elementary particles. This structure is usualy described by a form-factor which, so far, is to a large extent an arbitrary function. The first properly invariant formulation of a theory of extended particles is due to Peierls and McManus (McManus 1948). The form-factor may in principle be obtained from experiment, but one can also hope that it will be explained by a future theory of elementary particles. An attempt to construct a theory of this kind was already made by Yukawa (1950). In fact it was shown by Møller (1954) that Yukawa's theory is a particular case of a form-factor theory with the form-function chosen in a specific way.

A theory of the structure of particles may be viewed also as a theory of forces acting between point particles. This will become apparent from the considerations of the first section. It is mathematically expressed by the equivalence of certain integral equations with partial differential equations. From this point of view various modifications of the conventional theory consisting in the introduction of higher order differential operators are also special cases of an extended source theory with a particular choice of the form-function. This equivalence will give us means to construct tensor densities satisfying differential conservation laws, although these quantities will be expressed by (in general infinite) series of differential operators.

Integral equations are, however, a most suitable form for an extended source theory, and therefore one should try to define the energy-momentum and angular momentum tensor densities in terms of integral operators. To what extent this is possible we shall investigate in the second section. It will be shown that for scattering problems (inhomogeneous integral equations) the quantities in question must necessarily contain differential operators although their order may not exceed two. For bound problems (homogeneous integral equations) it is possible to define energy-momentum and angular momentum tensor densities by means of integral operators only. In both cases only integral conservation laws are satisfied. This

means that the integral quantities (densities integrated over a space-like surface) are conserved from one space-like hyper-surface σ_1 to a later surface σ_2. These surfaces, however, may not be taken arbitrarily near to each other, the closest distance being prescribed by the nature of the form-factor.

The present paper considers classical fields only. An attempt at quantization was published by the author elsewhere (Rzewuski 1951), see also Rayski (1951) and Møller (1952).

1. Transition to differential equations

As starting point of the considerations it is most convenient to take integral equations describing non-local interactions. For the simple case of a charged scalar field $\psi(x)$, $\psi^*(x)$ interacting with a neutral scalar field $\varphi(x)$ these equations have the form

$$\begin{aligned}\psi(1) &= \psi^0(1) + g\int K(12)\varphi(2)\psi(2)\,dx_2,\\ \psi^*(1) &= \psi^{0*}(1) + g\int K^*(12)\varphi(2)\psi^*(2)\,dx_2,\\ \varphi(1) &= \varphi^0(1) + g\int L(12)\psi^*(2)\psi(2)\,dx_2,\end{aligned} \tag{1}$$

Here ψ^0, φ^0, K and L are given functions, the numbers 1, 2, ... denote points in space time, g is a constant. For other types of fields (e. g. the electromagnetic field interacting with a spinor field) the equations are essentially the same and all following considerations remain valid.

Equations (1) may be viewed as Lagrange's equations of the following variational principle

$$\begin{aligned}W = \iint dx_1\,dx_2\,\{&-p^*(1)K(12)p(2) - \tfrac{1}{2}f(1)L(12)f(2)\\ &+ p^{0*}(1)K(12)p(2) + p^*(1)K(12)p^0(2) + f^0(1)L(12)f(2)\}\\ &+ \iiiint dx_1\,dx_2\,dx_3\,dx_4\,K^*(12)p^*(2)K(13)p(3)L(14)f(4),\\ &\delta W = 0,\end{aligned} \tag{2}$$

where p, p^* and f are connected with ψ, ψ^* and φ by the following equations

$$\begin{aligned}\psi(1) &= \int K(12)p(2)\,dx_2, \qquad \psi^*(1) = \int K^*(12)p^*(2)\,dx_2,\\ \varphi(1) &= \int L(12)f(2)\,dx_2\end{aligned} \tag{3}$$

under the condition that $K^*(12) = K(21)$ and $L(12) = L(21)$. This condition is not always satisfied in physical applications (various kinds of Green-functions). However, the physically most important cases of antihermiticity — $K^*(12) = K(21)$ and $-L(12) = L(21)$ may be dealt with analogously. The variational principle (2) is invariant under rotations in space time if K and L are invariant functions of their arguments. This is a demand which must be imposed on any physical theory. (2), however, is not invariant under translations because of the appearance of p^0 and f^0. These given functions have the meaning of boundary conditions and such conditions cannot of course be invariant under translations unless $p = \text{const.}$ and $f = \text{const.}$ The special choice $p = f = 0$ corresponds to the very important case of closed

systems. One has then to deal with the homogeneous integral equations corresponding to (1). Thus for bound states an energy-momentum and an angular momentum tensor may be derived from (2), for scattering problems, however, only an angular momentum tensor. We shall look, therefore, for other variational formulations which permit the derivation of both tensors in both cases. In the next section we shall come back to the formulation (2) and to the problem of bound states.

In this section we shall deal with that possibility of defining tensor densities which consists in a transition to differential equations. This transition is always possible if there exist differential operators $K^{-1}(-\Box)$, $L^{-1}(-\Box)$ for which the following equations are satisfied

$$K^{-1}(-\Box)\,K(x) = \delta(x), \qquad K^{*-1}(-\Box)\,K^{*}(x) = \delta(x),$$
$$L^{-1}(-\Box)\,L(x) = \delta(x). \tag{4}$$

To satisfy the demands of invariance under rotations and translations, $K(12)$ and $L(12)$ must be functions of the distance $(x^1_\mu - x^2_\mu)^2$ only. For the same reason K^{-1} and L^{-1} are functions of d'Alembert's operator

$$\Box = \partial_\mu \partial_\mu = \frac{\partial^2}{\partial x^2} + \frac{\partial^2}{\partial y^2} + \frac{\partial^2}{\partial z^2} - \frac{\partial^2}{\partial t^2}.$$

Operating with (4) on equations (1) one gets immediately

$$K^{-1}(-\Box)\,(\psi - \psi^0) = g\varphi\psi, \qquad L^{-1}(-\Box)\,(\varphi - \varphi^0) = g\psi^*\psi. \tag{5}$$

The third equation is complex conjugate to the first one. The meaning of (4) becomes apparent if Fourier transforms $K(k^2)$ and $L(k^2)$ of $K(x)$ and $L(x)$ exist. In this case (4) may be written in momentum space:

$$K^{-1}(k^2)\,K(k^2) = 1, \qquad L^{-1}(k^2)\,L(k^2) = 1. \tag{6}$$

In all physical applications the functions ψ^0 and φ^0 describing boundary conditions are chosen in such a way as to satisfy the unperturbed equations

$$K^{-1}(-\Box)\psi^0 = L^{-1}(-\Box)\varphi^0 = 0. \tag{7}$$

In this case (5) takes the simpler form

$$K^{-1}(-\Box)\psi = g\varphi\psi, \qquad L^{-1}(-\Box)\varphi = g\psi^*\psi. \tag{8}$$

Solutions of (1) with the special choice (7) for ψ^0 and φ^0 satisfy (8) and the solutions of (8) have always the form (1), where ψ^0 and φ^0 are general solutions of (7).

In all practical cases, so far, the operators $K^{-1}(\alpha)$, $L^{-1}(\alpha)$ regarded as functions of a complex variable α have no singular points for finite α. If so, a Taylor expansion is possible and we may write

$$K^{-1}(-\Box) = \sum_{n=0}^{\infty} \varkappa_n \Box^n,$$

$$L^{-1}(-\Box) = \sum_{n=o}^{\infty} \lambda_n \Box^n . \tag{9}$$

For equations of finite order these expansions are of course finite. Equations (8) become

$$\sum \varkappa_n \Box^n \psi = g \varphi \psi, \qquad \sum \lambda_n \Box^n \varphi = g \psi^* \psi. \tag{10}$$

They are Lagrange's equations of the following variational principle

$$\delta W = 0, \qquad W = \int_{\sigma_1}^{\sigma_2} L \, dx,$$

$$L = \sum_{n=o}^{\infty} (-1)^n \left\{ \frac{\lambda_n}{2} \varphi^2_{\nu_1 \ldots \nu_n} + \varkappa_n \psi^*_{\nu_1 \ldots \nu_n} \psi_{\nu_1 \ldots \nu_n} \right\} - g \varphi \psi^* \psi \tag{11}$$

with the assumption that K^{-1} is a real function, which is always satisfied in physical applications. In (11) the notation

$$f_{\nu_1 \ldots \nu_n} = \frac{\partial^n f}{\partial x_{\nu_1} \partial x_{\nu_2} \partial x_{\nu_n}}$$

is used. The integration is extended over a region of space time between two space-like surfaces σ_1 and σ_2. The Lagrangian (11) is invariant both under translations and rotations of space-time and, therefore, the construction of an energy-momentum and angular momentum tensor is possible.

The calculation of these tensors for equations of arbitrary order may be found in the papers by de Wet (1948) and Green (1948), so that we quote here only the results:

$$T_{\mu\nu} = \delta_{\mu\nu} L + \sum_{n=o}^{\infty} \sum_{m=o}^{\infty} (-1)^n \left[\lambda_{m+n+1} \varphi_{\nu a_1 \ldots a_n} \Box^m \varphi_{\mu a_1 \ldots a_n} \right.$$
$$\left. + \varkappa_{m+n+1} (\psi_{\nu a_1 \ldots a_n} \Box^m \psi^*_{\mu a_1 \ldots a_n} + \psi^*_{\nu a_1 \ldots a_n} \Box^m \psi_{\mu a_1 \ldots a_n}) \right]. \tag{12}$$

This tensor satisfies the conservation law $\delta_\mu T_{\mu\nu} = 0$ *if* ψ and φ are solutions of equations (8) and therefore also if they are solutions of the integral equations (1). To construct the angular momentum tensor, the symmetrical tensor

$$T'_{\mu\nu} = T_{\mu\nu} - \delta_\lambda f_{\lambda\mu\nu} \tag{13}$$

must be used, and we have

$$M_{\lambda\mu\nu} = T'_{\lambda\mu} x_\nu - T'_{\lambda\nu} x_\mu , \qquad \delta_\lambda M_{\lambda\mu\nu} = 0. \tag{14}$$

The additional term in (13) has no influence on the integral quantity

$$P_\nu(\sigma) = \int_\sigma d\sigma_\mu T_{\mu\nu} \tag{15}$$

since $f_{\lambda\mu\nu} = -f_{\mu\lambda\nu}$ and, therefore, $\partial_\mu \partial_\lambda f_{\lambda\mu\nu} = 0$.

The definition of current density and its conservation law follows immediately from the invariance of the variational principle under gauge transformations of the first kind. The result is

$$j_\mu = ie \sum_{n=0}^{\infty} \sum_{m=0}^{\infty} (-1)^n \varkappa_{m+n+1} \left(\psi_{\nu_1 \ldots \nu_n} \Box^m \psi^*_{\mu\nu_1 \ldots \nu_n} - \psi^*_{\nu_1 \ldots \nu_n} \Box^m \psi_{\mu\nu_1 \ldots \nu_n}\right),$$

$$\delta_\mu j_\mu = 0. \tag{16}$$

The formulae for j_μ, $T_{\mu\nu}$, $M_{\lambda\mu\nu}$ and $f_{\lambda\mu\nu}$ for the case of arbitrary Lagrangians are given in Appendix I.

The preceding calculations show that it is possible to construct expressions for the current, energy-momentum, and angular momentum in non-local field theories in which the fields satisfy equations of the form (1). These tensors satisfy differential conservation laws. Required is only the knowledge of the expansion coefficients $\varkappa_n$ and λ_n of the kernels $K(x)$ and $L(x)$.

It may be noted that the conventional theory with Klein-Gordon differential operators is obtained from (1) by putting

$$K^{-1}(k^2) = -k^2 - \varkappa^2, \qquad L^{-1}(k^2) = -k^2 - \lambda^2. \tag{17}$$

In this case the quantities j_μ, $T_{\mu\nu}$, $M_{\lambda\mu\nu}$ and $f_{\lambda\mu\nu}$ go over into those of the conventional theory, as must be required in accordance with the general correspondence principle.

The above definition of j_μ, $T_{\mu\nu}$, $M_{\lambda\mu\nu}$ and $f_{\lambda\mu\nu}$ has the disadvantage of containing series (in general infinite) of differential operators. It seems that a form appropriate for integral equations should contain integral operators. To what extent this is possible we shall investigate in the next section.

Another disadvantage of this formulation is the indefinitness of the total energy (for the definition of total energy see formula (32)). It gives rise to difficulties in the corresponding quantum theory. However, it seems that by means of the modern quantization techniques it will become possible to avoid these difficulties. For methods of constructing the S-matrix for non-local fieldtheories, we refer to the papers by Rzewuski (1951), Rayski (1951) and Møller (1952).

2. Integral conservation laws

To obtain integral conservation laws one has to start with a variational principle containing integral operators. We have seen that the principle (2) containing only integral operators is of no use, at least for scattering problems, because of its lack of invariance under translations. To get invariance one has to remove the functions p^0 and f^0 or ψ^0 and φ^0 from the theory. This may be done under the assumption that equations (7) have solutions different from zero which are expressible in form of Fourier integrals. In this case $K^{-1}(k^2)$ and $L^{-1}(k^2)$ have each at least one zero $k^2 = -\varkappa^2$ or $k^2 = -\lambda^2$ respectively. From the physical point of view this condition is necessary to obtain propagation character of the solutions. We may write now

$$K^{-1}(k^2) = -P^{-2}(k^2)\,(k^2 + \varkappa^2), \qquad L^{-1}(k^2) = -F^{-2}(k^2)\,(k^2 + \lambda^2). \quad (18)$$

Here squared functions are taken for conveniency, which has no other bearing upon the theory than that it allows square roots as form factors. Now, we assume that the functions ψ^0 and φ^0 are those particular solutions of (7) which satisfy the equations

$$(\Box - \varkappa^2)\psi^0 = (\Box - \lambda^2)\varphi^0 = 0. \quad (19)$$

We could, of course, take also more general solutions of (7), but this would increase the order of the differential operators introduced into the variational principle, which is against our purpose. The operators (19) will help to remove ψ^0 and φ^0 from the integral equations (1) by changing them into integro-differential equations. For this purpose it is convenient to introduce new fields by means of the equations

$$\psi(1) = \int P(12)\,\Psi(2)\,dx_2, \qquad \varphi(1) = \int F(12)\,\Phi(2)\,dx_2. \quad (20)$$

On the other hand it follows from (18) that

$$K(12) = \iint P(13)\,G_\varkappa(34)\,P(42)\,dx_3\,dx_4,$$

$$L(12) = \iint F(13)\,G_\lambda(34)\,F(42)\,dx_3\,dx_4, \quad (21)$$

with

$$G_\varkappa(x) = \frac{1}{(2\pi)^4}\int \frac{e^{ik_\mu x_\mu}}{-k^2 - \varkappa^2}\,dk.$$

By means of Fourier transforms we may now replace the equations for ψ and φ by equations for Ψ and Φ:

$$\Psi(1) = \Psi^0(1) + g\iint G_\varkappa(12)\,P(23)\,\psi(3)\,\varphi(3)\,dx_2\,dx_3,$$

$$\Phi(1) = \Phi^0(1) + g\iint G_\lambda(12)\,F(23)\,\psi^*(3)\,\psi(3)\,dx_2\,dx_3, \quad (22)$$

the only assumption being that $P(k^2)$ and $F(k^2)$ have no zeros for finite k^2. Due to (19), equations (20) take in Fourier space the form

$$\Psi^0(k) = \psi^0(k)\,\delta(k^2 + \varkappa^2)\,P^{-1}(k^2), \qquad \Phi^0(k) = \varphi^0(k)\,\delta(k^2 + \lambda^2)\,F^{-1}(k^2). \quad (23)$$

This shows that Ψ^0 and Φ^0 satisfy the same equations (19) as ψ^0 and φ^0. To prevent the trivial zero solution, one has to assume

$$P^{-1}(-\varkappa^2) \neq 0, \qquad F^{-1}(-\lambda^2) \neq 0. \quad (24)$$

Operating on both sides of (22) with the operators (19) and noticing that

$$(\Box - \varkappa^2)\,G_\varkappa(x) = (\Box - \lambda^2)\,G_\lambda(x) = \delta(x), \quad (25)$$

one gets

$$(\Box - \varkappa^2)\,\Psi(1) = g\int P(12)\,\varphi(2)\,\psi(2)\,dx_2, \quad (26)$$

$$(\Box - \lambda^2)\, \Phi(1) = g \int F(12)\, \psi^*(2)\, \psi(2)\, dx_2. \tag{26'}$$

These integro-differential equations correspond to the following variational principle

$$\delta W = 0, \tag{27}$$

$$W = \int dx \left\{ \Psi^*_\nu \Psi_\nu + \varkappa^2 \Psi^* \Psi + \frac{1}{2} \Phi^2_\nu + \frac{\lambda^2}{2} \Phi^2 + g \varphi \psi^* \psi \right\}.$$

It is convenient to replace (27) by a more general principle in which the domain of integration is contained between two arbitrary space-like surfaces σ_1 and σ_2, namely

$$\delta W = 0, \qquad W = \int_{\sigma_1}^{\sigma_2} \mathcal{L}^0(x)\, dx + g \iiint_{\sigma_1}^{\sigma_2} \mathcal{L}'(x\, x'\, x''\, x''')\, dx\, dx'\, dx''\, dx''',$$

$$\mathcal{L}^0 = \Psi^*_\nu \Psi_\nu + \varkappa^2 \Psi^* \Psi + \frac{1}{2} \Phi^2_\nu + \frac{\lambda^2}{2} \Phi^2, \tag{28}$$

$$\mathcal{L}'(x\, x'\, x''\, x''') = F(x - x')\, \Phi(x')\, P(x - x'')\, \Psi^*(x'')\, P(x - x''')\, \Psi(x''').$$

(26) and (27) correspond to that formulation of non-local field theory which was proposed by Rayski (1951). The Lagrange equations corresponding to (28) have the same form as (26) but with finite limits of integration. It may be noted that the transition from (26) to the integral equations (1) on the one hand and to the differential equations (8) on the other is simple only for infinite limits of integration.

The formulation (28) needs some explanations since it implies that wave functions are spread over a finite region of space-time only

$$\psi(1) = \int_{\sigma_1}^{\sigma_2} P(12)\, \Psi(2)\, dx_2, \qquad \varphi(1) = \int_{\sigma_1}^{\sigma_2} F(12)\, \Phi(2)\, dx_2, \tag{29}$$

$P(x)$ and $F(x)$ are for relativistic reasons functions of the invariant square x^2_μ. They must be chosen small for large x^2_μ to contain the old theory with a $\delta(x)$-function as a limiting case. It was shown by McManus (1948) that in the cases in which the Fourier transforms $P(k^2)$ and $F(k^2)$ of $P(x)$ and $F(x)$ are functions of $|k^2|$ only, it is even possible to define functions which are small for large x_μ. In any case, (29) implies that contributions from outside the region between the surfaces σ_1 and σ_2 are neglected. This indicates that these surfaces have not a merely mathematical meaning; they are surfaces on which something physical happens which prevents the influence of the outside of the integration domain on the inside. This physical event may be identified with an experiment fixing the initial values on σ_1 and measuring the final values on σ_2. The assumption that σ_1 and σ_2 are surfaces distinguished by physical conditions will become important in the discussion of the energy-momentum tensor.

The variational principle (28) is invariant both under translations and rotations and, therefore, energy-momentum and angular momentum may be defined

satisfying integral conservation laws. The derivation is carried out in a similar way as for the variational principles containing single integrals (see Appendix II). The tensor densities in question have the form (II, 9, 12)

$$T_{\nu\mu} = T^0_{\nu\mu} + \delta_{\nu\mu}\bar{\mathcal{L}}', \qquad M_{\lambda\nu\mu} = T_{\nu\lambda}x_\mu - T_{\lambda\mu}x_\nu,$$

$$\bar{\mathcal{L}}'(x) = g\iiint dx'dx''dx''' \{F(x-x')\Phi(x')P(x-x'')\Psi^*(x'')P(x-x''')\Psi(x''')$$
$$+ F(x'-x)\Phi(x)P(x'-x'')\Psi^*(x'')P(x'-x''') \qquad (30)$$
$$+ F(x''-x')\Phi(x')P(x''-x)\Psi^*(x)P(x''-x''')\Psi(x''')$$
$$+ F(x'''-x')\Phi(x')P(x'''-x'')\Psi^*(x'')P(x'''-x)\Psi(x)\},$$

where $T^0_{\nu\mu}$ denotes the unperturbed part (corresponding to the unperturbed Lagrangian) which has the same form for local and non-local interactions. $\bar{\mathcal{L}}'$ is that part of the energy momentum which is due to the interaction between the fields. For further discussion we shall rewrite it making use of the Lagrange equations (26) (with finite integration limits, cf. also II,3)

$$\bar{\mathcal{L}}' = g\varphi\psi^*\psi \pm \Phi(\Box - \lambda^2)\Phi \pm \Psi^*(\Box - \varkappa^2)\Psi \mp \Psi(\Box - \varkappa^2)\Psi^*. \qquad (31)$$

The minus sign corresponds to antisymmetrical P or F. For kernels which do not have the property of symmetry or antisymmetry somewhat more general considerations are necessary.

Defining the integral quantities

$$P_\nu(\sigma) = \int_\sigma d\sigma_\mu T_{\mu\nu}, \qquad M_{\nu\mu}(\sigma) = \int_\sigma d\sigma_\lambda M_{\lambda\nu\mu}, \qquad (32)$$

we may write the conservation laws (II,12) as follows

$$P_\nu(\sigma_1) = P_\nu(\sigma_2), \qquad M_{\nu\mu}(\sigma_1) = M_{\nu\mu}(\sigma_2). \qquad (33)$$

From these integral conservation laws one cannot go over to differential laws since the surfaces σ_1 and σ_2 cannot be chosen arbitrarily close together. Indeed, the surfaces σ_1 and σ_2 were distinguished by experiments carried out on the system. If, however, we introduce form-factors into the theory, which is equivalent with the introduction of an elementary length, it becomes in principle impossible to carry out experiments arbitrarily close together in space-time.

The quantities (31) have the disadvantage of not satisfying the correspondence principle. Indeed, in the limiting case $\varphi \to \Phi$, $\psi \to \Psi$ (29) goes over into $4g\,\Phi\Psi^*\Psi$, whereas in the corresponding local theory the interaction part is $g\Phi\Psi^*\Psi$. We hope to come back to this question in a forthcoming publication.*

*) Note added in proof: In the meantime differential conservation laws have been constructed by the author (Il Nuovo Cimento X, 182, 1953) corresponding to any variational principle (27) containing multiple integrals. These differential conservation laws satisfy automatically the correspondence principle and they are consistent with the integral conservation laws derived in this paper.

The current density derivable from the invariance of (27) with respect to gauge transformations of the first kind has the same form (in φ, ψ, ψ^*) as in the corresponding local theory (in Φ, Ψ, Ψ^*) and satisfies therefore the correspondence principle. This is due to the fact that the interaction term does not contain derivatives of the fields. The conservation law for this current has, of course, also an integral character.

Now we go back to the Lagrangian (2) and to the question of bound states. For closed systems we have $p^0 = f^0 = 0$ and the principle (2) becomes invariant under translations. Since it contains no derivatives of the fields, no current vector may be defined from the invariance under gauge transformations of the first kind. The invariance under translations and rotations yields in the same way as before (it is to be noticed that the unperturbed part contains also multiple integrals) the simple result

$$\mathcal{L} = \int_{\sigma_1}^{\sigma_2} dx' \left\{ -p^*(x) K(xx') p(x') - p^*(x') K(x'x) p(x) - \frac{1}{2} f(x) L(xx') f(x') - \frac{1}{2} f(x') L(x'x) f(x) \right\}$$

$$+ g \iiint_{\sigma_1}^{\sigma_2} dx' dx'' dx''' \{ K^*(xx') p^*(x') K(xx'') L(xx''') f(x''')$$

$$+ K^*(x'x) p^*(x) K(x'x'') p(x'') L(x'x''') f(x''')$$

$$+ K^*(x'x'') p^*(x'') K(x'x) p(x) L(x'x''') f(x''')$$

$$+ K^*(x'x'') p^*(x'') K(x'x''') p(x''') p(x''') L(x'x) f(x) \} = g \psi^* \psi \varphi, \tag{34}$$

$$T_{\mu\nu} = \delta_{\mu\nu} \mathcal{L}, \qquad P_\mu(\sigma) = \int_\sigma d\sigma_\nu T_{\nu\mu}, \qquad P_\mu(\sigma_1) = P_\mu(\sigma_2),$$

$$M_{\lambda\mu\nu} = T_{\lambda\mu} x_\nu - T_{\lambda\nu} x_\mu, \qquad M_{\mu\nu}(\sigma) = \int_\sigma d\sigma_\lambda M_{\lambda\mu\nu}, \qquad M_{\mu\nu}(\sigma) = M_{\mu\nu}(\sigma)_2.$$

Here the demand of correspondence with the local theory is automatically satisfied. This is evident if one replaces K by $G_\varkappa$ and L by G_λ.

Finally, we may remark that if the functions K^{-1} and L^{-1} have more zeros than one, there are more possibilities to define different tensor densities satisfying conservation laws. Indeed, instead of (19) we could take functions ψ^0 and φ^0 being general solutions of

$$\prod_i (\Box - \varkappa_i^2) \psi^0 = \prod_i (\Box - \lambda_i^2) \varphi^0 = 0, \tag{35}$$

where the products are over some of the zeros. In this case the annihilation of ψ^0 and φ^0 in the field equations requires the introduction of higher order derivatives. The corresponding calculations are simply a compilation of the methods described

in Appendices I and II. Thus we get a whole set of different tensor densities. On the one side we have tensor densities containing only integral operators, on the other only differential operators. We emphasize that only the last densities satisfy differential conservation laws. The rest of the whole set satisfies integral conservation laws. It is clear that the number of possibilities depends on the assumptions concerning ψ^0 and φ^0. For $\psi^0 = \varphi^0 = 0$ we have the greatest number of possibilities; for ψ^0 and φ^0 being general solutions of (7) there is exactly one possibility left, namely the tensor densities (16), (12) and (14).

Appendix I

Derivation of conservation laws for Lagrangians containing derivatives of arbitrary order (Ostrogradski 1850, de Wet 1948, Green 1948).

We give here some of the general formulae of which particular cases were discussed in the first section. If a given variational principle

$$\delta W = 0, \qquad W = \int_{\sigma_1}^{\sigma_2} \mathcal{L}\,[q^a(x),\ q^a_{\nu_1}(x),\ q^a_{\nu_1\nu_2}(x), \ldots]\, dx \tag{I,1}$$

containing derivatives $q^a_{\nu_1 \ldots \nu_n}$ of the fields q^a of arbitrary order is invariant with respect to gauge transformations of the first kind $\delta q^a_{\nu_1 \ldots \nu_n} = -ie\eta^a\, d\lambda\ q^a_{\nu_1 \ldots \nu_n}$ and translations and rotations of space time $\delta x_\nu = \varepsilon_\nu - \varepsilon_{\nu\mu} x_\mu$, then it is possible to define three tensor densities

$$j_\mu = -ie\eta^a \sum_{n=o}^{\infty} p^a_{\mu\nu_1 \ldots \nu_n}\ q^a_{\nu_1 \ldots \nu_n},$$

$$T_{\mu\nu} = \mathcal{L}\delta_{\mu\nu} - \sum_{n=o}^{\infty} p^a_{\mu\beta_1 \ldots \beta_n}\, q^a_{\nu\beta_1 \ldots \beta_n} - \partial_\lambda f_{\lambda\mu\nu}, \tag{I,2}$$

$$M_{\lambda\mu\nu} = T_{\lambda\mu} x_\nu - T_{\lambda\nu} x_\mu,$$

which satisfy the differential conservation laws

$$\partial_\mu j_\mu = \partial_\mu T_{\mu\nu} = \partial_\lambda M_{\lambda\mu\nu} = 0. \tag{I,3}$$

Here

$$p^a_{\nu_1 \ldots \nu_n} = \sum_{m=o}^{\infty} (-1)^m \frac{\partial^m}{\partial x_{\mu_1} \ldots \partial x_{\mu_m}} \frac{\delta \mathcal{L}}{\partial q_{\nu_1 \ldots \nu_n \mu_1 \ldots \mu_m}} \tag{I,4}$$

$\eta^a = 0, \pm 1$ according to whether q^a is a neutral field or one of the two complex conjugate fields, and

$$f_{\lambda\mu\nu} = -f_{\mu\lambda\nu} = \sum_{n=o}^{\infty} \Big\{ p^a_{\lambda\nu_1 \ldots \nu_n} S^{\alpha\beta}_{\mu\nu\nu_1 \ldots \nu_n \mu_1 \ldots \mu_n} + p^a_{\nu\nu_1 \ldots \nu_n} S^{\alpha\beta}_{\mu\lambda\nu_1 \ldots \nu_n \mu_1 \ldots \mu_n} + p^a_{\mu\nu_1 \ldots \nu_n} S^{\alpha\beta}_{\nu\lambda\nu_1 \ldots \nu_n \mu_1 \ldots \mu_n} \Big\} q^\beta_{\mu_1 \ldots \mu_n} \tag{I,5}$$

the meaning of $S^{\alpha\beta}_{\mu\nu\nu_1 \ldots \nu_n \mu_1 \ldots \mu_n}$ being analogous to that in (II,7).

Appendix II

The derivation of energy momentum and angular momentum from a variational principle defined by (28) is carried out by an extension of the usual methods (cf. e.g. Pauli 1942 or Schwinger 1951) to multiple integrals:

$$\delta W_{12} = 0, \qquad W_{12} = \sum W^n_{12} ;$$

$$W^n_{12} = \int_{\sigma_1}^{\sigma_2} \!\!\cdots\!\! \int dx^1 \ldots dx^n \, \mathcal{L}^n \left[q^a(x^1) \ldots q^a(x^n) \, , \, q^a_\nu(x^1) \ldots q^a_\nu(x^n) \right]. \tag{II,1}$$

The change in W^n_{12} introduced by an infinitesimal variation $\delta_0 q^a(x^i)$ of the fields $q^a(x^i)$ and by an infinitesimal translation and rotation δx_ν is

$$\delta W^n_{12} = \int_{\sigma_1}^{\sigma_2} \!\!\cdots\!\! \int dx^1 \ldots dx^n \sum_{m=1}^{n} \left\{ \frac{\partial \mathcal{L}^n}{\partial q^a(x^m)} \, \delta_0 q^a(x^m) + \right.$$

$$\left. + \frac{\partial \mathcal{L}^n}{\partial q^a_\nu(x^m)} \, \delta_0 q^a_\nu(x^m) + \frac{\partial \mathcal{L}^n}{\partial x^m_\nu} \, \delta x^m_\nu \right\}. \tag{II,2}$$

Changing the variable x^m into x we get

$$\delta W^n_{12} = \int_{\sigma_1}^{\sigma_2} \!\!\cdots\!\! \int dx dx^1 dx^{n-1} \left\{ \frac{\partial \sum_{m=1}^{n} \mathcal{L}^n_{x^m = x}}{\partial q^a(x)} \delta_0 q^a(x) \right.$$

$$\left. + \frac{\partial \sum_{m=1}^{n} \mathcal{L}^n_{x^m = x}}{\partial q^a_\nu(x)} \delta_0 q^a_\nu(x) + \frac{\partial \sum_{m=1}^{n} \mathcal{L}^n_{x^m = x}}{\partial x_\nu} \delta x^m_\nu \right\}, \tag{II 2'}$$

where $x^1 \ldots x^{n-1}$ denote the remaining set of the $n-1$ points of space-time. Denoting further

$$\int_{\sigma_1}^{\sigma_2} \!\!\cdots\!\! \int dx^1 \ldots dx^{n-1} \sum_{m=1}^{n} \mathcal{L}^n_{x^m = x} = \bar{\mathcal{L}}^n(x) \quad \text{and} \quad \sum_n \bar{\mathcal{L}}^n = \mathcal{L}, \tag{II,3}$$

we obtain

$$\delta W_{12} = \int_{\sigma_1}^{\sigma_2} dx \left\{ \frac{\partial \mathcal{L}}{\partial q^a(x)} - \frac{\partial}{\partial x_\nu} \frac{\partial \mathcal{L}}{\partial q^a_\nu(x)} \right\} \delta_0 q^a(x)$$

$$+ \left(\int_{\sigma_2} - \int_{\sigma_1} \right) d\sigma_\nu \left\{ \frac{\partial \mathcal{L}}{\partial q^a_\nu(x)} \, \delta^0 q^a(x) + \mathcal{L} \delta x_\nu \right\} \tag{II,4}$$

From (II,1) and (II,4) we get the Lagrange equations

$$\frac{\partial \mathcal{L}}{\partial q^a(x)} - \frac{\partial}{\partial x_\nu} \frac{\partial \mathcal{L}}{\partial q^a_\nu(x)} = 0 \tag{II,5}$$

and the generator of infinitesimal transformations on σ

$$F(\sigma) = \int_\sigma d\sigma_\nu \left[\frac{\partial \mathcal{L}}{\partial q^a_\nu(x)} \, \delta_0 q^a(x) + \mathcal{L} \delta x_\nu \right]. \tag{II,6}$$

Since the total change in q^α is

$$\delta q^\alpha = \delta_0 q^\alpha + q^\alpha_\mu \, \delta x_\mu + \partial_\mu \, \delta x_\mu \, S^{\alpha\beta}_{\mu\nu} \, q^\beta \tag{II,7}$$

$F(\sigma)$ becomes

$$F(\sigma) = \int_\varrho d\sigma_\nu \left[\frac{\partial \mathcal{L}}{\partial q^\alpha_\nu(x)} \, \delta q^\alpha(x) + T_{\nu\mu} \, \delta x_\mu \right] \tag{II,8}$$

with

$$T_{\nu\mu} = \delta_{\nu\mu} \mathcal{L} - \frac{\partial \mathcal{L}}{\partial q^\alpha_\nu(x)} \, q^\alpha_\mu(x) - \delta_\lambda f_{\lambda\nu\mu} \tag{II,9}$$

and

$$f_{\mu\lambda\nu} = -f_{\lambda\mu\nu} = \left[\frac{\partial \mathcal{L}}{\partial q^\alpha_\mu(x)} \, S^{\alpha\beta}_{\lambda\nu} + \frac{\partial \mathcal{L}}{\partial q^\alpha_\nu(x)} \, S^{\alpha\beta}_{\lambda\mu} + \frac{\partial \mathcal{L}}{\partial q^\alpha_\lambda(x)} \, S^{\alpha\beta}_{\nu\mu} \right] q^\beta(x). \tag{II,10}$$

Since δx_μ describes translations and rotations:

$$\delta x_\mu = e_\mu - e_{\mu\nu} \, x_\nu, \tag{II,11}$$

the conservation laws implied by the invariance of (II,1) with respect to the transformations (II,11) take the form

$$\begin{aligned} &P_\nu(\sigma_1) = P_\nu(\sigma_2), && M_{\nu\mu}(\sigma_1) = M_{\nu\mu}(\sigma_2), \\ &P_\nu(\sigma) = \int_\sigma d\delta_\mu \, T_{\mu\nu}, && M_{\nu\mu}(\sigma) = \int_\sigma d\sigma_\lambda \, M_{\lambda\nu\mu}, \\ &&& M_{\lambda\nu\mu} = T_{\lambda\nu} \, x_\mu - T_{\lambda\mu} \, x_\nu . \end{aligned} \tag{II,12}$$

For applications it is important to note that

$$\partial_\nu \, T_{\nu\mu} = \left(\frac{\partial \mathcal{L}}{\partial x_\mu} \right)_{expl.} \tag{II,13}$$

where $\left(\frac{\partial \mathcal{L}}{\partial x_\mu} \right)_{expl.}$ means differentiation with respect to x_μ appearing explicitly in $\mathcal{L}$.

REFERENCES

Green H. S., *Proc. Roy. Soc.*, **197**, 73 (1948).
McManus H., *Proc. Roy. Soc.*, **195**, 323 (1948).
Møller Ch., *Kgl. Dansk. Vidensk.* (1952) (to be published).
Ostrogradski M., *Mem. Acad. St. Petersbourg*, **6**, 385 (1850).
Pauli W., *Rev. Mod. Phys.*, **13**, 203 (1942).
Rayski J., *Acta. Phys. Polonica*, **11**, 25 (1951).
Rzewuski J., *Acta Phys. Polonica*, **11**, 9 (1952).
Schwinger J., *Phys. Rev.*, **82**, 914 (1951).
de Wet J. S., *Proc. Roy. Soc.*, **195**, 365 (1948); *Proc. Camb. Phil. Soc.* **44**, 546 (1948).
Yukawa H., *Phys. Rev.*, **77**, 219 (1950).

КРАТКОЕ СОДЕРЖАНИЕ

Я. Ржевуский, *Законы сохранения в теории нелокализуемых полей.*

Целью настоящей работы является исследование возможности удовлетворения законов сохранения в теории нелокализуемых полей.

SUR LES SPECTRES RAMANIENS DES SOLUTIONS DE PYRIDINE ET D'ACIDE ACÉTIQUE I

Par Roman Mierzecki

Institut de Physique Expérimentale de l'Université de Varsovie

(Manuscrit reçu le 5 juin 1952)

Dans les recherches présentées on a étudié les spectres ramaniens de la pyridine, de l'acide acétique et des solutions de ces deux substances contenant 61,0; 48,3; 41,4; 30,4 et 22,3% de pyridine par mole. On a constaté des faibles déplacements de fréquences des raies de la pyridine et de l'acide acétique dans les solutions. En outre on a mis en évidence deux raies nouvelles de fréquences $\Delta\nu = 881$ cm^{-1} et $\Delta\nu = 1005$ cm^{-1} n'apparaissant pas dans les substances pures.

On sait, que les fréquences ramaniennes provenant des oscillations respectives des atomes dans la molécule peuvent être modifiées sous l'influence des autres molécules. Les liaisons intermoléculaires dans les solutions des deux liquides donnant des molécules associées, exercent une certaine influence sur les oscillations des atomes. Ce fait se retrouve aussi dans les modifications des spectres ramaniens. Il serait intéressant d'étudier cette influence dans les solution donnant des mélanges azéotropiques.

De ce point de vue Whitting et Martin (1931) ont comparé les spectres ramaniens de la pyridine et de l'acide acétique avec le spectre d'une solution contenant 2 moles de pyridine pour 3 moles d'acide. Cette composition forme d'après Zawidzki (1900) une solution azéotropique (azéotrope négatif).

Ils ont observé un changement de fréquences des raies de la pyridine et de l'acide acétique de l'ordre de 10 cm^{-1}, mais n'ont trouvé aucune raie nouvelle. Toute fois la précision de leur mesures parait n'être pas suffisante pour le problème étudié. La pyridine utilisée pour les études présentes a été purifiée par distillation fractionnée à l'aide d'une colonne d'un mètre de hauteur[1]. De la même manière on a obtenu une solution de pyridine et d'acide acétique contenant 41,4% de pyridine par mole. A l'aide de ces deux liquides et de l'acide acétique glacial on a préparé des solutions de compositions mentionnées au début. L'eau, qui pouvait se trouver dans les solutions ou provenir de l'humidité des vases, a été éliminée en distillant quelques centimètres cubes de la solution des cuvettes ramaniennes. Comme la pyridine forme avec l'eau un azéotrope positif on peut

[1] Les distillations étaient éxécutées dans l'Institut de Chimie Physique de l'Université de Varsovie.

considérer la déhydratation comme suffisante. Pendant cette opération les gaz dissous étaient eliminés également. On a fermé les cuvettes par la fusion de leurs extrémités. Avant de fermer les tubes des cuvettes on a prélevé quelques centimètres cubes du mélange à titre d'échantillon. Pour déterminer sa composition l'acide acétique a été titré par 0,1 n NaOH en présence de phenolphtaléine comme indicateur.

Les spectres ramaniens étaient observés a l'aide d'un spectrographe à deux prismes de verre. Le spectrographe (production de la firme Huet) a une dispersion de 17 Å par millimètre de la plaque vers 4358 Å. Le spectre était excité par la raie $\lambda = 4358$ Å de mercure provenant d'une lampe de type S. 500 (PRK 2). La partie plus réfrangible du spectre de la lampe était arrêtée par un filtre composé de solution saturée de nitrite de sodium.

La courbe de dispersion a été obtenue à l'aide d'un microphotomètre enregistreur de Moll. Les courbes d'enregistrement des spectres ont permis au moyen de la courbe de dispersion de déterminer les fréquences des raies ramaniennes. Les valeurs obtenues de cette façon sont juste à 0,3 cm^{-1} prés. Les résultats des mesures sont réunis dans le tableau 1, où les raies sont indiquées par les mêmes lettres que sur la figure 1. Cette figure montre les spectres des substances pures, d'une solution contenant 41,4% de pyridine, et le spectre du benzène.

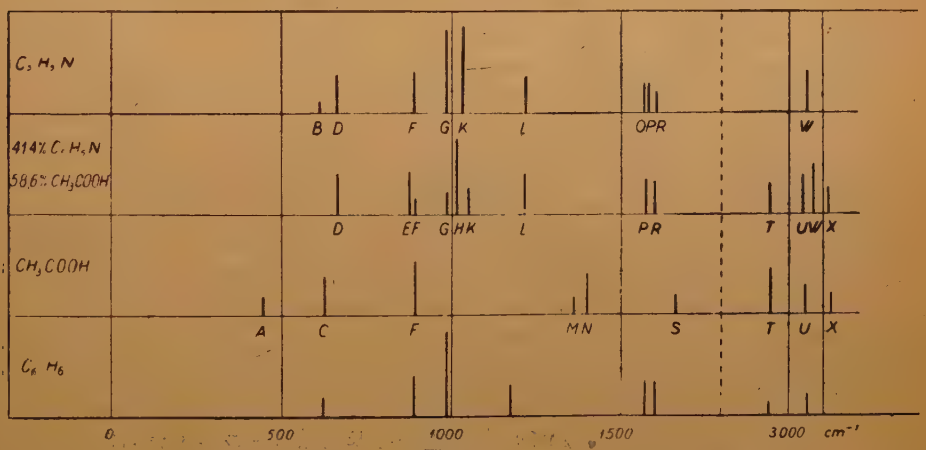

Fig. 1

Comme on le voit dans la figure 1, les raies les plus intenses dans le spectre de la pyridine sont les raies indiquées par les lettres G et K de fréquences $\Delta \nu = 990{,}5$ cm^{-1} et $\Delta \nu = 1030{,}7$ cm^{-1}. Le microphotogramme de ces deux raies est représenté dans la figure 2a. D'aprés Kline et Turkevich (1944) ces raies proviennent des oscillations symétriques de valence du noyau pyridique 1 et 12 de la classe A_1. La raie, dont l'intensité est la plus grande dans la solution, est une raie nouvelle H ($\Delta \nu = 1005$ cm^{-1}), qui n'existe pas dans les spectres des substances pures. Elle est située, comme le montrent les microphotogrammes suivants (fig. 2b, c, d), entre les deux raies de la pyridine mentionnées ci-dessus. Les microphotogrammes sont ceux des spectres des solutions contenant 61,0 (fig. 2b), 41,4

(fig. 2c), et 22,3 (fig. 2d)% de pyridine par mole. On voit alors, que même dans la solution contenant 61% de pyridine la raie nouvelle H est plus intense, que les raies de la pyridine pure G et K. Dans la solution contenant 41,4% de pyridine les raies G et K sont très peu intenses, tandis que l'intensité de la raie H est très grande. L'irrégularité de la courbe photométrique au point J (fig. 2d) semble indiquer la présence d'encore une raie nouvelle de fréquence voisine de 1020 cm^{-1} dans les solutions plus diluées avec de l'acide acétique. Comme l'indiquent les résultats des mesures des fréquences réunis dans le tableau 1 toutes les trois raies sont deplacées dans les solutions. Quand on diminue la quantité de pyridine jusqu'au voisinage de 40%, leur fréquences augmentent d'une façon appréciable; dans les solutions contenant 40—30% de pyridine les fréquences sont indépendantes de la concentration; dans les solutions plus diluées on observe un léger abaissement de fréquences.

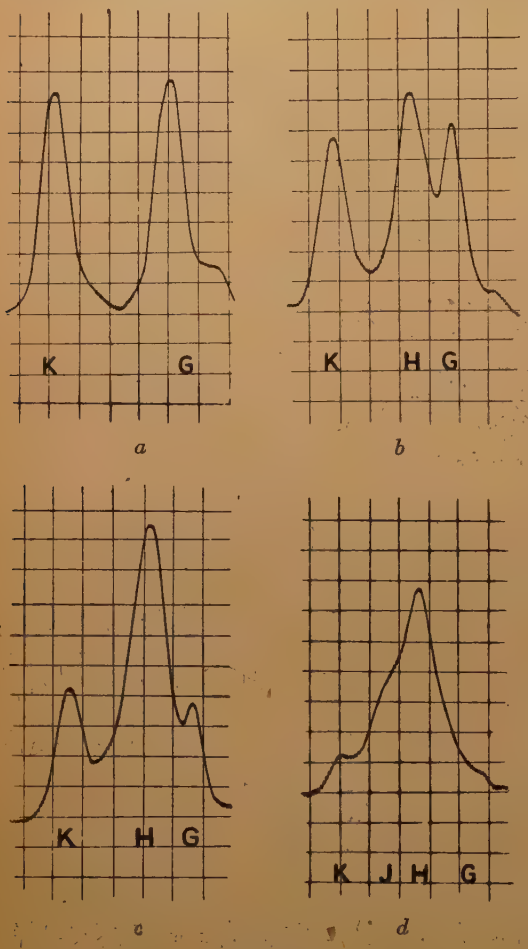

Fig. 2

Si l'on compare les résultats des mesures des fréquences des autres raies de différantes concentrations (tableau 1) on constate les déplacements des raies suivants:

La fréquence de la raie d'une intensité moindre $\Delta\nu = 650{,}9$ cm^{-1} provenant des oscillations symétriques de déformation du noyau 4 de la classe B_2 change très peu. Le changement le plus grand de fréquence peut être observé dans la solution contenant 41,4% de pyridine. L'intensité de la raie de la pyridine de fréquence $\Delta\nu = 602{,}3$ cm^{-1} provenant des oscillations antisymétrique de valence du noyau 6 de la classe B_1 diminue rapidement et la raie devient diffuse dans les spectres des solutions.

La fréquence de la raie de la pyridine $\Delta\nu = 1217{,}6$ cm^{-1} provenant des oscillations de déformation des liaison C—H est diminuée dans les solutions.

Au lieu de deux raies diffuses de la pyridine de fréquences $\Delta\nu = 1569{,}5$ et $\Delta\nu = 1574{,}7$ cm^{-1}, provenant des oscillations du noyau 8a de la classe B_1 et 8b de la classe A_1, on observe une raie, dont la fréquence augmente plus vite

dans les solutions plus concentrées et reste presque invariable dans les solutions contenant moins que 40% de pyridine.

La fréquence de la raie $\Delta\nu = 1594{,}4\ \mathrm{cm}^{-1}$, qui est une raie de combinaison des fréquences 990 et 602 cm^{-1}, est abaissée dans les solutions, mais augmente à mesure que la quantité de pyridine est diminuée. La fréquence de la raie de la pyridine $\Delta\nu = 3056{,}4\ \mathrm{cm}^{-1}$ provenant des oscillations de valence des liaisons C—H 3 de la classes A_1 augmente rapidement dans les mêmes conditions.

En comparant le spectre de l'acide acétique pure et de ses solutions dans la pyridine on constate, que la fréquence de la raie $\Delta\nu = 2943{,}5\ \mathrm{cm}^{-1}$ provenant probablement des oscillations de valence des liaisons C—H en dimères d'acide diminue dans les solutions à mesure qu'on dilue l'acide avec de la pyridine. La fréquence de la raie $\Delta\nu = 3126{,}3\ \mathrm{cm}^{-1}$ provenant d'aprés Kohlrausch (1943, p. 256) des oscillations des liaisons O—H en dimères d'acide passe par un maximum dans la solution contenant 41,4% de pyridine.

Les raies $\Delta\nu = 889{,}0\ \mathrm{cm}^{-1}$ de la pyridine et $\Delta\nu = 893{,}0\ \mathrm{cm}^{-1}$ de l'acide acétique sont difficiles à distinguer dans les spectres des solutions et forment une bande commune, dans laquelle on remarque toute fois deux maxima d'inégale intensité; la fréquence du maximum plus faible est intermédiaire entre les fréquences des raies mentionnées ci-dessus. La différence des deux maxima ci-dit est voisine de 10 cm^{-1}. Il semble que le maximum plus élevé indique la présence d'une raie nouvelle. Les autres raies de l'acide acétique dans les spectres des solutions possèdent une intensité tellement faible, qu'elles ne sont pas décelables.

L'explication de la présence des raies nouvelles ainsi que les variations des fréquences doit être cherchée dans l'action intermoléculaire entre les molécules de la pyridine et de l'acide acétique. Cette action semble être la plus forte dans la solution contenant 41,4% de pyridine. Grâce au caractère alcalin de la pyridine et caractère acide de l'acide acétique des liaisons facilement dissociables peuvent se former entre les molécules de ces substances.

Des modifications analogues mais moins marquées étaient observées par Hatem, Valladas-Dubois et Volkinger (1949) dans les spectres ramaniens des solutions de pyridine et d'éthanol. Malgré que l'éthanol n'a pas de caractère acide les investigateurs français suggérent, qu'il y a dans les solutions une liaison intermoléculaire.

Une raie de fréquence $\Delta\nu = 1005\ \mathrm{cm}^{-1}$ a été trouvée dernièrement aussi par Ham, Rees et Walsh (1952) dans les spectres infrarouges de la solution saturée d'iode dans la pyridine.

L'abaissement de fréquence de la raie de la pyridine provenant des oscillations des liaisons C—H est difficile à expliquer. Il est possible, que grâce aux liaisons intermoléculaires l'influence de l'azote du noyau devient plus faible. C'est ainsi, que dans la façon de se comporter dans les solutions le noyau de la pyridine se rapproche au noyau du benzène. On arrive aux mêmes suppositions en comparant les spectres de la pyridine, des solutions et du benzène (fig. 1). Certaines régions des spectres des solutions ressemblent plus au spectre du benzène que de la pyridine pure. Au lieu de deux raies de pyridine $\Delta\nu = 990{,}5$ et $\Delta\nu = 1030{,}7\ \mathrm{cm}^{-1}$ on

observe dans le benzène une raie $\Delta\nu = 992\ cm^{-1}$ correspondant à la nouvelle raie dans les solutions. Dans la région de $1600\ cm^{-1}$ on observe dans les spectres des solutions ainsi que dans le spectre du benzène deux raies à la place de trois dans le spectre de la pyridine.

Résultats:

En comparant les spectres ramaniens de la pyridine, de l'acide acétique et des solutions de ces deux substances on doit constater que:

1. Les raies de la pyridine $\Delta\nu = 650{,}9;\ 990{,}5;\ 1030{,}7;\ 3056{,}4\ cm^{-1}$ ont dans les solutions des fréquences augmentées. Pour certaines raies l'augmentation passe par un maximum dans la solution de concentration voisine de 40% de pyridine par mole.

2. La fréquence des raies de la pyridine $\Delta\nu = 1217{,}6$ et $1594{,}4\ cm^{-1}$ est diminuée dans les solutions.

3. La fréquence de la raie de l'acide acétique $\Delta\nu = 2943{,}5\ cm^{-1}$ est diminuée dans les solutions et des raies $\Delta\nu = 3046.9$ et $3126{,}3\ cm^{-1}$ est augmentée.

4. On a observé dans les solutions deux raies nouvelles de fréquence $\Delta\nu = 881$ et $1005\ cm^{-1}$.

Actuellement dans des recherches en cours sont étudiées les intensités des raies. Les mêmes études seront faites avec les solutions des picolines et lutidines dans l'acide acétique.

Je tiens à exprimer à MM. les Professeurs St. Pieńkowski et W. Świętosławski mes remerciements les plus sincères pour les conseils qu'ils m'ont prodigués et l'intérêt qu'ils ont porté à mon travail.

BIBLIOGRAPHIE

Ham N. S., Rees A. L. et Walsh A., *Nature*, Lond., **169**, 110 (1952).

Hatem S., Valladas-Dubois S. et Volkinger H., *C. R. Acad. Sci.*, Paris, **228**, 182 (1949).

Kline et Turkevich, *J. Chem. Phys.*, **12**. 300 (1944).

Kohlrausch, *Ramanspektren*, Leipzig, 1943.

Whitting R. E., Martin W. H., *Trans. Roy. Soc. Can. III*, **25**, 87 (1931).

Zawidzki J., *Z. Phys. Chem.*, **35** 129 (1900).

КРАТКОЕ СОДЕРЖАНИЕ

Роман Межецкий, *Исследование спектров комбинационного рассеяния смеси: пиридин — уксусная кислота.*

Исследовано спектр комбинационного рассеяния смеси пиридина и уксусной кислоты пяти различных составов и проведено сравнение со спектрами чистых веществ. Установлено, что в спектрах смесей выступает наряду с линиями чистых веществ, новая острая линия с частотой $\Delta\nu = 1005\ см^{-1}$. С ростом количества кислоты в смесях интенсивность этой линии увеличивается, а затем уменьшается. Вероятно, выступают линии с частотой около $\Delta\nu = 890\ см^{-1}$, а при большем содержании кислоты, также линии с частотой около $\Delta\nu = 1020\ см^{-1}$. Спектры смесей имеют больше сходства со спектром бензола, чем со спектром чистого пиридина. Установлено также изменение частоты наблюдаемых линий пиридина, смесей и уксусной кислоты в зависимости от состава смеси.

Tableau 1

Raies	1 100% C_5H_5N 0% CH_3COOH	2 61,0% C_5H_5N 39,0% CH_3COOH	3 48,3% C_5H_5N 51,7% CH_3COOH	4 41,4% C_5H_5N 58,6% CH_3COOH	5 30,4% C_5H_5N 69,6% CH_3COOH	6 22,3% C_5H_5N 77,7% CH_3COOH	7 0% C_5H_5N 100% CH_3COOH
A	—	—	—	—	—	—	444,3
B	602,3	—	—	—	—	—	—
C	—	—	—	—	—	—	620,8
D	650,9	650,9	651,1	651,4	650,9	649,9	—
E	—	879,8	880,9	881,6	881,8	883,8	—
F	889,0	889,3	?	891,7	892,0	893,0	893,0
G	990,5	990,8	991,9	992,0	992,2	991,0	—
H	—	1005,0	1005.8	1006,4	1007,5	1007,3	—
J	—	—	—	—	1021,0	1019,9	—
K	1030,7	1031,8	1033,9	1034,1	1034,8	1034,3	—
L	1217,6	1214,7	1214,3	1214,3	1214,0	1212,0	—
M	—	—	—	—	—	—	1363,6
N	—	—	—	—	—	—	1403,5
O	1569,5	—	—	—	—	—	—
P	1574,3	1571,0	1571,7	1572,8	1572,8	1573,2	—
R	1594,4	1592,2	1592,7	1593,8	1594,0	1593,6	—
S	—	—	—	—	—	—	1665,6
T	—	2938,2	2938,5	2939,2	2940,2	2940,8	2943,5
U	—	3049,5	3048,3	3048 2	3047,5	3047,8	3048,9
W	3056,4	3062,8	3070,4	3070,6	3072,7	3075,1	—
X	—	3126,1	3127,1	3127,1	3126,2	3126,5	3126,3

ON THE SPECTRAL DISTRIBUTION OF INTERNAL BREMSSTRAHLUNG EMITTED BY ^{32}P AND ^{90}Y

By B. Makiej

Institute of Experimental Physics, Jagellonian University, Kraków*

(received June 25, 1952)

Absorption curves of weak γ-radiation emitted by ^{32}P and ^{90}Y and absorbed in lead were taken with the help of a scintillation counter acting as a detector of high efficiency. The absorption curves obtained on experimental data were analysed and compared with absorption curves calculated on the basis of spectral distribution of internal Bremsstrahlung according to Knipp's and Uhlenbeck's theory. The results of experiments and calculation lead to the following conclusions: (1) the spectral distribution of internal Bremsstrahlung of ^{32}P calculated on theoretical grounds agrees with experimental results, (2) in the case of ^{90}Y a spectrum of hard γ-radiation of about 1,5 MeV energy and about 5 photons per 10000 β-transitions intensity is superimposed on the internal Bremsstrahlung spectrum.

1. Introduction

If a nucleus is in an energetically excited state owing to a β-radioactive transformation, then, while the nucleus passes to the ground state, either a monoenergetic γ-photon emission takes place, or an electron is emitted from any of the K, L, M... shells as an internal conversion electron. If the β-transition leads to the ground state no γ-radiation with a linear spectrum takes place and the detection becomes possible of a weak γ-radiation with a continuous spectrum. This radiation was first observed by Aston (1927) during measurements of RaE radiation. The theory of this observed weak radiation was independently elaborated by Knipp and Uhlenbeck (1936) and by Bloch (1936). They proved on the basis of quantum mechanics that the radiation with a continuous spectrum appears as a result of a sudden change of the charge of the nucleus caused by the formation of a β-particle and its subsequent leaving the nucleus. This radiation was called the internal Bremsstrahlung (IB) in contrast to the external Bremsstrahlung, or X-rays, appearing as a result of acceleration of the electron in the Coulomb field of the nucleus during the absorption of electrons in matter. Knipp-Uhlenbeck's and Bloch's theory concerns the allowed transitions of the radioactive nucleus and interaction of the polar vector type. Chang and Falkoff (1949) ex-

* The experimental part of this work was executed in the Physical Laboratory of Birmingham University (Gt. Britain).

tended the theory to cover forbidden transitions as well as other types of relativistically invariant interactions.

One of the recent experimental papers is that by Wu (1941) concerning the investigation of the whole range of the IB spectrum. Wu, with the help of an ionization chamber, measured absorption curves of the radiation emitted by a ^{32}P source, surrounded by targets absorbing the β-particles. An analysis of the absorption curves and measurements of the ratio of the ionization caused by X-rays (appearing during the absorption of β-particles in the target) and the ionization caused by β-particles, permitted to calculate the number of photons per β-particle and the IB mean energy per β-particle. Wu's experiments do not, however, answer the question whether the IB spectral distribution agrees with the spectral distribution to be expected on theoretical grounds; for, because of the employed geometry of the measurements, the IB intensity was only a fraction of the X-ray intensity.

The present paper, therefore, deals with the problem of examining the shape of the IB spectral distribution by comparing the IB absorption curves in lead with absorption curves calculated on the basis of the theoretical spectral distribution of ^{32}P and ^{90}Y IB. These isotopes were formerly considered to be pure β-emitters (Dzhelepov and Petrovic 1950). The problem could be solved thanks to the use of a more suitable geometry of the measurements, which caused the X-ray intensity to be only a fraction of the IB intensity. Besides, the high efficiency of the scintillation counter used as a detector facilitated fairly exact measurements in spite of the use of sources of comparatively low activity of order of 1 mC.

2. Theory

The β-transformation process may be considered to have two stages: (1) the passage from the initial to an intermediate state consisting of the formation and emission of a β-particle and a neutrino, and (2) the passage of the electron from the intermediate to the final state with a simultaneous emission of a γ-quantum. Classically the mechanism of the production of the radiation may be represented as follows: an electron produced during a β-transition is suddenly emitted from the nucleus and the subsequent change of the dipole moment causes the emission of electromagnetic radiation. In quantum mechanics this means that there exists a certain probability of a γ-quantum emission together with the emission of a β-particle. According to Knipp and Uhlenbeck the probability of the created electron of energy W_e (in mc^2 units) radiating a γ-quantum of energy k, is represented by the function

$$\Phi(W_e, k) = \frac{\alpha p}{\pi p_e k}\left[\frac{W_e^2 + W^2}{W_e p} \ln (W + p) - 2\right] \qquad (1)$$

where W is the energy of the electron after emitting the quantum, p_e is the electron

momentum before the emission, p — after the emission, $\alpha = \frac{e^2}{\hbar c}$ — the fine-structure constant. The IB spectrum $S(k)$ for the whole energy distribution of β-particles is obtained by multiplying the function $\Phi(W_e, k)$ by the probability $P(W_e)\,dW_e$ of the formation of an electron possessing initial energy in the $W_e + dW_e$ interval and integrating over the whole range of variability of W_e. Thus we get

$$S(k) = \int_{1+k}^{W_0} \Phi(W_e, k)\, P(W_e)\, dW_e, \tag{2}$$

where W_0 is the maximum energy of the β-spectrum. The function $P(W_e)$ is supplied by the theory of β-transformations or by experiment. If to calculate $S(k)$ we take the spectral distribution of the β-particles found by experiment, we eliminate any ambiguity inherent in the theory of β-transformations. Chang's and Falkoff's calculations led to the conclusion that also for other types of interaction and for forbidden transitions the shape of the IB spectrum differs only slightly from the same shape for allowed transitions, so that we cannot expect to be able to discern various degrees of interdiction on the basis of measurements of the spectrum shape. Hence a practical conclusion: the relatively simple equation (2) may also be employed for comparing theory with experiment for forbidden transitions.

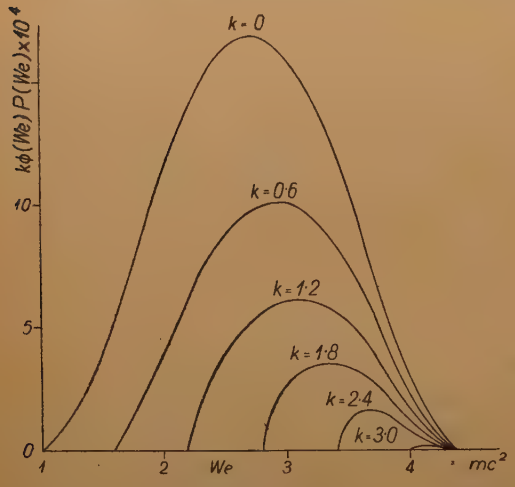

Fig. 1. Values of $k\Phi(W_e)P(W_e)$ for various energies of the photon, as a function of the energy of the ^{32}P β-particles

The energy spectrum of β-particles from Siegbahn's measurements (1944) was employed to calculate the ^{32}P IB spectrum distribution. Fig 1. shows the curves of the dependence of $k\Phi(W_e)P(W_e)$ on W_e for several values of the photon energy. On the basis of this diagram it is obvious that electrons responsible for emitting a quantum of a definite energy k possess various energies, but to every k there corresponds a certain energy W_e of the electrons at which the function $k\Phi(W_e)P(W_e)$ attains its maximum; the values of W_e corresponding to this maximum are higher for higher energies of the photon. After integrating, according to equation (2), for various values of k, we obtain the spectrum distribution of the ^{32}P IB intensity, as plotted on Fig. 2, where for comparison the diagram of the function according to Wu (1941) is also shown. Wu used in her calculations the

momentum distribution of the ^{32}P β-particles given by Lyman (1937). The IB energy per one β-particle is given by the surface enclosed by the axes of coordinates and the curve $kS(k)$. The calculated value of this energy for ^{32}P amounts in our case to $0{,}0025\ mc^2 = 1{,}28$ keV, which is in accordance with the value $0{,}0024\ mc^2$ calculated by Madansky and Rasetti (1951).

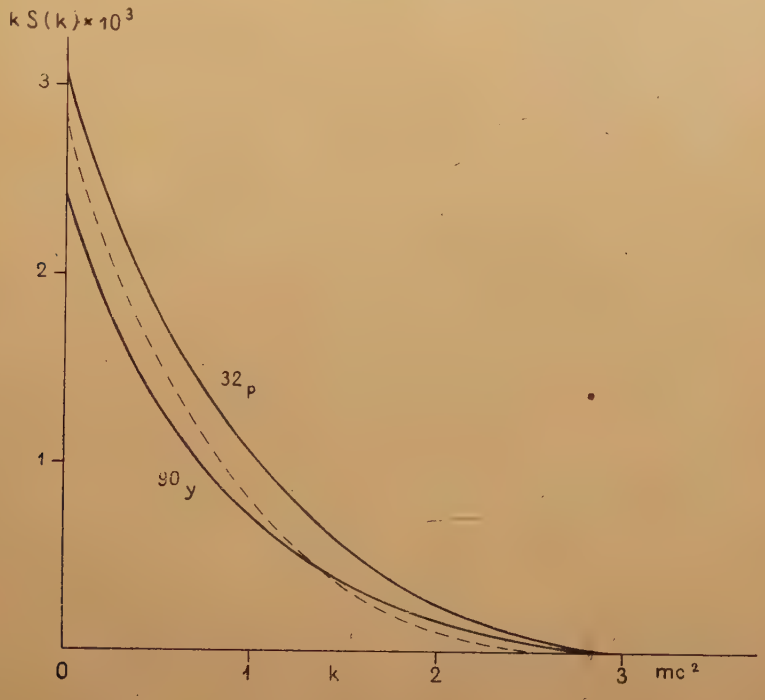

Fig. 2. Distribution of the ^{32}P and ^{90}Y IB spectrum expected on theoretical grounds. Dashed line IB spectrum distribution of ^{32}P according to Wu (1941)

The number of IB photons $L(k)$ of energy higher than k per one β-particle may be calculated from the function $kS(k)$ according to the equation

$$L(k) = \int_{k}^{W_0 - 1} S(k)\, dk \qquad (3)$$

In the case of ^{32}P only about 3,4 photons are emitted on an average per 1000 β-particles. In view of this, the difficulties encountered during measurements of so weak radiation are obvious.

As in the case of ^{32}P, the ^{90}Y IB spectral distribution was calculated from equations (1) and (2); the β-particle spectral distribution was reconstructed by calculation on the basis of Langer's and Price's paper (1949) in which Fermi's diagram for the forbidden transition $^{90}Y \rightarrow {}^{90}Zr$, i.e. the diagram of the function

$\left(\frac{P(p_e)}{\sigma p_e^2 F_B}\right)^{1/2}$, is shown to be a straight line cutting the axis of abscissae at a point corresponding to the maximum energy $W_0 = (2{,}180 \pm 0{,}007)$ Mev. In the above expression $\sigma = W^2 - 1 + (W_0 - W)^2$ is a factor characterizing the forbidden transition, and F_B is Fermi's function with Coulomb interaction, calculated on the basis of Bethe's and Bacher's approximation (1936). The linear form of Fermi's diagram proves that the Bethe-Bacher approximation yields a fairly good representation of the shape of the ^{90}Y β-particle spectrum, provided the factor σ characterizing the forbidden transition is also taken into account. On the basis of Konopinski's and Uhlenbeck's theory of β-transitions (1948) the introduction of the factor σ is justified for a transition with a spin change of 2 and a simultaneous change of parity; probably these changes take place during a ^{90}Y β-transition (Langer and Price 1949).

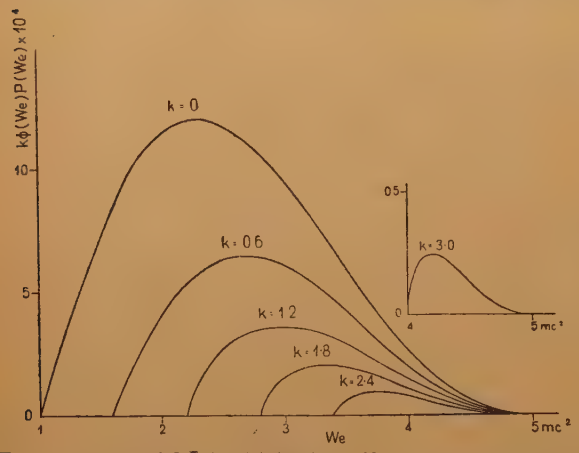

Fig. 3. Values of $k\Phi(W_e)P(W_e)$ of ^{90}Y for several values of the photon energy as function of the ^{90}Y β-particle energy

A plot of the function $k\Phi(W_e)P(W_e)$ of ^{90}Y for several values of the photon energy is shown in Fig. 3. After integrating this function with respect to W_e one obtains the spectrum of ^{90}Y IB intensity represented in Fig. 2. The total IB energy per one β-particle is in this case smaller than in the case of ^{32}P and ammounts to 0,0018 mc^2.

3. Apparatus

In the radiation detected, besides IB, X-rays formed during the absorption of β-particles were also present. The geometry of the measurements was chosen so that the ratio of intensities of X-rays and of the total photon radiation was as small as possible. For this purpose the absorber of β-particles was placed almost in the center of the distance source — detector. In Wu's experiments the β-particle absorber in the form of an aluminium plate was placed directly next to the source and the ratio of intensities of X-rays and of IB ammounted to about 4 : 1. In the present work the value of the ratio was lowered to about 1 : 10 in the case of ^{32}P and to about 1 : 2 in the case of ^{90}Y. This was possible thanks to a more suitable geometry of the measurements and thanks to the use of paraffin-wax as a β-particle absorber possessing a low effective atomic number.

A schematic diagram of the apparatus for measuring absorption curves of photon radiation is shown in Fig. 4. S is the radiodactive source. A scintillation counter with a phosphor adhering to the window of the photomultiplier F acts as a detector. The photomultiplier is placed in a light-tight brass screen B with a window of aluminium foil and protected with a 4 cm thick lead shield L having a cylindrical opening against the window of the photomultiplier. The wall of the lead shield facing the source is covered with a layer of wood W in order to weaken the X-ray background. The layer of wood has an opening for inserting absorbers. This opening is covered with a block of paraffin-wax of sufficient thickness to absorb completely the β-particles. As detector a scintillation counter was used with a natural crystal of calcium tungstate of about 0,8 cm^3 volume, with an 11-stage photomultiplier EMI type 5031 of 25 μ A/lumen sensitivity, possessing a multiplication factor of $2{,}5 \times 10^7$ at a potential difference of 160 V per each stage.

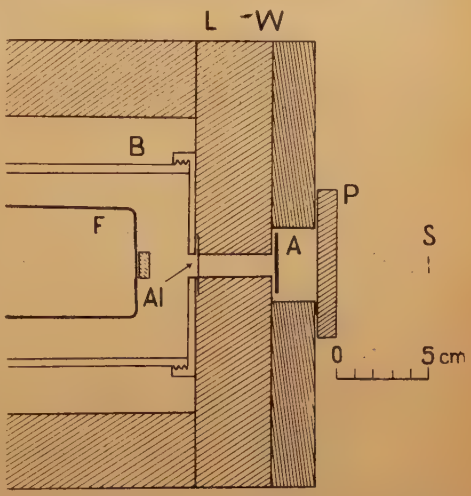

Fig. 4. Apparatus for measuring absorption curves of photon radiation

The diagram of the whole scintillation counting system is shown in Fig. 5. The electric impulse on the collector of the photomultiplier F, appearing as a result of a scintillation in the phosphor, is transmitted to the grid of the valve of the cathode follower K. The impulse passes next to the single-stage amplifier A and after passing through the discriminator D, which cutts off all small impulses, it is registered in the scaler S. The shape and duration of the impulses may be observed on the screen of the oscilloscope M.

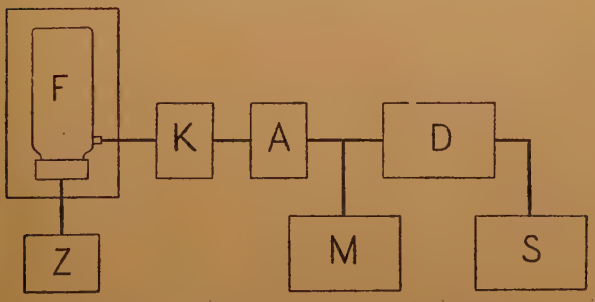

Fig. 5. Block diagram of the counting system for the electric impulses of the scintillation counter. Z-high voltage generator. K - cathode follower, A - amplifier, M - oscilloscope, D - discriminator, S - scaler

A circuit diagram of the scintillation counting system consisting of the initial stage, the amplifier and the discriminator is shown in Fig. 6. The accelerating voltages on the dynodes of the photomultiplier are collected from terminals of a potentiometer. The collecting plate C is conected directly with the grid of the cathode follower. The time constant of the element on the input of the cathode follower is fitted to the decay time of the luminescence of the calcium tungstate

and it ammounts to about 0,2μsec. The negative bias voltage on the grid of the first valve of the discriminator determines the hight of the impulses passing through the discriminator. Standard impulses, lasting about 30 μsec, which leave

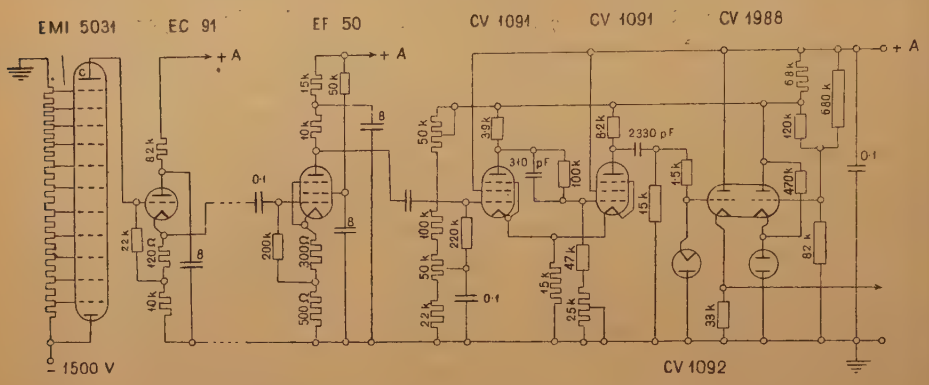

Fig. 6. Circuit diagram of the initial stage, amplifier and discriminator

the discriminator are counted subsequently with the help of a scaler 1 : 100 "Cintel" type UC2A produced by "Cinema Television LTD".

4. Measurements with ^{32}P

The radioactive source was prepared by evaporating of about 0,8 ml of a solution of phosphoric acid containing ^{32}P ($T = 14{,}3$ d, $W_0 = 1{,}71$ MeV) on a thin aluminium foil (2,3 mg/cm^2). The radioactive substance was covered with a very thin film of "Zapon" varnish formerly dissolved in amyl acetate to prevent any loss of the substance. As was later calculated from measurements by means of a Geiger-Müller counter for β-particles, the initial intensity of the source amounted to about 2,7 mC.

The main source of information about the IB spectrum distribution consists in our case in the measurements of absorption of this radiation in lead.

A series of measurements was started and finished by measuring the counter background; the bias voltage of the discriminator was kept constant during the whole time of measuring. Small fluctuations of the counter background during daytime (usually not over 5%) were due to temperature changes and changes in intensity of the X-ray and γ-ray background due to radioactive sources employed in researches in neighbouring rooms. In the detected radiation besides the IB there also appeared X-rays due to the absorption of β-particles in the paraffin-wax block, in air, and in the substance of the source. Separate auxiliary measurement. were undertaken to determine the percentage of the total radiation due to X-rayss As the source ^{32}P was thin, most of the β-particle absorption took place in the paraffin-wax plate covering the openings in the shield of the counter. In the first place, therefore the correctness of the analysis of the absorption curve depends

on an exact calculation of the correction δ_{par} due to the detection of X-rays formed in the paraffin plate. The ratio of the intensities of X-rays formed by β-particle absorption in paraffin and in aluminium was calculated with the help of measurements in which the paraffin or aluminium absorbers were placed directly next to the source. On the basis of the value of this ratio $N_{Al}/N_{par} = (2{,}95 \pm 0{,}05)$ and of measurements of the increase of the detected radiation intensity when instead of the paraffin plate placed in its usual position (Fig. 4) an aluminium plate absorbing β-particles has been inserted, the correction $\delta_{par} = (8{,}0 \pm 2{,}0)\,\%$ was calculated. The correction for X-rays formed by β-particle absorption in the aluminium foil on which the radioactive phosphorus was placed, in the layer of varnish covering the source, and in the air around the source, was calculated from measurements; the calculation was based on the experimental law of linear increase of X-radiation intensity with the increase of surface density of layers absorbing β-particles (Wu, 1941), provided the layers were sufficiently thin. The value of the correction for X-radiation in the source itself amounts to $\delta_s = (1{,}2 \pm 0{,}2)\%$, counting, as above, in proportion to the total detected radiation (without the *Pb* absorbers). Calculation of X-radiation appearing in the air surrounding the source in the solid angle of detection leads to the value of the correction $\delta_a = (1{,}3 \pm 0{,}5)\%$. Thus the total correction for X-radiation amounts to $\delta = (10{,}5 \pm 2{,}1)\%$.

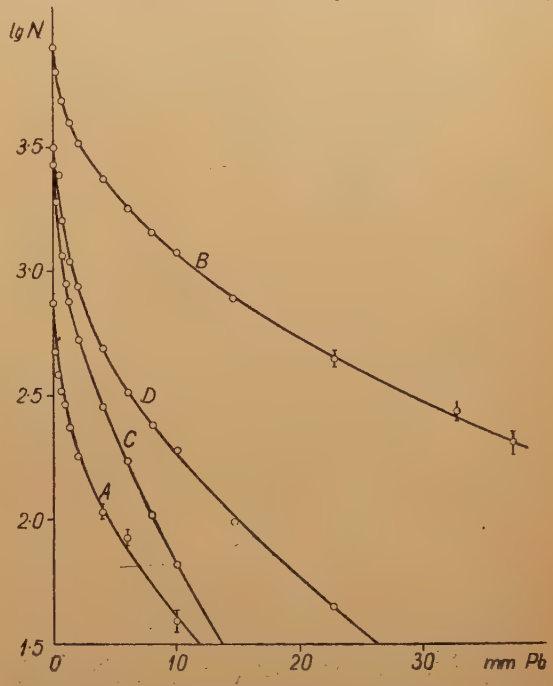

Fig. 7. Photon radiation absorption curves. On the axis of ordinates lg N is plotted, where N is a figure proportional to the counting rate. A — ^{32}P IB + some X-rays, C — X-radiation from the Cu target + some ^{32}P IB, B — ^{90}Y IB + some X-rays, D — X-radiation from the Cu target + some ^{90}Y IB

To obtain the pure IB absorption curve from the mixed absorption curve A on Fig. 7, a correction curve in the shape of an absorption curve of X-rays produced in an 0,8 mm copper target adhering to the source (Fig. 7, curve C) was substracted from the absorption curve found directly by measurements. This procedure seems perfectly correct, because in the first place the shape of the X-ray spectrum is approximately independent of the material of the target, and secondly the radiation leaving the copper target contains only about 13% of IB, hence the absorption curve of this radiation represents with a sufficiently good

approximation the shape of the X-ray absorption curve and therefore the shape of the correction curve.

5. Measurements with ^{90}Y

As a radioactive source containing ^{90}Y ($T = 60{,}5$ hrs, $W_0 = 2{,}18$ MeV) a sample of Y_2O_3 (from Johnson-Matthey, London) was used, irradiated with neutrons in the BEPO in Harwell (Gt. Britain) during 7 days. For measurements of photon radiation absorption a source of surface density of about 50 mg/cm^2 was used. The photon radiation absorption curve was determined in the same geometry as in the case of measurements with a ^{32}P source. Additional measurements of photon radiation with a screening of the counter with 9 cm of lead and the source - detector distance of 20,5 cm were undertaken with the purpose of verifying the correctness of the geometry of the measurements and of determining more exactly the shape of the end of the absorption curve. The shape of the absorption curve obtained on the basis of these additional measurements was the same as the shape of the curve obtained on the basis of the main measurements. This proves that the geometry employed was correct. The photon radiation absorption curve measured with the source ^{90}Y is plotted in Fig. 7. A comparison of the curves B and A leads to the conclusion that in the radiation due to ^{90}Y a much harder component appears than in the case of the radiation due to ^{32}P. To obtain the absorption curve of pure γ-radiation of ^{90}Y a correction curve in the shape of an absorption curve of X-rays formed by the absorption of the ^{90}Y β-particles in the copper target is substracted. The number of X-photons amounts in this case to about 34% of the total number of photons hitting the detector, with a lead absorber of zero thickness. This number is the sum of X-photons formed in the air in the vicinity of the source amounting to 1%, of X-photons formed in the paraffin-wax plate absorbing β-particles amounting to 6% and of photons formed in the source itself amounting to about 27%. The percentage of X-photons formed in the air and in the paraffin plate was measured in the same way as in the case of ^{32}P. The percentage of X-photons formed in the source was calculated from the surplus of X-photons after combining two sources of equal thickness to make one source of double thickness.

6. Discussion

Experimental results may be compared with theory by a graphic analysis of the experimental absorption curve into several monoenergetic components and by calculating the total IB energy per one β-particle. This method was used by Wu (1941) and Storruste (1951). The advantage of this method is in its simplicity; but its drawback is that it does not show whether the shape of the spectral distribution curve theoretically calculated is in agreement with the experimental results. This important observation was obtained in our experiments by calculating the ^{32}P and ^{90}Y IB absorption curves expected on a theoretical basis and comparing them with pure IB absorption curves found by experiments. As the efficiency of

the scintillation counter used drops suddenly for photons of an energy lower than 0,1 MeV (as was proved by experiment with the help of the lines 0,136 MeV (^{186}Re) and 0,081 MeV (^{166}Ho)), during the calculation of the absorption curve only the IB spectrum range of photon energy above 0,08 MeV was considered. Further, the simplifying assumption was made that the counting efficiency is constant in the photon energy range considered (see Fig. 2). Auxiliary measurements of γ-ray absorption coefficients of the employed absorbers were performed for the following γ-lines 1,2 MeV (^{60}Co); 0,48 MeV (^{181}Hf); 0,41 MeV (^{198}Au); 0,33 MeV (^{111}Ag)[1] and the Evans and Evans (1948) absorption coefficient curve was corrected on the basis of data obtained for the given geometry. This corrected absorption coefficient curve was used for the calculation of IB absorption curves.

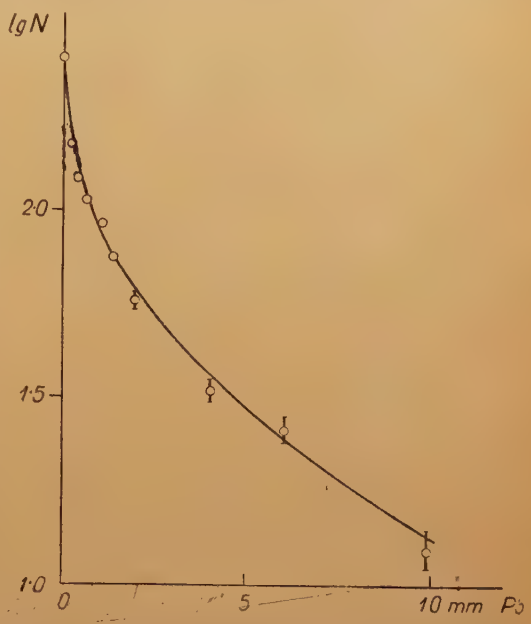

Fig. 8. ^{32}P IB absorption curve in lead. The continuous line is plotted on the basis of calculations according to Knipp's and Uhlenbeck's theory

The continuous line on Fig. 8 represents the theoretical ^{32}P IB absorption curve in lead. Points marked with circles represent experimental values obtained from the described analysis of direct experimental results, after taking into account the measured corrections for IB absorption in the paraffin-wax filter for the β-particles. Theoretical values were multiplied by a normalizing factor which was chosen so that the point corresponding to an absorber of 2 mm of lead on the theoretical curve should fall on the experimental curve. As may be seen from Fig. 8 the experimental values fall within the limits of experimental errors on the theoretical curve (the probable errors are indicated on the diagram as small vertical lines), and therefore, the ^{32}P IB spectrum distribution calculated on the basis of Knipp's and Uhlenbeck's theory may be considered as being in agreement with experiment. Madansky and Rasetti (1951) came to the similar conclusion on the basis of measurements of the ^{32}P IB spectrum in the range of 0,03 MeV — 0,3 MeV.

By comparing the number of IB photons per one β-particle found by experiment with the value following from theory, we may calculate the mean IB photon counting efficiency. In our arrangement this efficiency amounted to about 30% — in agreement with the measured value for the γ-line 0,411 MeV (^{198}Au).

[1] A. Storruste (1950).

The theoretical absorption curve and the absorption curve obtained from measurements are represented on Fig. 9. The shapes of both these curves are quite different. This indicates that a much higher percentage of hard radiation photons is present than would be expected theoretically. Two possibilities present themselves: either the shape of the IB spectrum for the forbidden transition $^{90}Y \rightarrow {}^{90}Zr$ differs from the shape expected on theoretical grounds, or the measured

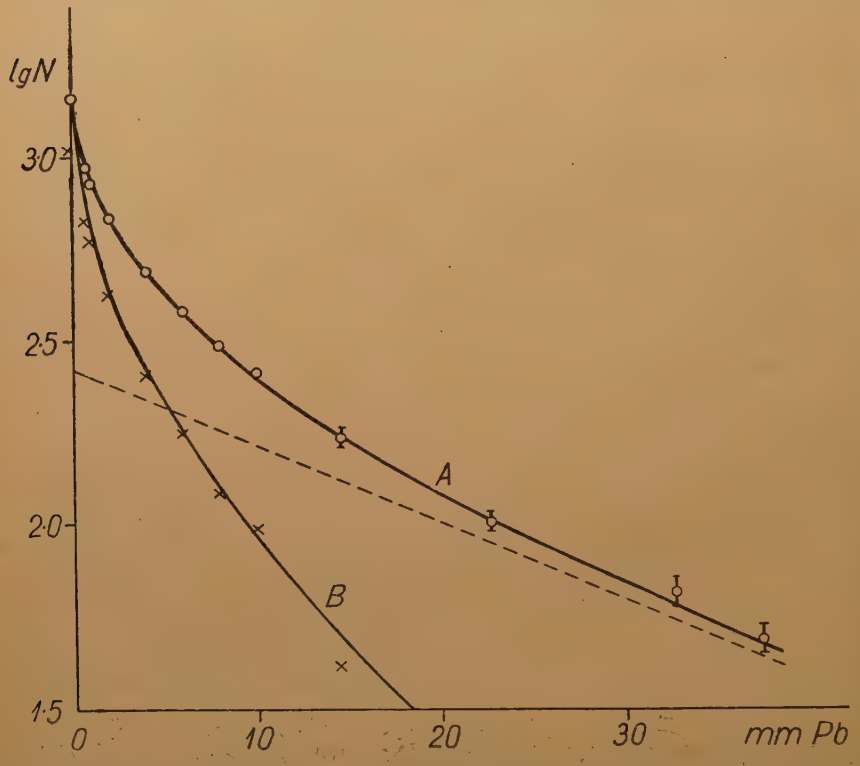

Fig. 9. Analysis of the absorption curve of radiation emitted by the ^{90}Y nucleus. Curve *B*-theoretical absorption curve. Circles — experimental values. Crosses - experimental values after subtracting the intensity of γ-ray line of 1,5 MeV energy

radiation emitted by ^{90}Y is not a pure IB. Madansky and Rasetti (1951) stated that the IB spectrum distribution of the forbidden transformation RaE $\rightarrow {}^{210}Po$ is not inconsistent with the IB spectrum distribution expected on the grounds of Knipp and Uhlenbeck's theory. It is, therefore, to be expected that in the corresponding case of a forbidden transformation of ytrium the calculation of the shape of the spectrum will also lead to a correct result. In view of this, it seems more probable that the measured radiation emitted by ytrium is not a pure IB, but that it is due in part to γ-ray lines. As no changes of the shape of the absorption curves were found during the measurements lasting longer than three times the half-life of ^{90}Y it must be assumed that the half-life of the transition in which linear γ-rays appear is the same as the half-life period of the transition $^{90}Y \rightarrow {}^{90}Zr$

and that some β-transitions lead to an excited state of ^{90}Zr emitting γ-radiation.

To estimate what percentage of all β-transitions are accompanied by genuine γ-photons, we assume, as the simplest possibility that the final part of the absorption curve is due mostly to a single line of hard γ-radiation. After subtracting the γ-absorption curve from the experimental absorption curve we obtain a pure ^{90}Y IB absorption curve. The results of such an analysis are marked on Fig. 9 with crosses. The shape of the curve as obtained approximately agrees with the theoretical IB absorption curve, which inversly proves that there is no contradiction between the above assumption and the experimental results. Thus the absorption curve of radiation emitted by the ytrium nucleus is probably the resultant of an absorption curve for γ-rays of a single γ-line of c. 1,5 MeV energy and c. 5 photons per 10000 β-particles intensity and the ^{90}Y IB absorption curve. The numerical values stated here are only a rough estimate, as the experimental results are encumbered with rather large errors (cf. Fig. 9). The energy values of the γ-photons cannot be exactly determined also due to the fact that in this range of energy the values of the absorption coefficients in lead depend only in a small degree on the value of the γ-ray energy.

The author wishes to express his gratitude to Professor M. L. Oliphant and to Professor P. B. Moon for their supervision of the experimental part of this investigation in the Physical Laboratory of Birmingham University (Gt. Britain) and to Professor H. Niewodniczanski for numerous valuable discussions and for his unabating interest in the progress of the whole work. He also wishes to tender his thanks to Dr A. Storruste for his collaboration in some measurements.

REFERENCES

Aston G. H., *Proc. Camb. Phil. Soc.*, **23**, 935 (1927).
Bethe H. A. and Bacher R. F., *Rev. Mod. Phys.*, **8**, 194 (1936).
Bloch F., *Phys. Rev.*, **50**, 272 (1936).
Chang C. S. W. and Falkoff D. L., *Phys. Rev.*, **76**, 365 (1949).
Dzhelepov B. and Petrovic S., *Usp. Fiz. Nauk*, **XL**, 497 (1950).
Evans R. D. and Evans R. O., *Rev. Mod. Phys.*, **20**, 305 (1948).
Konopinski E. J., *Rev. Mod. Phys.*, **15**, 209 (1943).
Knipp J. K. and Uhlenbeck G. E., *Physica*, **3**, 425 (1936).
Langer L. M. and Price Jr H. C., *Phys. Rev.*, **76**, 641 (1949).
Lyman E. M., *Phys. Rev.*, **51**, 1 (1937).
Madansky L. and Rasetti F., *Phys. Rev.*, **83**, 187 (1951).
Siegbahn K., *Phys. Rev.*, **70**, 127 (1944).
Storruste A., *Phys. Rev.*, **79**, 193 (1950); *Medd. Univ. Fys. Inst. Oslo*, Nr 185 (1951).
Wu C. S., *Phys. Rev.*, **59**, 481, (1941).

КРАТКОЕ СОДЕРЖАНИЕ

Б. Макей, *О спектральном распределении внутреннего тормозного излучения ^{32}P и ^{90}Y.*

Получена кривая поглощения в свинце, слабого γ—излучения ^{32}P ^{90}Y, при использовании в качестве детектора сцинтиляционного счетчика большой

чувствительности. Проведен анализ экспериментальных кривых поглощения и сравнение с расчетными кривыми спектрального распределения внутреннего тормозного излучения, полученными на основании теории Книппа и Уленбека.

Результаты измерений и расчетов позволяют сделать следующие выводы:

1. теоретическое предсказание спектрального распределения внутреннего тормозного излучения ^{32}P согласуется с экспериментальными данными.

2. в случае ^{90}Y на спектр внутреннего тормозного излучения налагается спектр жесткого γ—излучения с энергией около 1,5 MeV и интенсивностью около 5 фотонов на 10 000 β—превращений.

INVESTIGATION OF THE MOLECULAR STRUCTURE OF METHYL ALCOHOL BY THE SCATTERING OF THERMAL NEUTRONS

By J. A. Janik

Physical Institute, Jagellonian University, Kraków

(received June 30, 1952)

Measurements of the cross-section for scattering of slow neutrons show that the theory of Sachs and Teller (valid for molecular gases) is also true for many liquids. This may be verified on the examples of H_2, H_2O, H_2SO_4 and CH_3I molecules. The measurements of the cross-section for CH_3OH molecules give the value $(180 \pm 7) \cdot 10^{-24}\,cm^2$ which is much lower than $231 \cdot 10^{-24}\,cm^2$ obtained from the theory of Sachs and Teller. This discrepancy is interpreted as due to the influence of torsional oscillations between OH and CH_3 groups in the CH_3OH molecule, in agreement with the microwave experiments of Burkhard and Dennison.

1. Introduction

It is well known that the cross-section for scattering of slow neutrons by protons depends on the chemical binding of protons in the molecule. This dependence is based on the fact that a neutron may influence the vibrations of a proton in a molecule as well as cause a rotation of the whole molecule around one of its axis of inertia.

If a proton in the molecule vibrates with the frequency ν, the cross-section for scattering of a neutron by this proton (in the case of an isotropic vibration) is

$$\sigma = \frac{\sigma_0}{\varepsilon}(1 - e^{-4\varepsilon}), \qquad \text{(Bethe 1937)}$$

where $\sigma_0 = 20 \cdot 10^{-24}\,cm^2$ is the cross-section for scattering of slow neutrons by free protons, and $\varepsilon = \frac{E_n}{h\nu}$, E_n is the energy of the neutrons.

In the case of an anisotropic vibration

$$\sigma = 4\sigma_0\left[1 - 2\varepsilon' + \frac{32}{15}\left(\varepsilon'\varepsilon_2 + \frac{1}{4}\varepsilon_1^2\right) - \frac{64}{35}\left(\varepsilon'\varepsilon_2^2 + \right.\right.$$

$$\left.\left. + \frac{1}{4}\varepsilon_1^2\varepsilon_2 + \frac{5}{24}\varepsilon_1^3\right) + \ldots\right],$$

where

$$\varepsilon' = \frac{1}{3}\varepsilon_1 + \frac{2}{3}\varepsilon_2, \qquad \varepsilon_1 = \frac{E_n}{h\nu_1}, \qquad \varepsilon_2 = \frac{E_n}{h\nu_2}.$$

If the energy of a neutron is low in comparison to the vibrational quantum of a proton in the molecule the above equations give the value $4\sigma_0 = 80 \cdot 10^{-24}\,\mathrm{cm}^2$ for the scattering cross-section, in agreement with the theory of Fermi (1936), this being, however, exactly true only for zero-energy neutrons ($\varepsilon \to 0$).

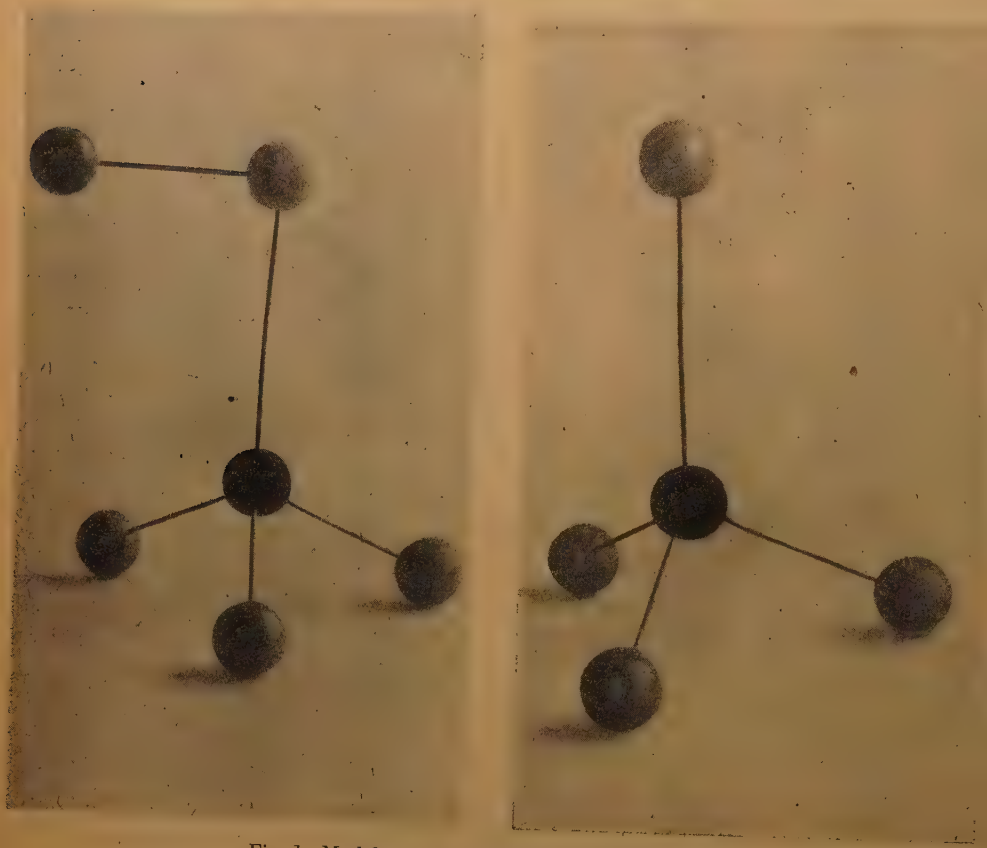

Fig. 1. Models of the CH_3OH and CH_3I molecules

In the case when the energy of a neutron is too small to produce vibrations of a proton, but much greater than the rotational quantum of the molecule, the neutron may cause a free rotation of the whole molecule around one of its axes of inertia. In this case the application of the theory of Sachs and Teller (1941) is necessary.

Taking into account all these considerations it seemed worth while to investigate the molecular structure of methyl alcohol by the scattering of slow neutrons by CH_3OH molecules. The general structure of the CH_3OH molecule, well-known from chemical and spectroscopic investigations, is shown in Fig. 1. The CH dis-

tance is about 1,10 Å, the CO distance about 1,44 Å, the OH distance about 0,958 Å, the HCH angle is equal to the tetrahedral angle of 109°28′, the COH angle is about 105°. (Burkhard and Dennison 1951).

The first conception of several investigators was that the hydrogen of the hydroxyl group rotates freely around the symmetry axis of the CH_3OH molecule (the CO axis). But the hydrogen of the hydroxyl group moves in a circle around the CO axis in a potential with three identical minima. If the potential barriers are sufficiently high the hydrogen atom will execute torsional oscillations. If the potential barriers are low there appears an approximately free rotation around the CO axis. Burkhard and Dennison (1951) interpret the obtained microwave frequency of 250 cm^{-1} as the frequency of torsional oscillations.

The scattering of slow neutrons by CH_3OH molecules may furnish another argument for the existence of these torsional oscillations. Evidently, the cross-section for scattering of a thermal neutron by the proton of a hydroxyl group will be different for free rotation of the hydrogen around the CO axis and for torsional oscillations. The measurements of the absorption coefficient for scattering of thermal neutrons by CH_3OH will decide on this detail in the molecular structure of methyl alcohol.

2. The application of the theory of Sachs and Teller to liquids

The theory of Sachs and Teller (1941) explains the phenomenon of the scattering of slow neutrons by molecular gases when the neutron energy is low as compared with the vibrational quantum of protons in the molecule but great as compared to the rotational quantum of the whole molecule ($E_{rot} \ll E_n \ll E_{vib}$, $E_n < (E_{rot}\, kT)^{1/2}$).

The cross-section for scattering of a slow neutron by a proton bound in a molecule is

$$\sigma = \sigma_\infty (\mu_1 \mu_2 \mu_3 \mu)^{1/2} (T_0 + T_1 + T_2 + \ldots),$$

where σ_∞ is the cross-section for scattering of slow neutrons by protons in the case of zero-energy neutrons when the protons are rigidly bound. $\sigma_\infty = 80 \cdot 10^{-24} cm^2$. $T_0, T_1, \ldots$ are terms which depend on the energy of the neutrons and on the energy of the molecules, $\mu = \frac{1}{3}(\mu_1 + \mu_2 + \mu_3)$, and μ_1, μ_2, μ_3 are the characteristic values of a tensor constructed in the following manner:

The molecule is replaced by a hypothetical mass point. The mass of this mass point is a tensor $\mathbf{M}$ defined by:

$$(M^{-1})_{ii} = \left(\frac{r_j^2}{I_{k_{\parallel}}} + \frac{r_k^2}{I_j} + \frac{1}{M_0}\right), \qquad (M^{-1})_{ij} = -\frac{r_i r_j}{I_k},$$

where r_1, r_2, r_3 are the coordinates of the considered proton as referred to the principal axis of inertia of the molecule, I_1, I_2, I_3 are the moments of inertia of the whole molecule as referred to these axes, $\mathbf{M_0}$ is the mass of the molecule.

We introduce a dimensionless tensor $\mathbf{n} = m\mathbf{M}^{-1}$, where m is the mass of the neutron, and a third tensor μ by

$$\mu^{-1} = 1 + n.$$

The characteristic values of this tensor μ are the μ_1, μ_2, μ_3.

The theory of Sachs and Teller is valid for molecular gases. The comparison with experiment, however, shows that it is possible to use it also for many liquids. In this case it is necessary to replace the bracket expression $(T_0 + T_1 + T_2 + \ldots)$ in the equation of Sachs and Teller by 1, so that

$$\sigma = \sigma_\infty (\mu_1 \mu_2 \mu_3 \mu)^{1/2}.$$

This may be experimentally verified on the examples of liquid H_2, H_2O, H_2SO_4, and CH_3I, as it is easy to see from Table 1.

Table 1

Scattering cross-section for slow neutrons

Liquid	Cross-section per molecule calculated from the theory of Sachs and Teller	Cross-section per molecule experimentally obtained	References
H_2	$48{,}6 \cdot 10^{-24}\,cm^2$	$48 \cdot 10^{-24}\,cm^2$	Carrol 1941
H_2O	$78{,}5 \cdot 10^{-24}\,cm^2$	$85{,}5 \cdot 10^{-24}\,cm^2$	Rossel 1947
		$81{,}9 \cdot 10^{-24}\,cm^2$	Janik 1951b
H_2SO_4	$119{,}1 \cdot 10^{-24}\,cm^2$	$115 \cdot 10^{-24}\,cm^2$	Janik 1952
CH_3I	$195 \cdot 10^{-24}\,cm^2$	$195{,}2 \cdot 10^{-24}\,cm^2$	this paper
CH_3OH	$231 \cdot 10^{-24}\,cm^2$	$180 \cdot 10^{-24}\,cm^2$	this paper

The *case of CH_3I.* We apply the theory of Sachs and Teller to liquid CH_3I Fig. 2 shows the CH_3I molecule in the coordinate system of the principal axe of inertia. The obtained values for n_1, n_2, n_4 are:

$$n_1 = 0{,}007, \qquad n_2 = 0{,}095, \qquad n_3 = 0{,}416.$$

$\sigma = 60 \cdot 10^{-24}\,cm^2$ /proton bound in the CH_3I molecule,

$\sigma_{CH_3I} = 195 \cdot 10^{-24}\,cm^2$

$(\sigma_C = 5 \cdot 10^{-24}\,cm^2$ and $\sigma_I = 10 \cdot 10^{-24}\,cm^2)$.

The *case of CH_3OH.* The same theory of Sachs and Teller applied to methyl alcohol on the assumption that the OH group can freely rotate around the CO axis, gives for protons of the CH_3 group $\sigma = 57 \cdot 10^{-24}\,cm^2$, for the proton of the OH group $\sigma = 51{,}2 \cdot 10^{-24}\,cm^2$, and therefore the cross-section for the scattering of slow neutrons by CH_3OH molecule is

$\sigma_{CH_3OH} = 231 \cdot 10^{-24}\text{cm}^2$.
$(\sigma_0 = 3{,}8 \cdot 10^{-24}\text{cm}^2)$.

4. Apparatus

In this work a boron lined ionization chamber was used as a counter of thermal neutrons. The apparatus was described in detail in a previous paper on the absorption of slow neutrons (Janik 1951 a). A source of photoneutrons slowed down by 6 cm of paraffin was used. The necessary γ-ray source consisted of 200 mg of radium enclosed in platinum tubes and needles. The scatterers were placed in flat brass vessels, between the chamber and the neutron source, at a distance of 11 cm from the ionization chamber.

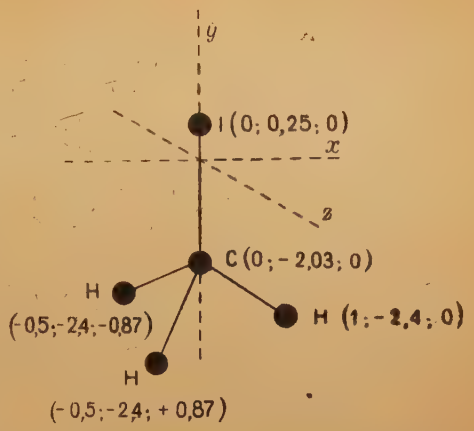

Fig. 2. CH_3I molecule in the coordinate system of the principal axes of inertia. The figures in brackets are the coordinates of the atoms as referred to these axes of inertia. The unit is 1 Å . CI = 2,28 Å, CH = 1,1 Å, HCH angle = 109°

5. Results

The experimentally obtained cross-sections for scattering of thermal neutrons by CH_3I and CH_3OH molecules are:

$$\sigma_{CH_3I} = (195{,}2 \pm 10) \cdot 10^{-24}\text{cm}^2$$

$$\sigma_{CH_3OH} = (180 \pm 7) \cdot 10^{-24}\text{cm}^2$$

The value for CH_3I is in agreement with that calculated from the theory of Sachs and Teller. This value (together with the previous values for H_2, H_2O, and H_2SO_4) furnishes a new argument for the applicability of the theory of Sachs and Teller to liquids.

But the value obtained for methyl alcohol is quite different from the calculated one (see Table 1). The calculation by means the theory of Sachs and Teller on the assumption that the OH group rotates freely around the CO axis yields $231 \cdot 10^{-24}\text{cm}^2$.

It is very natural to regard this discrepancy as being due to torsional oscillations of the OH and CH_3 groups in agreement with the microwave experiments. The OH and CH_3 groups oscillate relatively to one another with the frequency of 250 cm^{-1} so that the four hydrogen atoms in the molecule of methyl alcohol shall be considered each as a harmonical oscillator with $\varepsilon = \frac{E_n}{h\nu} = 1$. The neutron scattering cross-section will in this case depend on the frequency of this oscillation as well as on the rotation possibility of the whole CH_3OH molecule.

It is therefore not possible to use either formula of Bethe or the equation of Sachs and Teller ($E_n = E_{vib}$). But if we neglect the effect of rotation (as in the case of very heavy molecules), we have for the scattering cross-section of neutrons by the vibrating protons according to Bethe's formula

$$\sigma = 209 \cdot 10^{-24}\text{cm}^2 \qquad (\varepsilon_1 = 1, \quad \varepsilon_2 = 0)$$

The possibility of rotation will of course cause further diminishing of the scattering cross-section.

Thus, the value of the cross-section obtained in the experiments, which is small in comparison with the theory of Sachs and Teller may be understood only on the assumption of torsional oscillations in the CH_3OH molecule.

6. Acknowledgements

My thanks are due to the Sekcja Naukowa Komisji Popierania Tworczości Naukowej i Artystycznej przy Prezydium Rady Ministrów R. P. for the award of a scholarship. I wish also to express my gratitude to Professor H. Niewodniczański for interesting and helpful discussions, as well as to Dr E. Wyrobek for permitting me to use 200 mg Ra belonging to the Instytut Onkologiczny in Cracow.

REFERENCES

Bethe H. A. *Rev. Mod. Phys.*, **9**, 69 (1937).
Burkhard D. G. and Dennison D. M., *Phys. Rev.*, **84**, 408 (1951).
Carrol H., *Phys. Rev.*, **60**, 702 (1941).
Fermi E., *Ricerca Scient.*, **7**, No 2, 13 (1936).
Janik J. A., *Acta Phys. Polonica*, **10**, 261 (1951a); **11**, 146 (1951b); **11**, (1952).
Rossel J., *Helv. Phys. Acta.*, **20**, 105 (1947).
Sachs R. G. and Teller E., *Phys. Rev.*, **60**, 18 (1941).

КРАТКОЕ СОДЕРЖАНИЕ

Г. Яник, Исследование структуры молекулы метилового спирта при рассеянии медленных нейтронов.

Измерения эффективного сечения рассеяния медленных нейтронов показывают, что теория Закса и Теллера (разработанная для газов) применима также к жидкостям. Этот факт проверен на примерах H_2, H_2O, H_2SO_4 и CH_3I. Теория Закса—Теллера, примененная к молекуле CH_3OH дает для эффективного сечения рассеяния значение $231 \cdot 10^{-24}$ см^2, в то время как опыт дает $(180 \pm 7) \cdot 10^{-24}$ см^2. Это расхождение можно объяснить влиянием взаимных крутильных колебаний групп OH и CH_3, в качественном согласии с радиоспектроскопическими измерениями Буркгарда и Деннисона.

ON LARGE PULSES IN PURE-VAPOUR G.-M. COUNTERS

By J. Wesołowski

Institute of Physics, B. Bierut University, Wrocław

(received July 15, 1952)

Large pulses produced by α-particles in pure-vapour G.-M. counters have been investigated in some detail. A typical operating characteristic is given of such a counter exposed to a divergent beam of α-radiation. A new luminous phenomenon associated with large pulses is described.

Introduction

A few years ago some experiments with boron-lined, slow-neutron counters were made by the author. The all-metal type counters used in those experiments were filled with pure organic vapours. For calibrating purposes small mica windows were mounted on the cathodes through which Po α-particles could be projected into the sensitive volume. The observations on an oscilloscope screen of the height and shape of the pulses showed that under the influence of the α-radiation there appeared occasionally some unusual, very large pulses. Some of these pulses exhibited a characteristic stepwise structure.

It was also observed that the counting rate of the large pulses increases with the voltage applied to the counter. These phenomena were evidently caused by discharges of a particular kind and of abnormal magnitude produced by α-particles. The observations mentioned above, as having no direct connexion with slow-neutrons experiments have not been published.

Since then several papers appeared in which essentially the same phenomenon was described and the results of more detailed investigations were presented. Huber, Hunzinger and Baldinger (1947) used argon-alcohol counters in which a movable α-particle source was placed on the wire. They observed that large pulses are produced only by those α-particles the paths of which are inclined to the normal to the wire at an angle smaller than a certain critical one. The value of this critical angle increases with the voltage across the counter. In consequence, the counting rate of large pulses also increases. In a series of papers Fünfer and Neuert (1950) and Neuert (1950) have reported results of their more detailed examinations of pure-vapour counters exposed to α-radiation. On the basis of a number of indirect observations they concluded that:

a) In contradistinction to ordinary Geiger discharges which propagate in a narrow layer along the wire, a discharge corresponding to a large pulse is localised in a narrow space extending from the wire to the cathode.

b) The abnormal discharges produced by α-particles are accompanied by long wave photons, and are similar in their mechanism to a streamer type discharges (Loeb and Meek 1940, Raether 1938).

Considering some interest evoked by recent investigations in this field, the author repeated his former experiments and supplemented them with new ones.

II. Experimental procedure

An earlier observation made in connexion with slow-neutron counters was the starting point of experiments described below. During some measurements with a counter in which the wire was incidentally insufficiently stretched, it was

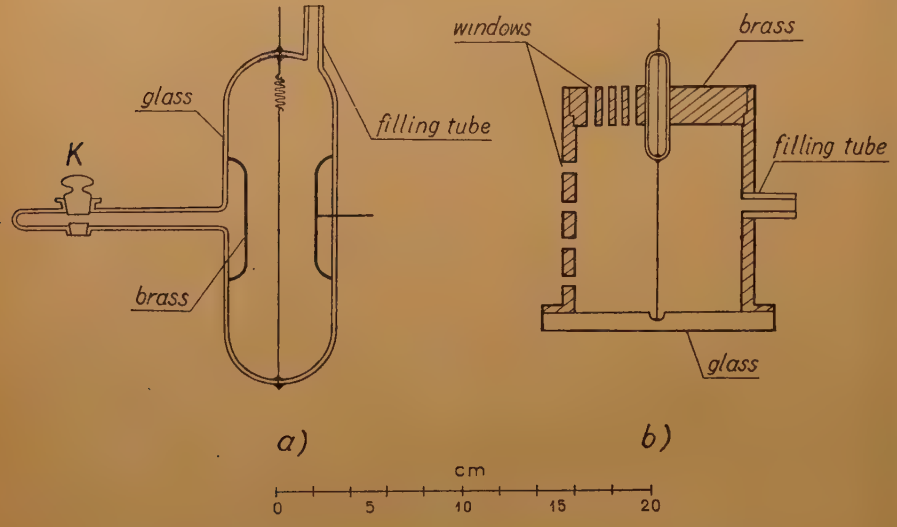

Fig. 1. Two types of counters used. Mica windows not to scale

observed that each large pulse was accompanied by an audible, mechanical oscillation of the wire. This suggested that large pulses are produced by a particular kind of spark discharges.

In order to test directly the correctness of this supposition, several types of counters were constructed in such a manner as to make possible visual observation of their interiors. Fig. 1 shows schematically the construction of two types of counters.

In counter 1(a), completely enclosed in a glass envelope, the Po α-particle source was placed in the hollow of the stopcock K of a lateral glass tube. Just opposite to the source a hole, of 0,5 mm diameter, was drilled in the cylinder of the cathode. The geometry of the arrangement was such that α-particles were falling almost normally to the wire.

Counters of type 1(b) were closed at one end with a thick glass window making possible visual observation of the interior. In the opposite brass wall four radially located, mica windows of 0,5 mm diameter were mounted. Through these windows α-particles could be projected almost parallelly to the wire and in various

distances from it. A number of similar windows was mounted in the cylinder of the cathode. By changing the distance between the source and the mica windows it was possible to alter to some extend the divergence of the beam of α-particles entering the counter. In order to obtain a distinct difference in magnitude of large and normal pulses, the length of the cathodes was limited to 50 mm. The

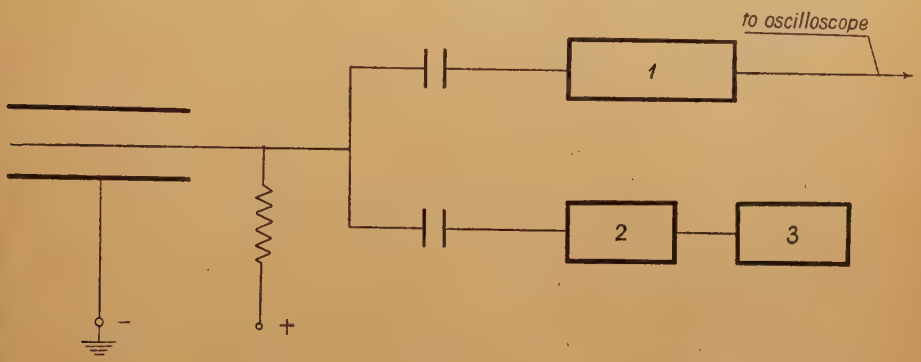

Fig. 2. Block diagram of the circuit: (1) amplifier, (2) pulse discriminator, (3) recording circuit

counters were filled with vapours of ethyl-alcohol, ether, methylal or with various mixtures of these substances, the total pressures ranging from 15 to 40 mm Hg.

A block diagram of the circuit used is shown in Fig. 2.

Negative pulses from the counter passed simultaneously to the oscilloscope circuit and, through a pulse discriminator, to the multivibrator of the recording circuit. In this way it was possible to observe simultaneously the size of the pulses on the oscilloscope screen and the luminous phenomena occuring in the counter. At the same time pulses of a given amplitude could be counted.

III. Experimental results

A rather small effective length of the counters greatly facilitated the sepaph tion and observation of the large pulses. According to the voltage applied to he counter the size of these pulses was about 20 to 100 times as large as that ttre to the cosmic ray or β-particle background. In agreement with the results repordet by other authors it was ascertained that α-particles projected parallelly to the wire did not produce large pulses. Strictly speaking, large pulses were not observed in such a geometry in which the α-particles did not hit the wire or the cylinder. Therefore, in all experiments described below α-particles were projected through the windows of the cylinder.

First of all the existence of a large-pulses threshold was found; it lies in the proportional region of the usual operating characteristic of the counter. Large pulses appear at a rather sharply defined voltage, depending on the type of the vapour used, the pressure and the geometrical parameters of the counter.

As the voltage is raised above this threshold, the counting rate at first rapidly increases, then reaches a maximum value, and, with a further increase of the

voltage, gradually diminishes. Nevertheless, large pulses are still observed even in a voltage region where the counter passes into a continuous discharge.

A typical curve showing the counting rate versus voltage is presented in Fig. 3. The maximum of the counting rate is reached at a voltage lying in the vicinity of what may be called: "The Geiger threshold".

It is known from Fünfer and Neuert's investigations that pure vapour counters do not exhibit a Geiger threshold in the common meaning of the word. The term

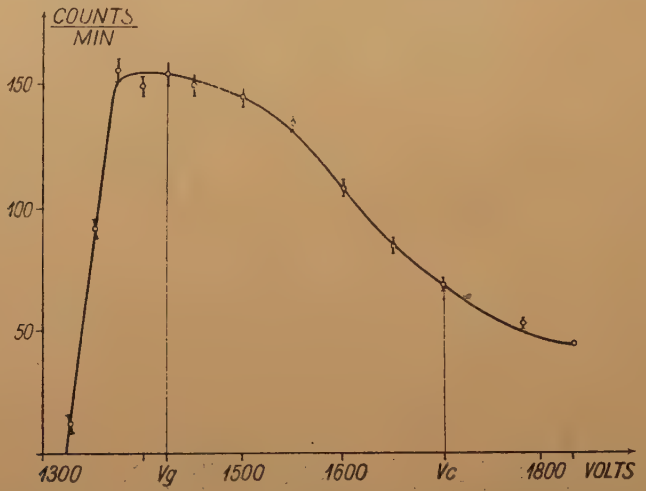

Fig. 3. Counting rate vs. voltage. Counter of the type 1(b). Po α-source a few mm. away from the mica window. Vg-Geiger threshold, Vc-beginning of the continuous discharge

„Geiger threshold" is understood here in a sense used by the above authors, i.e. an unsharply defined voltage at which Geiger pulses are almost of the same size.

IV. Correlation of luminous phenomena with the counting rate and magnitude of large pulses

At this stage of the investigation a quantitative description of such a correlation is rather difficult. In order to facilitate a qualitative description, let us distribute the values of the voltage applied to the counter into two regions: one below, the other above the Geiger threshold.

As the voltage of the first region is progressively raised and the threshold of large pulses reached, luminous phenomena begin to take place in the sensitive volume of the counter. Each large pulse is accompanied by bluish, sparklike stripes of light. The stripes extend from the mica window to the wire or reach the diametrically opposite side of the cylinder passing near the wire. Fig. 4 (a, b).

For the sake of simplicity, let us call the stripes extending between the window and the wire: "the inlet-stripes", and those between the wire and some other point of the cathode "the outlet-stripes". When the voltage is further raised the bright-

ness of the stripes increases and their appearance alters. Most frequently both kinds od stripes, inlet and outlet ones, appear simultaneously in the same event caused by the passage of a single α-particle. Fig. 4(c). The angle φ between these stripes decreases with increasing voltage, but when a more collimated beam of α-particles is directed on the wire then the stripes are situated almost in a straight line, independently of the voltage applied. In the second voltage region, i.e., above the Geiger threshold, the increase of the voltage causes a reduction of the counting rate and of the magnitude of the pulses Luminous phenomena change their aspect: the number of double stripes gradually diminishes, single outlet

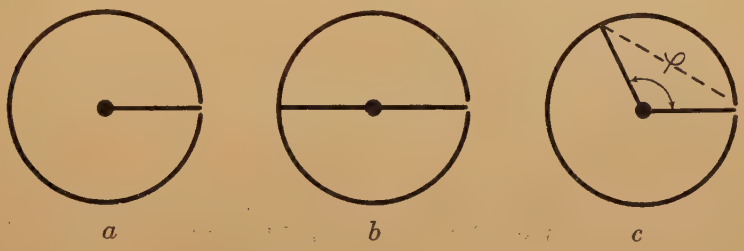

Fig. 4. (a), (b) Stripes just above the large-pulse threshold. (c) Stripes in the middle of the firs region. Dotted line supposed trajectory of α-particle

stripes predominate. As the voltage is further raised, the gas near the wire begins to glow and the counter passes into a continuous discharge. Yet, on the background of this discharge large pulses, though considerably reduced in number, are still observed. Finally, when the voltage is still further increased, typical overshootings occur in the counter.

The phenomena just described seem to indicate that the stripes connect the wire with two points on the cylinder: one, where an α-particle enters the counter (inlet-stripe), the other — where it is absorbed in the cathode. It seems that a single inlet-stripe appears when an α-particle falls directly on the wire.

As to the relative magnitude of the large pulses, the observations on the oscilloscope screen have shown that the height of these pulses is not uniform. Generally a pulse corresponding to a double stripe is about two times larger than that related to a single one.

V. Concluding remarks

The direct observations of the luminous phenomena taking place in pure organic vapour counters confirm Fünfer and Neuert's conclusions on the character of the discharge associated with large pulses. These discharges are in fact localized in small, narrow columns of the stripes and are accompanied by a visible radiation.

There are many obscure points yet; for instance, it is not clear why in the second voltage region the counting rate decreases with increasing voltage. It follows from what is already known on large pulses that pure vapour counters

might be in principle used as detectors of heavily ionizing particles in the presence of β-or γ-ray background and, at least to some extent, as indicators of the direction of motion of these particles.

Further investigations should decide whether and for what practical purposes these counters might be used.

The author is indebted to Mr. Z. Lewandowski for his assistance in carrying out some of the observations.

REFERENCES

Huber P., Hunzinger W., and Baldinger E., *Helv. Phys. Acta*, **20**, 525 (1947).

Fünfer E. and Neuert H., *Naturwiss.*, **37**, 20 (1950); *Helv. Phys. Acta*, **23**, Suppl. 3 (1950); *Z. angew. Phys.*, **2**, 241 (1950); *Z. Phys.*, **128**, 530 (1950).

Neuert H., *Z. Phys.*, **129**, 27 (1950).

Loeb L. B. and Meek J. M., *J. Appl. Phys.*, **11**, 438, 459 (1940).

Raether H., *Z. Phys.*, **110**, 611 (1938).

КРАТКОЕ СОДЕРЖАНИЕ

Я. Весоловский, *О больших импульсах в счетчике Гейгера-Мюллера наполненном чистым паром.*

Исследованы некоторые детали больших импульсов, вызванных α—частицами в счетчиках Гейгера-Мюллера, наполненных чистым паром.

Дана типичная характеристика счетчика, освещаемого расходящимся пучком α—частиц. Описывается новое световое явление, связанное с большими импульсами.

THIRD ORDER ABERRATIONS OF A MIRROR LENS

By J. Bartkowska

Optical Laboratory of the Institute of Precision Mechanics, Warszawa

(received September 16, 1952)

Formulae for third-order aberrations of a mirror lens are proved. As compared with analogous formulae for simple refracting lenses, these formulae show explicitly the advantages of using such a kind of lenses for the design of optical instruments.

The purpose of this article is to find expressions for third-order aberrations of mirror lenses and compare the properties of simple lenses (i.e. twice refracting) with the properties of mirror lenses. In the mirror lens the reflection occurs at its back surface. The light is refracted at the limiting surface, is then reflected and refracted again at the limiting surface. We shall use the sign convention adopted by J. Fluegge (1937, pp. 495—500). In this manner the direction of light remains positive to the right (Fig. 1). The law of reflection becomes (see the Index at the end of the paper)

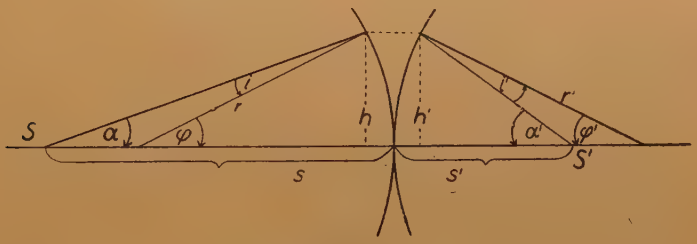

Fig. 1

$$\frac{1}{s'}-\frac{1}{s}=-\frac{2}{r}, \tag{1}$$

or

$$\Delta\frac{1}{s}=-\frac{2}{r}. \tag{2}$$

According to Fluegge $n'=n$; $i'=i$; $r'=-r$.
and Abbe's invariant

$$Q=n\left(\frac{1}{r}-\frac{1}{s}\right)=n\left(-\frac{1}{r}-\frac{1}{s'}\right). \tag{3}$$

Our computational practice proved this method to be very convenient for numerical calculations and to leave less possibilities for errors. In what follows we assume the lens to be infinitely thin. We shall use the method of the "basic parameters" (Slusarev 1937) to prove the formulae for Seidel's sums. This metod, when applied to a system of infinitely thin components, enables us to divide all the parameters into two groups of external and internal parameters.

External parameters depend only upon the focal lengths of several components, their reciprocal distances, and the positions of the object and the entrance pupil. Internal parameters depend only upon the radii of curvature and the indices of refraction of the sorts of glass used in the different components. Slusarev applies the method of "basic parameters" to the computation of systems of infinitely thin refracting lenses, single or cemented. In this article we use Slusarev's method for the computation of systems composed of infinitely thin mirror lenses.

We call "basic parameters" of an infinitely thin component the following expressions

$$\overline{P} = \sum_{i}^{k} \overline{h}_i^2 \overline{Q}_i^2 \Delta_i \frac{\overline{a}}{n}, \tag{4}$$

$$\overline{W} = -\sum_{i}^{k} \overline{h}_i \overline{Q}_i \Delta_i \frac{\overline{a}}{n}, \tag{5}$$

$$\pi = \sum_{i}^{k} \overline{h}_i \frac{f}{r_i} \Delta_i \left(\frac{1}{n}\right). \tag{6}$$

The summation is performed over all the surfaces of a very thin component, assuming

$$\overline{a}_1 = 0; \qquad \overline{a}'_k = 1.$$

The symbol Δ_i denotes the difference of a given magnitude before and after refraction by the i-th surface; for reflection

$$\Delta \frac{1}{n} = -\frac{2}{n}.$$

The focal length is determined by the equation

$$\frac{1}{f} = -\frac{2n}{r_2} + \frac{2(n-1)}{r_1}. \tag{7}$$

It is now necessary to calculate all the image distances and substitute their values in (4) — (6). We express r_2 by r_1 assuming in (7) $f = 1$. Thus we get the following formulae

$$\overline{P} = \frac{2(n-1)}{n^2} \varrho_1^3 + \frac{n^2+2n-3}{n^2} \varrho_1^2 + \frac{4n^2+n-5}{2n^2} \varrho_1 + \frac{4n^2-3}{4n^2}, \tag{8}$$

$$\overline{W} = \frac{n^2-1}{n^2}\varrho_1 + \frac{2n^2-1}{2n^2}, \tag{9}$$

$$\Pi = \frac{2n^2-2}{n^2}\varrho_1 - \frac{1}{n^2}, \tag{10}$$

where $\varrho_1 = \frac{f}{r_1}$.

Special attention should be paid to the results represented by formulae (8) and (10). The parameter $\overline{P}$ of a mirror lens is a third-order function, while in a refracting lens it is a quadratic function of the variable r_1. The graph (Fig. 2) shows us this function for different values of the refractive index. From the examiantion of the first and second derivatives it is clear that this function is monotonically increasing and has one point of inflexion. Parameter Π forms a linear function of the curvature, in contradistinction to the case of refracting lenses, where Π is approximately equal to 0,7.

For $n = 1{,}5$, $\overline{P} = 0$ and $\overline{W} = 0{,}222$ when $r_1 = -1$. This is the case of the so called Mangin's mirror (1876) which has the advantage of corrected spherical aberration and slight comatic aberration.

From (8)—(10) we can eliminate ϱ_1. Then $\overline{P}$ and Π become functions of $\overline{W}$, namely

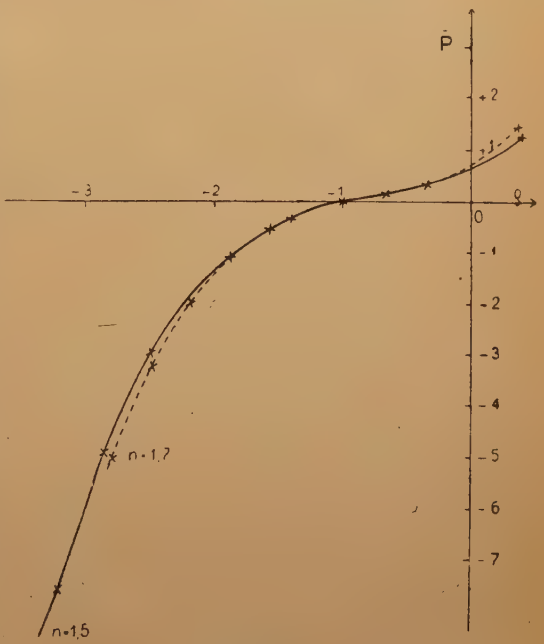

Fig. 2

$$\overline{P} = \frac{2n^4\overline{W}^3}{(n+1)^3(n-1)^2} + \frac{n^3(n^2-3n-1)\overline{W}^2}{(n+1)^3(n-1)^2} + \frac{(2{,}5n^4-n^3-2n^2+n+1)\overline{W}}{(n+1)^3(n-1)^2} + \frac{-2n^4+n^3+2n^2-n-1}{4(n+1)^3(n-1)^2} \tag{11}$$

$$\Pi = 2\overline{W} - 2. \tag{12}$$

The continuous graph in Fig. 3 represents the function $\overline{P}(\overline{W})$ for $n = 1{,}5$. The shape of this graph changes very little for other values of the refractive index n. The dashed line represents the same function for $n = 1{,}7$.

Formula (11), as it stands, is too complicated to be of much use for practical computations. However, mirror lenses are usually applied in systems with a great light gathering power, where the main role is played by spherical and comatic aberrations. The value of the parameter $\overline{W}$ varies then between -1 and $+1$, and is usually very small. Then, in first approximation, we can omit second and third powers of $\overline{W}$. We obtain thus linear equations, which are easy to solve.

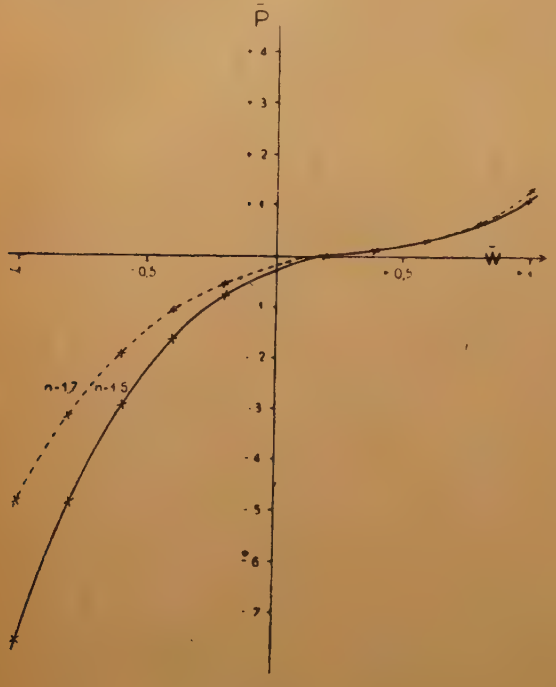

Fig. 3

It may be also remarked here that great negative values of $\overline{W}$ correspond to large curvatures.

Slusarev also introduces two new parameters P and W

$$P = \sum_{i}^{k} h_i^2 Q_i^2 \Delta_i \frac{\alpha}{n}, \quad (13)$$

$$W = -\sum_{i}^{k} h_i Q_i \Delta_i \frac{\alpha}{n}, \quad (14)$$

where α and h are now arbitrary. He proves the following formulae

$$P = (\alpha' - \alpha)^3 \overline{P} + 4\alpha(\alpha' - \alpha)^2 \overline{W} + \alpha(\alpha' - \alpha)\,[2\alpha(2 + \Pi)^{-}\alpha'], \quad (15)$$

$$W = (\alpha' - \alpha)^2 \overline{W} + \alpha(\alpha' - \alpha)\,(2 + \Pi). \quad (16)$$

If in formulae (15) and (16) we replace Π by its value from (12), we obtain

$$P = (\alpha' - \alpha)^3 \overline{P} + (\alpha' \cdot \alpha)\,(\alpha' - \alpha)\,(4\overline{W} - 1), \quad (17)$$

$$W = (\alpha'^2 - \alpha^2)\,\overline{W}. \quad (18)$$

We can arrive at the same result, by computing successive object distances of an incident ray on a mirror lens from any point, substituting the results in formulae (13) and (14), and eliminating by the aid of (8) and (9).

From formula (17) it is evident that Mangin's mirror has a very small spherical aberration for any object position. The following formulae express Seidel's sums as functions of the parameters P, W and Π (Slusarev 1937). The summation is extended over all the infinitely thin components of the optical system.

$$S_I = \sum_{l}^{m} h_l P_l\,; \quad (19)$$

$$S_{II} = \sum_{l}^{m} y_l P_l - J \sum_{l}^{m} W_l ; \tag{20}$$

$$S_{III} = \sum_{l}^{m} \frac{y_l^2}{h_l} P_l - 2J \sum_{l}^{m} \frac{y_l W_l}{h_l} + J^2 \sum_{l}^{m} \Phi_l ; \tag{21}$$

$$S_{IV} = \sum_{l}^{m} \Phi_l \Pi_l ; \tag{22}$$

$$S_V = \sum_{l}^{m} \frac{y_l^3}{h_l^2} P_l - 3J \sum_{l}^{m} \frac{y_l^2}{h_l^2} W_l + J^2 \sum_{l}^{m} \frac{y_l}{h_l} \Phi_l (3 + \Pi_l). \tag{23}$$

In the case of an object at finite distance

$$\alpha'_p = 1, \qquad \beta_1 = 1, \qquad h_1 = s_1 \alpha_1, \qquad y_1 = x_1 ;$$
$$J = \alpha_1 (x_1 - s_1).$$

In the case of an object at infinity

$$\alpha^1 = 0, \qquad \alpha' = 1, \qquad h^2 = 1, \qquad y_1 = \frac{x_1}{F} ;$$
$$J = -1.$$

where p is the index of the last medium.

In telescopic systems $\alpha_1 = 0$, $\alpha'_p = 0$, $\overline{\alpha'_q} = 1$,

where q is the index of the medium before the eye piece. Formulae (19), (20) and (21) are valid in the case of mirror lenses. We express in (22) and (23) Π by its value from (12) and get

$$S_{IV} = \Sigma (2\overline{W}_l - 2) \Phi_l ; \tag{24}$$

$$S_V = \sum \frac{y_l^2}{h_l^2} P_l - 3J \sum \frac{y_l^2}{h_l^2} W_l + J^2 \sum \frac{y_l}{h_l} \Phi l (2\overline{W} + 1) \tag{25}$$

From (24) it is clear that the curvature of field depends on the bending of the mirror lens, and that for $\overline{W}$ lying near 0,25 it has the value —1,5. Hence it follows that in systems composed of refracting and mirror lenses, we can succeed in balancing the curvature of field without using negative lenses.

In the formula for distortion an essential role is played by its last term since, when spherical and comatic aberrations are already corrected, the values of P and $\overline{W}$ for individual components are usually small. The factor $2\overline{W} + 1$ appearing in the formula for mirror lenses is less than the factor $3 + \Pi = 3{,}7$ appearing in the same place for refracting lenses. Furthermore in systems in which mirror lenses occur distorsion is very small. The balancing of astigmatism causes the greatest difficulty because of the factor $2\Phi_i$.

We resume in a few words the essential differences and similarities between refracting and reflecting lenses. In the former the parameter $\overline{P}$ is a quadratic

function of curvature of the surface, in the latter-a third-order function. In the former spherical aberration cannot be corrected, it can only be brought to a minimum, in the latter it can be corrected and the function has no extremum. In both the parameter $\overline{W}$ is a linear function of the curvature. The value of the parameter $\overline{\Pi}$ for refracting lenses varies very little and is approximately equal to 0,7, while for reflecting lenses it is a linear function of curvature in the interval from —1,5 to —2.

The systems with mirror lenses can be easily corrected for spherical and comatic aberrations, and for distortion. The curvature of field has large values of opposite signs as in the case of refracting lenses. We get a chance of balancing the curvature of field by combining reflecting with refracting lenses. The chief difficulty is caused by astigmatism which is not easy to remove in systems with great light gathering power.

Index of signs and symbols used

α — angle of first auxiliary ray with optical axis
β — angle of second auxiliary ray with optical axis
ϱ — reciprocal of radius of curvature related to focal length 1
Φ — reciprocal of focal length, power of a lens
Π — parameter connected with curvature of the field, formula (6)
f — focal length
h — height of first auxiliary ray
i — angle of incidence
i' — angle of refraction or reflection
i — as index denotes successive number of the surface of a given lens
J — normative factor appearing in formulae (19)—(25)
k — number of lens surfaces
$\mathfrak{I}$ — index denoting successive number of a given lens in a system
m — number of lenses in a given system
n — refractive index
P — parameter defined by formulae (4) and (13) connected with spherical aberration
Q — Abbe's invariant, formula (3)
r — radius of curvature of a lens
s — object or image distance of first auxiliary ray
$S_I, S_{II}, S_{III}, S_{IV}, S_V$ — Seidel's sums, formulae (19)—(23)
W — parameter connected with comatic aberration, formula (5) and (14)
x — object or image distance of 2-nd auxiliary ray
y — height of 2-nd auxiliary ray
— — a dash above a symbol means that a given magnitude is computed for an object at infinity and focal length 1 (e.g. $\overline{P}$)
' — an accent means that a given magnitude is computed after refraction or reflection at a given surface (e.g. s')
Δ — denotes the difference of a given magnitude before and after refraction or reflection on a given surface

REFERENCES

Bouvers, *Achievements in Optics*, Amsterdam 1946.
Czapski-Eppenstein, *Grundzüge der Theorie der optischen Instrumente*, *Leipzig* 1924

Fluegge J., *Z. Instr. Kunde* 495, (1937).
Fluegge J., Z. Instr. Kunde, (1941).
Maksutov, *Astronomical Optics*, Moscow 1946 (in Russian).
Mangin, *Etude de divers dispositifs optiques destinés a projeter la lumiére électrique sur les objets éloignés*, Paris 1876.
Slusarev, *Methods of Computation of Optical Systems*, Moscow 1937 (in Russian).
Sonnenfeld, *Der Hohlspiegel.*
Volosov, *Method of Computation of Compound Photographic Systems*, Moscow 1948 (in Russian).

КРАТКОЕ СОДЕРЖАНИЕ

Я. И. Бартковская, *Аберрации III порядка отражательных линз.*

В работе дан вывод формул аберации III порядка отражательных линз. Сравнение этих формул с соответствующими формулами для преломляющих линз показывает преимущества употребления отражательных линз при постройке оптических приборов.

ANGULAR CORRELATION OF THREE SUCCESSIVE GAMMA QUANTA*

By Janusz Dąbrowski

Institute of Theoretical Physics III, University of Warsaw, Warszawa
National Institute of Mathematics, Warszawa

(received September 22, 1952)

Formulas are given for the angular correlation of three successive γ-quanta. The assumption is made that each γ-quantum is of a given multipolarity. The z-axis is taken along the direction of propagation of the second quantum. The Racah summation formulas are used twice. The final correlation formula is given in terms of $P_{2\mu,\lambda}(\cos\vartheta_1)P_{2\nu,\lambda}(\cos\vartheta_3)\cos\lambda\varphi$, where $\vartheta_1(\vartheta_3)$ is the angle between the direction of the first (third) and the second quantum, and φ is the dihedral angle between the planes of the first-second and third-second quanta. Numerical values of the correlation coefficients for dipole transitions are given. Results are given for the limitations of anisotropy. The formalism describes also the case in which some of the emission processes are replaced by absorption processes.

1. Introduction

The investigation of the angular correlations of successive γ-radiation is an important method used in order to determine the total angular momenta of excited nuclear levels and the multipolarity of γ-radiations. All the papers up to now investigated the case of two radiations emitted in cascade (Hamilton 1944, Goertzel 1946, Brady and Deutsch 1950, Falkoff and Uhlenbeck 1950, and Racah 1951, where also further literature may be found; see also the report by Rubinowicz 1949). This limited this method of determination of the angular momenta and the multipolarity of the corresponding transitions to the first and the second excited levels. In order to extend this method to the next, i.e. the third, excited level, I started to work out the theory of the angular correlation of three successive γ-radiations — as suggested to me by Profesor A. Rubinowicz. While I was working on this problem, there appeared a paper on the same subject by Arfken, Biedenharn and Rose (1951 and then still another one by the same authors (1952). During the execution of correlation experiments on triple transitions, the magnetic quantum numbers of the intermediate states of the nucleus are unknown (in contradistinction to the case of double transitions). Therefore, in the correlation formulas for triple transitions interference terms appear (Lippman 1951). This circumstance makes

* This work is part of a thesis submitted in partial fulfillment of the requirements for the degree of Candidate of Science.

he theory of angular correlation much more complicated in the case of triple ransitions than in the case of double transitions. Therefore, in their calculations he three authors mentioned confine themselves only to the special cases in which wo of the radiations are parallel or antiparallel and the interference terms vanish. Besides they consider the case of two radiations in triple cascade with one ra- liation unobserved. The corresponding experiments are only of importance when ne of the three quanta is difficult to observe, e.g., on account of its small energy. Of course, most of the informations and the clearest results are yielded by exper- ments in which one is not limited to special positions of the counters. Hence I ndertook the laborious task of calculating the correlation formulas for triple γ-radiation for arbitrary directions of emission.

The distinction between emission and absorption is irrelevant in the corre- ation formulas. Thus the theory of triple correlation describes also the case of bsorption followed by emission of two cascade radiation. In this case it is of impor- ance to avoid the necessity of observing the emitted quanta parallel to the direction f propagation of the exciting quanta, which could perturb the registration of he counter. When additional effects (scattering, pair production) possess rota- ional symmetry with respect to the direction of propagation of the exciting quanta, ne can place the counters on a half-cone the axis of which is parallel to this di- ection and the vertex of which is in the emitting nucleus. Then the anisotropy n the coincidences is due solely to the angular correlation of the two emitted adiations. If most of the scattering is a forward-scattering, one should observe he radiation emitted backwards with respect to the direction of propagation of the xciting quanta.

I. Theory

The following process is considered: A nucleus in the initial excited state j_1 ass over to the first intermediate excited state j_2 by emitting a γ-quantum $(\vec{k}_1 2^{L1})$. he nucleus in the state j_2 pass then over to the second intermediate excited state j_3 y emitting a γ-quantum $(\vec{k}_2 2^{L2})$. Finally the nucleus in the state j_3 makes a tran- ition to the ground state j_4 by emitting a γ-quatum $(\vec{k}_3 2^{L3})$; j are the quantum umbers of the total angular momentum of the four states; $(\vec{k} 2^{L})$ are the wave ector and multipolarity of the successive γ-quanta. It is assumed that the nuclear states which differ only in respect to the magnetic quantum numbers m_r $(r = 1, 2, 3, 4)$ have the same energy, and that the initial nuclei are oriented t random.

The probability of the above process is given by the formula

$$w = \sum \{m_1 m_4 M_1 M_2 M_3\}$$

$$\times \left| \sum \{m_2 m_3\} (j_1 m_1 \,|\, H(\vec{k}, M_1) \,|\, j_2 m_2)\ (j_2 m_2 \,|\, H(\vec{k}_2 M_2) \,|\, j_3 m_3) \right.$$

$$\times (j_3 m_3 | H(\vec{k}_3 M_3) | j_4 m_4)|^2, \qquad (1$$

where $H(\vec{k}M)$ is the interaction hamiltonian for emission of a γ-quantum wi the wave vector $\vec{k}$; $M = \pm 1$ corresponds to a left- or right-handed circular polarized wave respectively. The summation is to be performed over the indic in the { }-braces.

This formula can be derived by solving the perturbation theory equatio by the Weisskopf-Wigner method (see Appendix).

In Eq. (1) and further on we omit constant factors, which are irrelevant f the correlation formulas.

The matrix elements of the interaction hamiltonian $H(\vec{k}_s M_s)$ $(s = 1, 2,$ for emision of a γ-quantum with the wave vector

$$\vec{k}_s = k_s (\vec{i}_x \cos\varphi_s \sin\vartheta_s + \vec{i}_y \sin\varphi_s \sin\vartheta_s + \vec{i}_z \cos\vartheta_s) \qquad (2$$

and multipolarity 2^{Ls} have the form (Goertzel 1946)

$$(j_s m_s | H(\vec{K}_s M_s) | j_{s+1} m_{s+1})$$

$$= \text{const} \sum_{\mu|-Ls}^{Ls} D^{(Ls)}(\varphi_s \vartheta_s 0)_{\mu M s} M_s^{\varepsilon} (j_{s+1} L_s j_s m_s | j_{s+1} L_s m_{s+1} \mu), \qquad (3$$

where $\varepsilon = 0,1$ for magnetic and electric transitions respectively and the "const is independent of m_s, m_{s+1}, M_s. $D^{(Ls)}(\varphi_s \vartheta_s 0)_{\mu Ms}$ are matrices of the irreducibl representation of the three-dimensional rotation group and $(j_{s+1} L_s j_s m_s | j_{s+1} L$ $m_{s+1} \mu)$ are the Clebsch-Gordan coefficients (Wigner 1931).

The value of w is independent of the direction chosen for the axis of quanti zation, hence we take the z-axis along the direction of propagation of the secon quantum. This choice of the z-axis simplifies essentially further calculations, sinc it enables us to perform most summations in the same manner as Racah (195 did it for double correlations.

$D^{(L_2)}(000)_{\mu M_2} = \delta(\mu M_2)$, hence inserting expressions (3) in Eq. (1), we hav with our choice of the z-axis the following formula for w

$$w = \sum \{m_1 m_2 m_2' m_3 m_3' m_4 \mu\mu' \nu\nu' M_1 M_2 M_3\} (j_2 L_1 j_1 m_1 | j_2 L_1 m_2 \mu)(j_2 L_1 j_1 m_1 | j_2 L_1 m_2' \mu')$$

$$\times D^{(L_1)}(\varphi_1 \vartheta_1 0)^*_{\mu M_1} D^{(L_1)}(\varphi_1 \vartheta_1 0)_{\mu' M_1} (j_3 L_2 j_2 m_2 | j_3 L_2 m_3 M_2)(j_3 L_2 j_2 m_2' | j_3 L_2 m_3' M_2)$$

$$\times (j_4 L_3 j_3 m_3 | j_4 L_3 m_4 \nu)(j_4 L_3 j_3 m_3' | j_4 L_3 m_4 \nu') D^{(L_2)}(\varphi_3 \vartheta_3 0)^*_{\nu M_3} D^{(L_2)}(\varphi_3 \vartheta_3 0)_{\nu' M_3}. \qquad (4$$

Now making use of the formula

$$D^{(L)}(\alpha\beta\gamma)^*_{\mu'\mu} = (-)^{\mu-\mu'} D^{(L)}(\alpha\beta\gamma)_{-\mu'-\mu}$$

we split up the products D^*D appearing in Eq. (4) into sums of matrices of irre ducible representations with help of the well-known formulas (Wigner 1931):

$$D^{(L_1)}(\varphi_1 \vartheta_1 0)^*_{\mu M_1} D^{(L_1)}(\varphi_1 \vartheta_1 0)_{\mu' M_1} = (-)^{M_1 - \mu} \sum \{k\varrho\} (L_1 L_1 - \mu\mu' | L_1 L_1 k\varrho)$$

$$\times D^{(k)}(\varphi_1 \vartheta_1 0)_{\varrho 0} (L_1 L_1 - M_1 M_1 | L_1 L_1 k 0),$$

$$D^{(L_3)}(\varphi_3\vartheta_3 0)^*_{\nu M_3} D^{(L_3)}(\varphi_3\vartheta_3 0)_{\nu' M_3} = (-)^{M_3-\nu} \sum \{l\lambda\}(L_3L_3 - \nu\nu'|L_3L_3 l\lambda)$$
$$\times D^{(l)}(\varphi_3\vartheta_3 0)_{\lambda 0}(L_3L_3 - M_3M_3|L_3L_3 l0). \quad (5)$$

Taking into account Eq. (5), Eq. (4) takes the form

$$w = \sum \{lk\varrho\lambda M_2 m_2 m_3 m_2' m_3'\} \Big[\sum \{m_1\mu\mu'\} (-)^{\mu} (L_1L_1 - \mu\mu'|L_1L_1 k\varrho)$$
$$\times (j_2L_1 j_1 m_1|j_2L_1 m_2\mu)(j_2L_1 j_1 m_1|j_2L_1 m_2'\mu') \Big]_1 (j_3L_2 j_2 m_2|j_3L_2 m_3 M_2)$$
$$\times (j_3L_2 j_2 m_2'|j_3L_2 m_3' M_2) \Big[\sum \{\nu\nu' m_4\} (-)^{\nu} (L_3L_3 - \nu\nu'|L_3L_3 l\lambda)(j_4L_3 i_3 m_3|j_4L_3 m_4\nu)$$
$$\times (j_4L_3 j_3 m'_3|j_4L_3 m_3\nu') \Big]_2 D^{(k)}(\varphi_1\vartheta_1 0)_{\varrho 0} D^{(l)}(\varphi_3\vartheta_3 0)_{\lambda 0}$$
$$\times \sum \{M_1\}(L_1L_1 - M_1M_1|L_1L_1 k0) \sum \{M_3\}(L_3L_3 - M_3M_3|L_3L_3 l0). \quad (6)$$

Now making use of the Racah (1942) summation formulas, we can write the brackets $[\,]_1$, $[\,]_2$ of Eq. (6) as follows

$$[\,]_1 = (-)^{\varrho+k+m'_2-m_2}(2k+1)^{\frac{1}{2}} W(j_2j_2L_1L_1|kj_1)(j_2km'_2\varrho|j_2kj_2m_2)$$
$$[\,]_2 = (-)^{\lambda}(2l+1)^{\frac{1}{2}} W(j_3j_3L_3L_3|lj_4)(j_3lm'_3 - \lambda|j_3lj_3m_3), \quad (7)$$

where W are the Racah coefficients.

Now using the relation

$$(j_1j_2 - m_1 - m_2|j_1j_2j - m) = (-)^{j_2+j-j_1-2m_2}(j_1j_2m_1m_2|j_1j_2jm), \quad (8)$$

we obtain

$$\sum \{M_1\}(L_1L_1 - M_1M_1|L_1L_1k0) = \begin{cases} 2(L_1L_1 1 - 1|L_1L_1k0) & \text{for even } k, \\ 0 & \text{for odd } k, \end{cases}$$

$$\sum \{M_3\}(L_3L_3 - M_3M_3|L_3L_3l0) = \begin{cases} 2(L_3L_3 1 - 1|L_3L_3l0) & \text{for even } l, \\ 0 & \text{for odd } l. \end{cases} \quad (9)$$

We see that k and l take even values only; we put, therefore,

$$k = 2\mu; \qquad l = 2\nu. \quad (10)$$

Making use of Eqs. (7) and (9), with (10), we can write Eq. (6) in the following form

$$w = \sum \{\mu\nu\lambda\varrho\} D^{(2\mu)}(\varphi_1\vartheta_1 0) D^{(2\nu)}(\varphi_3\vartheta_3 0)_{\lambda 0} (-)^{\varrho+\lambda} W(j_2j_2L_1L_1|2\mu j_1)$$
$$\times W(j_3j_3L_3L_3|2\nu j_4)(L_1L_1 1 - 1|L_1L_1 2\mu 0)(L_3L_3 1 - 1|2\nu 0)[(4\mu+1)(4\nu+1)]^{\frac{1}{2}}$$
$$\times \sum \{m_2m_3m_2'm_3'M_2\}(-)^{m'_2-m_2}(j_2 2\mu m'_2\varrho|j_2 2\mu j_2 m_2)(j_3 2\nu m'_3 - \lambda|j_3 2\nu j_3 m_3)$$
$$\times (j_3L_2 m_3 M_2|j_3L_2 j_2 m_2)(j_3L_2 m'_3 M_2|j_3L_2 j_2 m'_2). \quad (11)$$

The sum over m_2, m_3', m_2', m_3' is reduced to a single sum. Indeed, since $(j_1j_2m_1m_2|j_1j_2jm)$ has a factor $\delta(m_1+m_2, m)$, we have

$$\lambda = -\varrho \qquad m'_3 = m_3 + \lambda,$$
$$m'_2 = m_3 + M_2 + \lambda, \qquad m_2 = m_3 + M_2. \tag{12}$$

Hence Eq. (11) takes the form

$$w = \sum \{\mu\, \nu \lambda\} D^{2\mu}(\varphi_1 \vartheta_1 0)_{-\lambda 0} D^{(2\nu)}(\varphi_3 \vartheta_3 0)_{\lambda 0} [(4\mu+1)(4\nu+1)]^{1/2} \times (-)^{\lambda} R_{\mu\nu\lambda}(j_1 j_2 j_3 j_4 | L_1 L_2 L_3), \tag{13}$$

where

$$R_{\mu\nu\lambda}(j_1 j_2 j_3 j_4 | L_1 L_2 L_3) = r_{\mu\nu}(j_1 j_2 j_3 j_4 | L_1 L_3) A_{\mu\nu\lambda}(j_2 j_3 | L_2),$$
$$r_{\mu\nu}(j_1 j_2 j_3 j_4 | L_1 L_3) = W(j_2 j_2 L_1 L_1 | 2\mu j_1)\, W(j_3 j_3 L_3 L_3 | 2\nu j_4)\, (L_1 L_1 1 - 1 | L_1 L_1 2\mu 0) \times (L_3 L_3 1 - 1 | L_3 L_3 2\nu 0),$$
$$A_{\mu\nu\lambda}(j_2 j_3 | L_2) = \sum \{m_3 M_2\} (j_3 2\nu m_3 + \lambda, -\lambda | j_3 2\nu j_3 m_3) \times j_2 2\mu m_3 + M_2 + \lambda, -\lambda | j_2 2\mu j_2 m_3 + M_2)(j_3 L_2 m_3 M_2 | j_3 L_2 j_2 m_3 + M_2) \times (j_3 L_2 m_3 + \lambda M_2 | j_3 L_2 j_2 m_3 + M_2 + \lambda). \tag{14}$$

Replacing in expression for $A_{\mu\nu\lambda}$ the summation indices m_3, M_2 by $-m_3$, $-M_2$ and taking into account the symmetry properties of the Clebsch-Gordan coefficients, we easily get

$$A_{\mu\nu\lambda} = A_{\mu\nu-\lambda}. \tag{15}$$

Hence Eq. (13) takes the form

$$w = \sum \{\mu\, \nu \lambda \geqslant 0\} (-)^{\lambda} [(4\mu+1)(4\nu+1)]^{1/2} R_{\mu\nu\lambda} [D^{(2\mu)}(\varphi_1 \vartheta_1 0)_{-\lambda 0} \times D^{(2\nu)}(\varphi_3 \vartheta_3 0)_{\lambda 0} + D^{(2\mu)}(\varphi_1 \vartheta_1 0)_{\lambda 0} D^{(2\nu)}(\varphi_3 \vartheta_3 0)_{-\lambda 0}]. \tag{16}$$

Now we use the following relation (Goertzel 1946)

$$D^{(L)}(\alpha\beta\gamma)_{M0} = \left(\frac{4\pi}{2L+1}\right)^{1/2} Y_L^M(\beta\alpha)^*. \tag{17}$$

Here the Condon and Shortley (1951) choice of phases for associated Legendre polynomials is used. Taking into account Eq. (17) and introducing the angle $\varphi = \varphi_1 - \varphi_3$, we get finally

$$w = \sum \{\mu\, \nu \lambda \geqslant 0\} R_{\mu\nu\lambda}(j_1 j_2 j_3 j_4 | L_1 L_2 L_3) P_{2\mu,\lambda}(\cos\vartheta_1) P_{2\mu\nu,\lambda}(\cos\vartheta_3) \cos\lambda\varphi. \tag{18}$$

The values of the Clebsch-Gordan coefficients are tabulated by Condon and Shortley (1951) and the Racah coefficients by Biedenharn (1952). Thus all the quantities occurring in expression (14) for $R_{\mu\nu\lambda}$ are known.

III. Discussion

In the final formulas (14) for the correlation coefficients there remains only one sum, over m_3 (disregarding the trivial sum over $M_2 = \pm 1$). But this single sum is not formidable, since it depends upon j_2, j_3, L_2 only, so that there are comparatively few cases in which this summation, e.g. for given L_2, must actually be performed.

We shall discuss now the limitation imposed on anisotropy. The Racah coefficients W does not vanish for the following triplets of numbers

$$(L_1 j_2 j_1),\ (L_1 L_1 2\mu),\ (j_2 j_2 2\mu),$$
$$(L_3 j_3 j_4),\ (L_3 L_3 2\nu),\ (j_3 j_3 2\nu), \tag{19}$$

which satisfy the triangle condition. So we conclude that

$$\mu \leqslant \min(L_1 j_2), \qquad \nu \leqslant \min(L_3 j_3), \tag{20}$$

where, e.g., min $(L_1 j_2)$ is the smaller of the two numbers L_1, j_2. Moreover, thanks to the properties of the associated Legendre polynomials, we have

$$\lambda \leqslant \min(2\mu 2\nu). \tag{21}$$

Eq. (18) takes a simpler form for some special positions of the counters. The case when two counters lie on a straight line going through the emitting nucleus was investigated by Arfken, Biedenharn and Rose (1951). In this case one must draw the z-axis parallel to this straight line. Therefore our formulas take simpler forms in the case in which one of the two counters is the counter registering the second quantum. Thus setting $\vartheta_1 = \pi, 0$ or $\vartheta_3 = \pi, 0$ all the terms vanish except those for which $\lambda = 0$, this being a consequence of the properties of $P_{l,m}$.

A simplification occurs for $\vartheta_1 = \frac{\pi}{2}$ or $\vartheta_3 = \frac{\pi}{2}$. Then, due to the properties of $P_{e,m}$, only the terms with even λ remain. The same occurs for $\varphi = \pi/2$ and is caused by the factor cos $\lambda\varphi$.

An interesting special case is the position $\vartheta_1 = \frac{\pi}{2}$ or $\vartheta_3 = \frac{\pi}{2}$ with $\varphi = \frac{\pi}{4}$ when the first or third transition is a dipole one. Then, on account of the properties of $P_{l,m}$, there remain only the terms with even λ, but because of the factor cos $\lambda\varphi$ and the inequality $\lambda \leqslant 2$ valid for dipole transitions, finally only the terms with $\lambda = 0$ remain.

The numerical values of the correlation coefficients for three dipole transitions are tabulated below. Only the values of r and A are given and not those of R, thus reducing the number of cases. Since the matrix elements of Eq. (1) are hermitean, it is sufficient to consider the cases $j_2 = j_3,\ j_3 + 1$ only. The values of the Clebsch-Gordan coefficients used here were given by Condon and Shortley (1951). The ratios of the Racah coefficients occurring in the expressions for r' are taken from the paper of Arfken, Biedenharn and Rose (1952).

Table of correlation coefficients for three dipole transitions.

$R'_{\mu\nu\lambda} = r'_{\mu\nu} A'_{\mu\nu\lambda} = R_{\mu\nu\lambda}/R_{000}$; $\quad r'_{\mu\nu} = r_{\mu\nu}/r_{00}$; $\quad A'_{\mu\nu\lambda} = A_{\mu\nu\lambda}/A_{000}$

R'_{100}

$$r'_{10}(j_2 j_2 j_3 j_4|11) = -\sqrt{\frac{(2j_2-1)(2j_2+3)}{20j_2(j_2+1)}} = r'_{10}(j_2 j_2 \quad|11) \text{ independent of } j_3,\ j_4$$

$$r'_{10}(j_2-1 j_2 j_3 j_4|11) = \sqrt{\frac{(j_2+1)(2j_2+3)}{20j_2(2j_2-1)}} = r'_{10}(j_2-1 j_2 \quad|11) \qquad ,, \quad ,, \quad ,,$$

$$r'_{10}(j_2+1 j_2 j_3 j_4|11) = \sqrt{\frac{j_2(2j_2-1)}{20(j_2+1)(2j_2+3)}} = r'_{10}(j_2+1 j_2 \quad|11) \ ,, \quad ,, \quad ,,$$

$$A'_{100}(j_3 j_3|1) = \frac{3-4j_3(j_3+1)}{10\sqrt{(2j_3-1)j_3(j_3+1)(2j_3+3)}}$$

$$A'_{100}(j_3+1 j_3|1) = -\frac{2j_3^2+9j_3+10}{10\sqrt{(2j_3+1)(j_3+1)(j_3+2)(2j_3+5)}}$$

R'_{010}

$$r'_{01}(j_1 j_2 j_3 j_4|11) = r'_{01}(\quad j_3 j_4|11) = r'_{10}(j_4 j_3 \quad|11) \qquad \text{independent of } j_1\, j_2$$

$$A'_{010}(j_3 j_3|1) = A'_{100}(j_3 j_3|1)$$

$$A'_{010}(j_3+1 j_3|1) = \frac{j_3[3-14j_3(j_3+1)]}{10(2j_3+3)\sqrt{(2j_3-1)j_3(j_3+1)(2j_3+3)}}$$

R'_{11}

$$r'_{11}(j_1 j_2 j_3 j_4|11) = r'_{10}(j_1 j_2 \quad|11)\, r'_{01}(\quad j_3 j_4|11)$$

$$A'_{110}(j_3 j_3|1) = \frac{20j_3^4+40j_3^3-91j_3^2-111j_3+72}{35j_3(j_3+1)(2j_3-1)(2j_3+3)}$$

$$A'_{110}(j_3+1 j_3|1) = \frac{(2j_3+3)j_3(64j_3^4+352j_3^3-979j_3-240)}{35(j_3+1)\sqrt{(2j_3-1)(2j_3+1)(2j_3+3)(2j_3+5)j_3(j_3+2)}}$$

$$A'_{111}(j_3 j_3|1) = \frac{3(-24j_3^4+148j_3^3+14j_3^2-165j_3+265)}{140(2j_3-1)j_3(j_3+1)(2j_3+3)}$$

$$A'_{111}(j_3+1 j_3|1) = \frac{3j_3(8j_3^4+44j_3^3+175j_3^2+274j_3-93)}{14(2j_3+3)(j_3+1)\sqrt{(2j_3-1)(2j_3+1)(2j_3+3)(2j_3+5)j_3(j_3+2)}}$$

$$A'_{112}(j_3 j_3|1) = \frac{9(8j_3^4+16j_3^3-84j_3^2-92j_3-15)}{70(2j_3-1)(j_3+1)j_3(2j_3+3)}$$

$$A'_{112}(j_3+1 j_3|1) = \frac{6j_3(8j_3^4+44j_3^3+70j_3^2+13j_3-30)}{35(j_3+1)(2j_3+3)\sqrt{(2j_3-1)(2j_3+1)(2j_3+3)(2j_3+5)j_3(j_3+2)}}.$$

The tabulation of separate values of r and A has the following advantage. A depends only upon j_2, j_3, L_2. Consequently the values of A given in the above table includes also, e.g., the case of the two first dipole transitions and the third quadripole transition for $j_2 \leqslant 1$.

In principle only dipole transitions are considered in this table, though some very special cases of higher multipolarity are also included. That is so because the number of cases of higher order transitions increases rapidly with the order. In general, however, the angular momenta of the two first excited states of the nucleus and the multipole character of the transitions between these states as well as between the first excited state and the ground state can be investigated with help of double correlation experiments. If this is the case, one has to insert in Eqs.(14) the known values of j_4, j_3, j_2, L_3, L_2 and to calculate the correlation coefficients as depending on j_1, L_1.

It should be pointed out that in the correlation formula (18) we assume that the counters distinguish the three quanta emitted in succession. In the case when the energies of the three quanta differ this can be done by bringing to coincidence those impulses only which correspond to γ-quanta whose energies lie in appropriate energy intervals or by applying suitable absorbers. Another possibility is the application of delayed coincidences. This application, however, is difficult for the correlation investigation, since at present the experimentally obtainable delay times are rather small ($>10^{-9}$ sec as compared with 10^{-12} sec which is in general the order of the half-life time of nuclear states). If it is impossible to distinguish between the three quanta, one must permute the directions of the three quanta appearing in Eq. (18) and add all the obtained expressions for w. Or alternately, one can place the counters in such directions that the angles between every two of them are equal. But the informations obtainable from such observations are rather poor.

Since the correlation formula (18) is sensitive to the sequence of the successively emitted quanta, the observation of triple γ-correlations can give information about the location of the nuclear levels.

Now, we shall discuss the possibility of measurement of triple γ-correlations. We assume that the number of triple cascade processes in the source used in our experiment is the same as the number of double processes in the sources used in similar experiments concerning double γ-correlations. With N_3 we denote the number of triple coincidences which should be observed in our experiment, whereas N_2 is the number of double coincidences observed in the experiments mentioned above. The efficiency for γ-quanta of modern scintilation counters is near to 100% (see the review article on scintilation counters by Haule (1951)). Thus the main factor which makes N_3 smaller than N_2 is the solid angle subtended by the counter. If, for instance, this solid angle is equal to 0,25 steradian, then this factor causes that $N_3 \approx 2 \cdot 10^{-2} N_2$. Taking into account the fact that in the case of double correlations the counters do not distinguish the two successive quanta, we get $N_3 \approx 10^{-2} N_2$. This result is obtained by neglecting such effects as absorption of the γ-rays in the apparatus. N_3 is also reduced by making the

apparatus sensitive only to γ-quanta with energies lying in special intervals. But the number of accidental coincidences is for the case of three counters much smaller then for the case of two counters. Besides, we must take into account the fact that the experiments concerning double correlations were performed with the use of counters, the efficiency of which was far from 100%. Therefore we conclude that the measurement of triple γ-correlations might be quite possible.

In conclusion I express my sincere thanks to Professor A. Rubinowicz for suggesting the problem and to Komisja Popierania Twórczości Naukowej i Artystycznej przy Prezydium Rady Ministrów for granting me a scholarship which enabled me to perform this work. I wish also to express my gratitude to Dr L. C. Biedenharn for sending me his "Tables of the Racah Coefficients".

Appendix

We shall outline here the solution of the perturbation theory equations describing triple γ-cascade processes by the method of Weisskopf and Wigner (1930, 1931, 1933). The energy levels of the nucleus considered are given in Fig. 1.

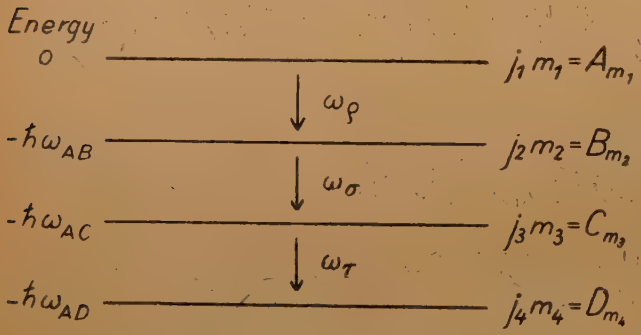

Fig. 1. Energy levels of the nucleus

The states of the system which we need for the calculation are: The initial state $(A_{m_1}; \ldots n_\varrho \ldots n_\sigma \ldots n_\tau \ldots)$ with probability amplitude a_{m_1}, the first intermediate state $(B_{m_2}; \ldots n_\varrho + 1 \ldots n_\sigma \ldots n_\tau \ldots)$ with prob. amp. $b_{m_2\varrho}$, the second intermediate state $(C_{m_3}; \ldots n_\varrho + 1 \ldots n_\sigma + 1 \ldots n_\tau \ldots)$ with prob. amp. $c_{m_3\varrho\sigma}$ and the final state $(D_{m_4}; \ldots n_\varrho + 1 \ldots n_\sigma + 1 \ldots n_\tau + 1 \ldots)$ with prob. amp. $d_{m_4\varrho\sigma\tau}$.

The equations of the perturbation theory are

$$i\hbar\dot{a}_{m_1} = \sum_{m_2\varrho}(a_{m_1}|H|b_{m_2\varrho})b_{m_2\varrho},$$

$$i\hbar\dot{b}_{m_2\varrho} = \sum_{m_1}(b_{m_2\varrho}|H|a_{m_1})a_{m_1} + \sum_{m_3\sigma}(b_{m_2\varrho}|H|c_{m_3\varrho\sigma})c_{m_2\varrho\sigma} + \hbar(\omega_\varrho - \omega_{AB})b_{m_2\varrho},$$

$$i\hbar\dot{c}_{m_3\varrho\sigma} = \sum_{m_2}(c_{m_3\varrho\sigma}|H|b_{m_2\varrho})b_{m_2\varrho} + \sum_{m_4\tau}(c_{m_3\varrho\sigma}|H|d_{m_4\varrho\sigma\tau})d_{m_4\varrho\sigma\tau} + \hbar(\omega_\varrho + \omega_\sigma - \omega_{AC})c_{m_3\varrho\sigma},$$

$$i\hbar\dot{d}_{m_4\varrho\sigma\tau} = \sum_{m_3}(d_{m_4\varrho\sigma\tau}|H|c_{m_3\varrho\sigma})c_{m_3\varrho\sigma} + \hbar(\omega_\varrho + \omega_\sigma + \omega_\tau - \omega_{AD})d_{m_4\varrho\sigma\tau}. \quad \text{(A1)}$$

H is the hamiltonian of interaction between the nucleus and the radiation field. The following solutions of Eqs. (A1) are assumed

$$a_{m_1} = \alpha_{m_1} e^{-\gamma(A_{m_1})t/2},$$

$$b_{m_2\varrho} = \sum_{m_1} \beta_{m_1 m_2 \varrho} \left\{ e^{-\gamma(A_{m_1})t/2} - e^{-[\gamma(B_{m_2})/2 + i(\omega_\varrho - \omega_{AB})]t} \right\},$$

$$c_{m_3\varrho\sigma} = \sum_{m_1} \varepsilon_{m_1 m_3 \varrho\sigma} \left\{ e^{-\gamma(A_{m_1})t/2} - e^{-[\gamma(C_{m_3})/2 + i(\omega_\varrho + \omega_\sigma - \omega_{CA})]t} \right\},$$

$$+ \sum_{m_2} \delta_{m_2 m_3 \varrho\sigma} \left\{ e^{-[\gamma(B_{m_2})/2 + i(\omega_\varrho - \omega_{AB})]t} - e^{-[\gamma(C_{m_3})/2 + i(\omega_\varrho + \omega_\sigma - \omega_{AC})]t} \right\},$$

$$d_{m_4\varrho\sigma\tau} = \sum_{m_1} \xi_{m_1 m_4 \varrho\sigma\tau} \left\{ e^{-\gamma(A_{m_1})t/2} - e^{-i(\omega_\varrho + \omega_\sigma + \omega_\tau - \omega_{AD})t} \right\}$$

$$+ \sum_{m_2} \eta_{m_2 m_4 \varrho\sigma\tau} \left\{ e^{-[\gamma(B_{m_2})/2 + i(\omega_\varrho - \omega_{AB})]t} - e^{-i(\omega_\varrho + \omega_\sigma + \omega_\tau - \omega_{AD})t} \right\},$$

$$+ \sum_{m_3} \zeta_{m_3 m_4 \varrho\sigma\tau} \left\{ e^{-[\gamma(C_{m_3})/2 + i(\omega_\varrho + \omega_\sigma - \omega_{AC})]t} - e^{-i(\omega_\varrho + \omega_\sigma + \omega_\tau - \omega_{AD})t} \right\}. \quad \text{(A2)}$$

Substitution of Eqs. (A2) into Eqs. (A1) gives the following results

$$\xi_{m_1 m_4 \varrho\sigma\tau} = \sum_{m_3} (d_{m_4\varrho\sigma\tau} | H | c_{m_3\varrho\sigma})\, \varepsilon_{m_1 m_3 \varrho\sigma} / \hbar[\omega_{AD} - \omega_\varrho - \omega_\sigma - \omega_\tau - i\gamma(A_{m_1})/2],$$

$$\eta_{m_2 m_4 \varrho\sigma\tau} = \sum_{m_3} (d_{m_4\varrho\sigma\tau} | H | c_{m_3\varrho\sigma})\, \delta_{m_2 m_3 \varrho\sigma} / \hbar[\omega_{BD} - \omega_\sigma - \omega_\tau - i\gamma(B_{m_2})/2],$$

$$\zeta_{m_3 m_4 \varrho\sigma\tau} = -(d_{m_4\varrho\sigma\tau} | H | c_{m_3\varrho\sigma}) \left\{ \sum_{m_1} \varepsilon_{m_1 m_3 \varrho\sigma} + \sum_{m_2} \delta_{m_2 m_3 \varrho\sigma} \right\} / \hbar[\omega_{CD} - \omega_\tau - i\gamma(C_{m_3})/2],$$

$$\varepsilon_{m_1 m_3 \varrho\sigma} = \sum_{m_2} (c_{m_3\varrho\sigma} | H | b_{m_2\varrho})\, \beta_{m_1 m_2 \varrho} / \hbar[\omega_{AC} - \omega_\varrho - \omega_\sigma - i(\gamma(A_{m_1}) - \gamma(C_{m_3}))/2]$$

$$\delta_{m_2 m_3 \varrho\sigma} = -\sum_{m_1} (c_{m_3\varrho\sigma} | H | b_{m_2\varrho})\, \beta_{m_1 m_2 \varrho} / \hbar[\omega_{BC} - \omega_\sigma - i(\gamma(B_{m_2}) - \gamma(C_{m_3}))/2],$$

$$\beta_{m_1 m_2 \varrho} = \alpha_{m_1} (b_{m_2\varrho} | H | a_{m_1}) / \hbar[\omega_{AB} - \omega_\varrho - i(\gamma(A_{m_1}) - \gamma(B_{m_2}))/2],$$

$$\gamma(C_{m_3}) = \sum_{m_4} W^{C_{m_3}}_{D_{m_4}} = W^{C_{m_3}}_{D},$$

$$\gamma(B_{m_2}) = \sum_{m_3} W^{B_{m_2}}_{C_{m_3}} = W^{B_{m_2}}_{C},$$

$$\gamma(A_{m_1}) = \sum_{m_2} W^{A_{m_1}}_{B_{m_2}} = W^{A_{m_1}}_{B}. \quad \text{(A3)}$$

W^F_G is the probability of transition of the nucleus from state F to state G by emitting a γ-quantum.

For $t \to \infty$ we get

$$d_{m_4\varrho\sigma\tau} = \frac{1}{\hbar^3}\sum_{m_1m_2m} a_{m_1} \tag{A4}$$

$$\times \frac{(d_{m_4\varrho\sigma\tau}|H|c_{m_3\varrho\sigma})(c_{m_3\varrho\sigma}|H|b_{m_2\varrho})(b_{m_2\varrho}|H|a_{m_1})}{\{\omega_{AD}-\omega_\varrho-\omega_\sigma-\omega_\tau-i\gamma(A_{m_1})/2\}\{\omega_{BD}-\omega_\sigma-\omega_\tau-i\gamma(B_{m_2})/2\}\{\omega_{CD}-\omega_\tau-i\gamma(c_{m_3})/2\}}$$

Making use of the known dependence of the matrix elements on the occupation numbers of the field oscillators and neglecting constant factors, we get Eq. (1). The assumption is made that the initial nuclei are oriented at random. Since the nuclear states which differ only in respect to magnetic quantum numbers have the same energy, one must sum over m_4. The summation over the directions of polarization corresponds to the case of observation with the help of three counters which do not distinguish between the directions of polarizations (see Hamilton 1944).

REFERENCES

Arfken G. B., Biedenharn L. C., Rose M. E., *Phys. Rev.* **83**, 586 (1951); *Phys. Rev.* **86**, 761 (1952).

Biedenharn L. C., *Tables of Racah Coefficients*, Oak Ridge National Laboratory No1098 (1952).

Brady E. L. and Deutsch M., *Phys. Rev.*, **78**, 558 (1950).

Condon and Shortley, *The Theory of Atomic Spectra*, Cambridge 1951.

Falkoff D. L. and Uhlenbeck G. E., *Phys. Rev.*, **79**, 323 (1950).

Goertzel G., *Phys. Rev.*, **70**, 897 (1946).

Hamilton D. R., *Phys. Rev.*, **58**, 122 (1944).

Haule W., *Naturwis*, **38**, 176 (1951).

Lippman B. A., *Phys. Rev.*, **81**, 162 (1951).

Racah G., *Phys. Rev.*, **62**, 438 (1942), *Phys. Rev.*, **84**, 910 (1951).

Rubinowicz A., *Rep. Prog. Phys.*, **22**, 233 (1949).

Weisskopf *V.*, *Ann. Phys. Lpz.*, **9**, 53 (1931); *Z. Phys.*, **85**, 451 (1933).

Weisskopf V. and Wigner E., *Z. Phys.*, **63**, 54 (1930); **65**, 18 (1930).

Wigner, *Gruppentheorie und ihre Anwendung auf die Quantenmechanik der Atomspektren*. Braunschweig 1931.

Я. Домбровский, *Угловые корелляции для трехступенчатой каскадной γ — эмиссии.*

Возбужденное ядро переходит в основное состояние через два последовательные действительные промежуточные состояния, испуская три последовательные γ—кванты. В работе получено взаимное угловое распределение этих трех γ—квантов. Система уравнений теории возмущений, описывающих весь процесс, решается методом Вейсскопфа—Вигнера. Для получения формулы вероятности каскадной эмиссии при условии, что каждый γ—квант соответствует переходу определенной мультипольности, используется теория групп. Вследствие выбора оси z параллельно к направлению второго кванта, возможно двухкратное применение формул суммирования Рака. Окончательно получаем разложение по выражениям

$$P_{2\mu,\lambda}(\cos\vartheta_1)P_{2\nu,\lambda}(\cos\vartheta_3)\cos\lambda\varphi,$$

где $\vartheta_1(\vartheta_3)$ — угол между направлением первого (третьего) и второго кванта, φ—угол между плоскостями, в которых лежат направления первого и второго кванта (третьего и второго). $P_{k,\lambda}$ — сферические функции. Коэффициенты разложения содержат коэффициенты Рака и Клебша—Жордана. Рассмотрена анизотропия углового распределения. Для дипольных переходов приведены числовые значения корелляционных коэффицентов в зависимости от квантовых чисел полного момента количества движения, участвующих в процессе ядерных уровней. Формулы описывают также процесс абсорпции, после которого наступает двухступенчатая каскадная эмиссия.

LETTERS TO THE EDITOR

RELATIVISTIC QUANTUM DYNAMICS OF A SYSTEM OF INTERACTING PARTICLES

By Jan Rzewuski

University of Wrocław, Institute of Theoretical Physics

(November 18, 1953)

Quantum mechanics, so far, was applied either to non-relativistic systems of particles, that is systems in which the interaction is of a static type, or to systems in which the particles move in a given external field. Extension to relativistic systems of particles interacting by means of retarded or advanced forces was hindered by the fact that the corresponding variational principle (1) contains double integrals in the interaction terms besides single integrals in the terms corresponding to unperturbed motion. Such systems are of a non-local type and it is impossible to describe them by a set of commuting observables corresponding to one time or, generally speaking, to one space-like surface. In fact all quantities appearing in the theory show besides an explicit dependence on the observables on a certain surface also an implicit dependence on these observables at points outside this surface. The intervention of points from the outside occurs by means of integrals of certain functions of the observables taken over the whole domain of time considered and is unavoidable in any non-local theory.

It is well known from the field theory, however, (Rzewuski 1951, Rayski 1951) that even in non-local cases, where the traditional quantization procedures are not directly applicable, one may calculate Heisenberg's S-matrix by means of direct methods such as the method of Feynman (1949) or Yang and Feldman (1950).

It is the aim of the present letter to describe briefly the construction of an S-matrix for relativistic dynamics of interacting particles. Such dynamics is in general described by an action integral of the following form

$$W = -\sum_n \varkappa_n \int_{\sigma_1}^{\sigma_2} \sqrt{1-(v_i^k)^2}\, dt^n + \frac{1}{2}\sum_n \sum_m e_n e_m \int_{\sigma_1}^{\sigma_2}\int v_\mu^n G(q^n - q^m) v_\mu^m dt^n\, dt^m \quad (1)$$

Here Latin indices run from 1 to 3, Greek indices from 1 to 4. For both types the convention about summation over dummy indices is adopted. $v_i^n = \dfrac{dq_i^n}{dt^n}$

is the velocity of the n-th particle, $v_0^n = 1$. The integration limits are denoted by σ_1 and σ_2 which means that one has to integrate over t^n between points at which the line $q_i^n(t^n)$ intersects two given space like surfaces σ_1 and σ_2. We may imagine that on these surfaces some experiments are arranged and for most practical problems we may move them to $-\infty$ or $+\infty$ resp. The function G gives account of the interaction and must for relativistic reasons depend on $q^n - q^m$ by means of the invariant $(q_\mu^n - q_\mu^m)^2$. For electrodynamics $G(q^n - q^m) = \delta[(q_\mu^n - q_\mu^m)^2]$ but we shall carry out the calculations for a general G, thus including into the considerations also mesodynamics and theories with extended particles. For simplicity the term $n = m$ is excluded. It gives account of the action of one particle on itself and may be considered to be contained in the mass constant $\varkappa_n$ as a renormalization effect (cf. Wheeler and Feynman 1949 and Feynman 1948). e_n is the charge of the n-th particle. Units are chosen in which $\hbar = c = 1$.

The equations of motion following from (1) are

$$\frac{d}{dt^n}\left(\frac{\varkappa_n v_i^n}{\sqrt{1-(v_k^n)^2}}\right) = e_n F_{i\nu}^n v_\nu^n, \tag{2}$$

where

$$F_{i\nu}^n = \frac{\partial A_\nu^n}{\partial q_i^n} - \frac{\partial A_i^n}{\partial q_\nu^n}; \quad A_\nu^n(q^n) = \sum_{m \neq n} e_m \int_{\sigma_1}^{\sigma_2} \frac{1}{2}\{G(q^n - q^m) v_\nu^m +$$

$$+ v_\nu^m G(q^m - q^n)\}\, dt^m. \tag{3}$$

Introducing a new variable $\pi_i^n = \dfrac{\varkappa_n v_i^n}{\sqrt{1-(v_k^n)^2}}$, we may write equations (2) in a simple form

$$\frac{d\pi_i^n}{dt_n} = e_n F_{i\nu}^n v_\nu^n. \tag{4}$$

Integration yields

$$\pi_k^n = p^{1n}{}_k + e_n \int_{\sigma_1}^{\sigma_2} \eta^{ret}(t^n - t^{n'}) F_{k\nu}^{n\prime} v_\nu^{n'}\, dt^{n'},$$

$$\pi_k^n = p^{2n}{}_k + e_n \int_{\sigma_1}^{\sigma_2} \eta^{adv}(t^n - t^{n'}) F_{k\nu}^{n\prime} v_\nu^{n'}\, dt^{n'}. \tag{5}$$

Primes denote dependence on $t^{n'}$. $p^{1n}{}_k$ and $p^{2n}{}_k$ are the boundary values of π_k^n at σ_1 or σ_2 resp. They satisfy the unperturbed equations $\dfrac{dp^{1n}{}_k}{dt^n} = \dfrac{dp^{2n}{}_k}{dt^n} = 0$. In the limiting case of no interaction $\pi_k^n \to p_k^n$. $\eta^{ret}(t)$ and $\eta^{adv}(t)$ are defined by

$$\eta^{ret}(t) = \begin{matrix} 1 \text{ for } t > 0, \\ 0 \quad ,, \quad t < 0, \end{matrix} \qquad \eta^{adv}(t) = \begin{matrix} 0 \text{ for } t > 0. \\ -1 \text{ for } t < 0. \end{matrix} \tag{8}$$

Equations (5) may be treated by means of the Yang-Feldman method (1950). The commutation rules for non interacting particles may be derived by application of Schwingers method (1951) to quantum mechanics with

$$W^0 = -\sum_n \varkappa_n \int_{\sigma_1}^{\sigma_2} \sqrt{1-(v_i^n)^2}\, dt^n \tag{9}$$

as action integral. They are

$$[q_i^{0n}, p_k^{0m}] = i\delta^{nm}\,\delta_{ik}, \qquad [q_i^{0n}, q_k^{0m}] = 0, \qquad [p_i^{0n}, p_k^{0m}] = 0, \tag{10}$$

where

$$p_i^{0n} = \frac{\varkappa^n\, v_i^{0n}}{\sqrt{1-(v_k^{0n})^2}}$$

(the superscript o denotes non-interacting particles). The second of the commutation rules (10) holds only if t^n and t^m correspond to the same space-like surface σ. For arbitrary t^n and t^m the commutation rules are derived by the usual methods but we shall not use them in this letter. The remaining commutation rules are valid generally because of the constancy of p_k^{0n}.

Now introducing the unitary operator S by the equations

$$p_k^{2n} = S^{-1} p_k^{1n}\, S, \tag{12}$$

combining equations (5) and (12), and using the notation

$$p_k^{0n} = \frac{1}{2}(p_k^{1n} + p_k^{2n}), \quad \varepsilon(t) = \eta^{ret}(t) + \eta^{adv}(t) = \begin{matrix} 1 \text{ for } t > 0, \\ -1 \text{ for } t < 0, \end{matrix} \tag{13}$$

we obtain two equations

$$\pi_k^n = p_k^{0n} + e^n \int_{\sigma_1}^{\sigma_2} \frac{1}{2}\,\varepsilon(t^n - t^{n'})\, F_{k\nu}^{n'}\, v_\nu^{n'}\, dt^{n'}, \quad [p_k^{0n}, S] = \frac{1}{2}\left\{S, e_n \int_{\sigma_1}^{\sigma_2} F_{k\nu}^n\, v_\nu^n\, dt^n\right\} \tag{14}$$

for π_k^n and S which may be solved by successive approximation. The first two terms in an expansion of π_k^n and S in powers of e_n are

$$\pi_k^n = p_k^{0n} + e_n \int_{\sigma_1}^{\sigma_2} \frac{1}{2}\,\varepsilon(t^n - t^{n'})\, F_{k\nu}^{0n'}\, v_\nu^{0n'}\, dt^{n'} + \ldots \tag{15}$$

$$S = 1 + \frac{i}{2}\sum_n e_n \int_{\sigma_1}^{\sigma_2} A_\nu^{0n}\, v_\nu^{0n}\, dt^n + \ldots$$

$$= 1 + \frac{i}{2}\sum_{n\neq m}\sum e_n e_m v_\nu^{0n} \iint_{\alpha_1}^{\sigma_2} G\,(q^{0n} - q^{0m})\, dt^n\, dt^m\, v_\nu^{0m} + \ldots \tag{16}$$

Thus the relativistic problem of interacting particles seems to be solved in principle in the framework of quantum dynamics without use of the field concept.

It may be regarded as an extension to quantum theory of the ideas of action at a distance advocated by Wheeler and Feynman (1945, 1949).

Applications to practical problems shall be given in a detailed account of this work.

REFERENCES

Feynman R. P., *Phys. Rev.*, **74**, 939 (1948); **76**, 749, 769 (1949).
Rayski J., *Acta Phys. Polonica*, **11**, 25 (1951).
Rzewuski J., *Acta Phys. Polonica*, **11**, 9 (1951).
Schwinger J., *Phys. Rev.*, **82**, 914 (1951).
Wheeler J. A. and Feynman R. P., *Rev. Mod. Phys.*, **17**, 157 (1945); **21**, 425 (1949).
Yang C. N. and Feldman D., *Phys. Rev.*, **79**, 972 (1950).

Czasopismo ukazuje się corocznie w jednym tomie złożonym z czterech kwartalnych zeszytów.

Maszynopisy prac w 2 egzemplarzach w językach rosyjskim, angielskim, francuskim lub niemieckim, zaopatrzone w krótkie streszczenia w języku pracy oraz rosyjskim należy nadsyłać pod adresem redakcji niżej podanym. Wszystkie ryciny powinny być zaopatrzone w krótkie objaśnienia jako podpisy do klisz. Autorzy mogą otrzymać najwyżej 50 odbitek swych prac po cenie kosztów produkcji.

Журнал издаваемый ежегодно в одном томе состоящем из четырех выпусков.

The periodical appears yearly in one volume of four quarterly issues.

Le périodique paraît dans un volume par an en quatre fascicules trimestriels.

Die Zeitschrift erscheint in einem Bande von vier Heften jährlich.

Adres redakcji — Адрес Редакции — Adresse de la Rédaction:
Kraków 2, al. Słowackiego 15 m. 9

Adres wydawnictwa: Warszawa 1, Krakowskie Przedmieście 79, skrytka pocztowa 455

Cena zeszytu pojedynczego wynosi 12 zł, prenumerata roczna 48 zł, półroczna 24 zł

Wszelkie wpłaty za rocznik 1953 należy przekazywać na konto Państwowego Wydawnictwa Naukowego: PKO Warszawa Nr 1-110-28504

Cena zł 12.—